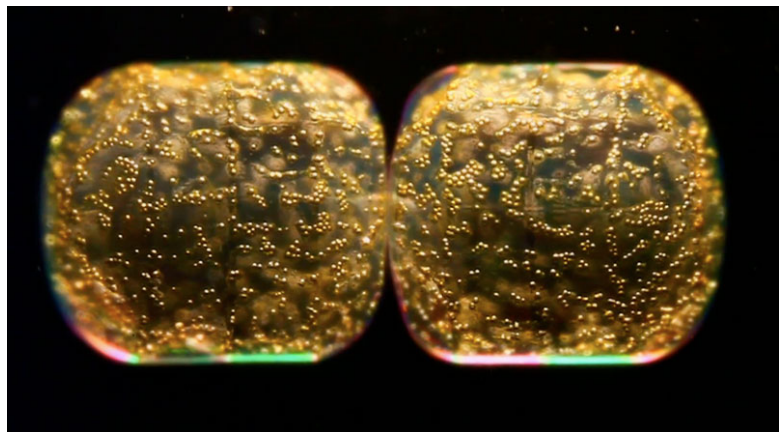


# Variability in the relationship between in situ fluorescence and chlorophyll-*a* concentration in Faroese waters (2002-2019): Recommendations for database management

Tórshavn · May 2020



*Credit: C. Sardet, CNRS, TARA Oceans*

**Ian Salter**  
**Sólvá Káradóttir Eliassen**  
**Sólvá Jacobsen**

# Variability in the relationship between in situ fluorescence and chlorophyll-*a* concentration in Faroese Waters (2002-2019): Recommendations for internal database management.

Ian Salter, Sólvá Káradóttir Eliassen, Sólvá Jacobsen

## Summary

Phytoplankton form the base of marine foodwebs and sustain productivity throughout all trophic levels, upto and including commercially important fish species. In addition they impact climate through the sequestration of atmospheric carbon dioxide and the production of climatically-active gases. Understanding natural variability and anthropogenic-driven changes in the spatial and temporal distribution of phytoplankton biomass is thus an important objective of both regional and global observing programs. The photosynthetic pigment chlorophyll-*a* (chl-*a*) serves as a proxy for phytoplankton biomass and can be either measured directly or inferred from in situ fluorescence. In situ fluorometry is widely-used because it is cost-effective and enables monitoring of phytoplankton biomass from multiple observing platforms that integrate across the relevant range of spatial and temporal scales. In order to correctly interpret fluorescence profiles it is necessary to characterise the relationship between in situ fluorescence and measured chl-*a* concentrations, with a view to producing field-corrected fluorescence datasets.

The objective of this technical report was to examine the observed variability in fluorescent yield per chl-*a* in Faroese waters and provide recommendations for internal database management regarding the storage of field-corrected fluorescence datasets. We analysed survey data collected by R/V Magnus Heinason during the period 2002-2019 and compared measured chl-*a* values with in situ fluorescence. There was significant seasonal and inter-annual variability in fluorescence yield per chl-*a* covering several orders of magnitude ( $0.06 - 13.3 F_{\text{chl}}:\text{chl}^{-1}$ ). Differences in water-column stratification and nutrient stoichiometry appear to explain some degree of the observed variability, most likely mediated through changes in phytoplankton community dynamics and photophysiological response. A significant shift in fluorescence yield per chl-*a* and silicate:nitrate ratios was observed from 2014 onwards, indicative of a potential shift in phytoplankton community dynamics on the Faroese shelf. Based on our analysis we conclude that it is not advisable to use a single empirical conversion to produce field-corrected fluorescence datasets in Faroese waters. Consequently we have modified the FAMRI database such that all in situ fluorescence data are stored as raw data with no field corrections. We have provided guidance that all future data collections should be stored this way. In addition, we recommend that fluorometers should be sent for factory calibration once every three years to carefully monitor changes in sensitivity and analytical performance.

## Contents

<b>1. Introduction</b>	<b>3</b>
<b>2. Materials and Methods</b>	<b>6</b>
<b>2.1. Fluorescence measurements</b>	<b>6</b>
<b>2.1.1. Theoretical background</b>	<b>6</b>
<b>2.1.2. Measurement principle</b>	<b>7</b>
<b>2.1.3. Sensitivity settings</b>	<b>7</b>
<b>2.1.4. Data smoothing</b>	<b>7</b>
<b>2.1.5. Calibration and units</b>	<b>8</b>
<b>2.2. Chlorophyll-a</b>	<b>8</b>
<b>2.2.1. Sample collection</b>	<b>8</b>
<b>2.2.2. Spectrophotometric determination of chl-<i>a</i></b>	<b>8</b>
<b>2.3. Sampling area</b>	<b>9</b>
<b>2.3.1. Selecting data from FAMRI database</b>	<b>10</b>
<b>3. Results</b>	<b>11</b>
<b>4. Discussion</b>	<b>20</b>
<b>4.1. Recommendations for storage of Fchl and extracted chl-a values in the FAMRI database</b>	<b>20</b>
<b>4.2. Possible explanations for variable fluorescent yields per chl-a in Faroese waters</b>	<b>21</b>
<b>4.3. Fluorometer performance</b>	<b>22</b>
<b>5. Conclusions</b>	<b>23</b>
<b>6. References</b>	<b>24</b>
<b>7. Appendix 1</b>	<b>28</b>
<b>8. Appendix 2</b>	<b>29</b>

# 1. Introduction

Phytoplankton are single-celled photosynthetic organisms that play an essential role in aquatic ecosystems and the Earth's biosphere. They are estimated to contribute approximately 50% of global net primary production (Field et al., 1998). The export of photosynthetically-fixed organic carbon out of the surface ocean is reported to range from 5 to 10 Pg yr<sup>-1</sup> (Lima et al., 2014), lowering atmospheric CO<sub>2</sub> concentrations by upto 200 ppm (Sarmiento and Toggweiler, 1984; Sarmiento et al., 1988) exerting a significant impact on global climate. The same processes of vertical organic carbon export are the principal supply of energy that sustains benthic ecosystems (Billet et al., 2001; Ruhl and Smith, 2004). In the upper ocean primary production by phytoplankton forms the base of aquatic food-webs that sustain all trophic levels. On the Faroese shelf phytoplankton biomass has been linked to the copepods (Gaard, 1999, 2000; Debes and Eliassen, 2006; Debes et al., 2008) which connect phytoplankton to commercially important fish species (Gaard and Steingrund, 2001). In fact there is substantial evidence of positive associations between primary production and 0-group stages cod, haddock, sandeel and Norway pout (Gaard et al., 2002; Steingrund and Gaard, 2005; Jacobsen et al., 2019). Understanding the distribution and regulation of phytoplankton biomass therefore represents an important challenge at both regional and global scales.

All phytoplankton contain the light-harvesting pigment chlorophyll-*a* (hereafter chl-*a*), and as a consequence it has been extensively applied as a proxy for autotrophic biomass and production in the global ocean (Behrenfeld et al., 2006). It is necessary to acknowledge that chl-*a* serves only as a proxy for phytoplankton biomass due to known variations of chl-*a* content and carbon biomass (chl-*a* / C) within phytoplankton. Variability in chl-*a* / C ratios has been linked to nutrient status (Riemann et al., 1989; Cullen et al., 1992), light availability (Geider et al., 1998; Moore et al., 2006), growth rates (Geider, 1987; Kruskopf and Flynn, 2006), allometric scaling (Álvarez et al., 2017) and taxonomic differences (Yacobi and Zohary, 2010; Rembauville et al., 2016). Despite these apparent complications, the analytical simplicity of reliable chl-*a* measurements has resulted in its widespread use for determining phytoplankton biomass in the ocean. Significantly, chl-*a* can be estimated from in situ fluorescence, thus facilitating measurements from multiple observation platforms across a wide range of spatial and temporal scales.

When chlorophyll molecules within phytoplankton cells absorb light, a small fraction of the energy is emitted as fluorescence. A first order relationship exists between the concentration of chl-*a* and in situ chlorophyll fluorescence ( $F_{chl}$ ), justifying the analytical basis for fluorescence measurements to quantify chl-*a* (Lorenzen, 1966; Falkowski and Kiefer, 1985). The actual relationship between fluorescence and chl-*a* is described by Equation 1:

$$F_{chl} = PAR \cdot [chl - a] \cdot \bar{a}^* \cdot Q_a^* \cdot \phi_F \quad \text{Eq.1}$$

where,  $F_{chl}$  = flux of in situ fluorescence emitted by an elementary volume (in this case it is  $\mu\text{mol photons m}^{-3} \text{ s}^{-1}$ ), PAR is photosynthetically active radiation ( $\mu\text{mol photons m}^{-2} \text{ s}^{-1}$ ),  $[chl - a]$  is the concentration of chlorophyll-*a* ( $\text{mg m}^{-3}$ ),  $\bar{a}^*$  ( $\text{mg m}^{-2}$ ) is the chl-*a*-specific spectrally-averaged absorption coefficient of phytoplankton weighted by the irradiance spectrum,  $Q_a^*$  (dimensionless) is the fluorescence intracellular reabsorption factor and  $\phi_F$  ( $\text{mol emitted photons (mol absorbed photons)}^{-1}$ ) is the quantum yield of  $F_{chl}$  (Babin, 2008).

Essentially, the product  $\{\text{PAR} \cdot [\text{chl}] \cdot \bar{a}^*\}$  reflects the amount of light absorbed by phytoplankton,  $Q_a^*$  is the fraction of fluorescence that is not reabsorbed within the cells and  $\phi_F$  indicates the fraction that is converted to fluorescence (Collins et al., 1985). The assumption that justifies the fluorometric approach is straightforward if PAR is generated using a constant artificial light source and the product  $(\bar{a}^* \cdot Q_a^* \cdot \phi_F)$  remains constant, because then  $F_{chl}$  is proportional to chl-*a* (Babin, 2008).

There are numerous factors that differ among phytoplankton species and their response to environmental conditions that result in variability of the product  $(\bar{a}^* \cdot Q_a^* \cdot \phi_F)$ . Fluctuating irradiance induces photophysiological regulatory mechanisms within cells. Non photochemical quenching (NPQ) is a process through which phytoplankton can dissipate the excess energy absorbed by photosynthetic pigments (Huot and Babin, 2010). When exposed to high irradiance, NPQ mechanisms suppress the transfer of photon energy from light-harvesting antennae to chl-*a* in photosynthetic reaction centres, consequently reducing emitted fluorescence (Horton et al., 1996). The differential packaging of photosynthetic pigments within cells can also result in “shading” effects that reduces chl-*a* fluorescence (Sosik and Mitchell, 1991; Kirk, 1994). In contrast, the composition and concentration of photosynthetic accessory pigments can increase apparent chl-*a* fluorescence efficiency (López-Sandoval et al., 2011). Macronutrient limitation (or rather starvation) inhibits the production of functional photosynthetic reaction centres, thereby modifying the quantum yield of fluorescence (Kolber et al., 1988; Geider et al., 1993a). Although both photosynthetic reaction centres (photosystems I and II; PSI and PSII) contain chl-*a*, because of the nature of pigment-protein complexes within the reaction centres, they are characterised by different fluorescent yields. Consequently, the majority of  $F_{chl}$  originates from chl-*a* bound in PSII (Falkowski and Kiefer, 1985), whilst chl-*a* in PSI emits virtually no fluorescence. Limitation of the micronutrient iron can increase chl-*a*-normalized fluorescence (Geider et al., 1993b; Schrader et al., 2011) due to a shift in the ratio of PSII and the non-fluorescing but iron-rich PSI (Strzepek and Harrison, 2004). Furthermore, the distribution of chl-*a* between PSI and PSII differs between species, resulting in variations of fluorescent yield per chl-*a* amongst different phytoplankton communities (Vincent, 1983; Proctor and Roesler, 2010).

The factors described above highlight the complexity in constraining fluorescent yield per chl-*a*. In practical terms, this imposes a challenge in calibrating  $F_{chl}$  as a function of chl-*a* as there are no suitable primary standards for chlorophyll. Such a primary standard should be chemically stable and have consistent optical properties. These requirements render it difficult to use algal cultures as primary standards because growth conditions, species selection, strain specificity, culture medium and physiological state all result in variable fluorescent yields. A chemical alternative, such as pure chl-*a*, is also problematic because it needs to be dissolved in a solvent that is compatible with fluorometer devices. Organic solvents (e.g. ethanol or acetone) that are required to dissolve chl-*a* are not compatible with the plastic components of most field devices. Another constraint is that most fluorometers use light-emitting diodes with a peak at 470 nm, and chl-*a* dissolved in acetone does not absorb strongly at 470 nm resulting in a weak fluorescence signal.

A common approach to circumvent the problems of primary calibration of fluorometers is to carry out so-called “field-calibration”. Using this approach, discrete water samples are taken at specific or nominal depths concomitantly with the acquisition of a continuous fluorescence profile. The extraction of filtered samples in acetone releases all chl-*a* bound within cells, from photosynthetic reaction centres and protein complexes, into pure solution thus nullifying the product  $(\bar{a}^* \cdot Q_a \cdot \phi_F)$  in Eq.1. Under these circumstances, fluorescence becomes a primary function of chl-*a*, and linear regression analyses can be used to determine an empirical conversion factor, known as fluorescent yield per chlorophyll, to convert  $F_{chl}$  to a concentration of phytoplankton-derived chl-*a*, typically expressed as either  $\mu\text{g L}^{-1}$  or  $\text{mg m}^{-3}$ . However, understanding the variability of fluorescent yield per chl-*a* is necessary before deciding if a single empirical conversion can be applied to specific fluorescence datasets.

$F_{chl}$  measurements are a core ecosystem observing component of the Faroe Marine Research Institute (FAMRI) and have been carried out since the nineties. Specifically, water-column profiles of fluorescence have been acquired on biological survey cruises alongside discrete water samples for analytical determination of chl-*a* concentrations. In 2011, a comparison of chl-*a* and fluorescence data, collected by FAMRI (2002-2010), was used to derive an empirical conversion factor of 1.23 (Appendix 1). The report concluded that all fluorescence data collected by FAMRI could be calibrated by this factor to generate field-corrected profiles. Data from this period were stored in the FAMRI database as “calibrated data” (QF\_FLU = 2). However, in the years that followed, the fluorescent yield per chl-*a* continued to display significant, and possibly enhanced, variability both between survey cruises and years. Consequently data from the period 2011-2019 have been stored in the database mainly as “raw data” (QF\_FLU = 1).

The purpose of this technical report is to carry out an extended analysis of the entire fluorescence and chl-*a* measurements conducted in the period 2002-2019. The main objectives are as follows:

- i) Characterise the variability in fluorescent yield per chl-*a*
- ii) Assess the validity of a single empirical conversion factor
- iii) Based on (i) and (ii), provide recommendations to the FAMRI database regarding the storage of  $F_{chl}$  measurements.

## 2. Materials and Methods

All data included in this report have been sampled by R/V Magnus Heinason during the period 2002-2019 and are stored in the FAMRI database. During the period 2002-2019 in situ fluorescence has been measured with two separate fluorometers, both manufactured by Seapoint (Table 1). In addition, since 2009 FAMRI has operated a WETLabs fluorometer interfaced to a SBE 25 CTD. Although this CTD-frame has no bottles, and thus data from the WETLabs fluorometer cannot be compared with chl-*a* measurements, the CTD has occasionally been deployed together with the SBE 911 CTD. Prior to 2002 FAMRI used a SeaTech fluorometer. Data from the WETLabs and SeaTech fluorometers are omitted from this report.

**Table 1.** Details of Seapoint fluorometers used by FAMRI since 2002 to collect  $F_{chl}$  measurements.

Instrument ID	Start Date	End Date	CTD	Information
HFSPA Serial # 2438	21-02-2002	11-02-2016	Seabird 911	Calibrated upon purchase (2002) by Seapoint. Range = 50µg/l, (gain setting = 3X). Lost with the CTD on the Faroe Shelf in February 2016
HFSPC Serial # SCF3747	27-01-2016	ongoing	Seabird 911	Calibrated upon purchase (2016) and at three years (2019) by Seapoint. Range = 50µg/l, (gain setting = 3X)

### 2.1 Fluorescence measurements

#### 2.1.1 Theoretical background

In algal cells, chl-*a* is contained in the functional units, photosystems I and II that comprise the photosynthetic reaction centres of the cell. The energy of an incoming photon excites an electron in accessory pigments located in light-harvesting complexes and the energy is transferred towards central pigment complexes in the photosynthetic reaction centres. This results in a suite of photochemical reactions that convert light-energy into chemical bonds, providing the basis for primary productivity. Although the trapping of photochemical energy by reaction centres is efficient, a small fraction, not utilized by the reaction centres, is emitted as fluorescence. The underlying principle of using fluorescence measurements is that the amount of emitted fluorescence is proportional to the quantity of chl-*a* in a sample, such that it can be used as a proxy for phytoplankton biomass.

### 2.1.2 Measurement principle

The Seapoint Chlorophyll Fluorometer is used for in situ fluorescence-based measurements of chl-*a* in aqueous solutions (Seapoint manual). The fluorometer uses modulated blue LED lamps and a blue excitation filter to excite chl-*a* in the sensing volume. The fluorescent light emitted by chl-*a* passes through a red emission filter and is detected by a silicon photodiode. The low level signal is then processed using synchronous demodulation circuitry which generates an output voltage proportional to chl-*a* concentration. The sensing volume is defined as the intersection of the lamp beams and the detectors cone of reception allowing the fluorometer to be used with or without a pumping system. The fluorometer operated by FAMRI is deployed without a pump, but water flows freely while the CTD is profiling.

### 2.1.3 Sensitivity settings

The range and sensitivity of the Seapoint fluorometer can be modified for different applications (Table 2).

**Table 2.** Sensitivity settings for Seapoint fluorometers (Seapoint manual).

Gain	Sensitivity	Range
30X	1.0 V / ( $\mu\text{g L}^{-1}$ )	5 $\mu\text{g L}^{-1}$
10X	0.33 V / ( $\mu\text{g L}^{-1}$ )	15 $\mu\text{g L}^{-1}$
3X	0.1 V / ( $\mu\text{g L}^{-1}$ )	50 $\mu\text{g L}^{-1}$
1X	0.033 V / ( $\mu\text{g L}^{-1}$ )	150 $\mu\text{g L}^{-1}$

Choosing the appropriate gain setting depends on the target concentration of chl-*a*, the resolution of the analogue to digital converter in the data recorder, and the expected level of smoothing that will be applied to the data. For most oceanographic applications, a range of 15 or 50  $\mu\text{g L}^{-1}$  is appropriate. Certain oligotrophic (low productivity) systems might benefit from a lower range of 5  $\mu\text{g L}^{-1}$ , although the noise level at 30X gain is likely to exceed the resolution of most data recorders. A range of 150  $\mu\text{g L}^{-1}$  could be necessary for certain systems such as lakes or protected fjords. For the standard oceanographic monitoring conducted by FAMRI, a gain of 3X (Setting 2) corresponding to a range of 50  $\mu\text{g L}^{-1}$ , has been chosen.

### 2.1.4 Data smoothing

The Seapoint Chlorophyll Fluorometer has a low pass filter with a 0.1 second time constant on its output (1.6 Hz cut-off frequency). For profiling applications where fluorescence values are changing rapidly, the low pass filter can be useful in resolving features that might be missed with a slower response. It is possible to increase this time interval to reduce noise and allow lower concentrations to be detected. This can be appropriate for moored applications. For all deployments covered in this report, smoothing has been carried out with the default 0.1 second time constant.

### 2.1.5 Calibration and units

The Seapoint Fluorometer provides an estimate of chl-*a* concentration according to Equation 2 (Seapoint manual):

$$\text{Output } (\mu\text{g L}^{-1}) = (\text{Voltage} \cdot \text{Range} / 5) + \text{Offset} \quad \text{Eq. 2}$$

where Voltage is the measured electrical signal, Range is the value at the corresponding gain setting (Table 2) and Offset is a numerical constant that can be used to correct the equation following calibration of the device.

The fluorometer is adjusted at the factory for a nominal range and sensitivity at a given gain setting (Table 2). The manufacturer (Seapoint) recommends devices should be calibrated if greater accuracy is required than that afforded by the nominal settings. The accuracy of the measurements at nominal settings is not reported by the manufacturer. In addition, changes in the accuracy of the sensor over time can occur. Factors such as biofouling, reductions in lamp efficiency and scratches on the optical measuring window can reduce sensitivity. Calibration can be carried out routinely to correct output through including an offset in Equation 2.

As a standard procedure, all fluorescence data are quality checked by standard check methods (Check program for all CTD-data) before being stored in the FAMRI database. In addition to this, the program Parflox is available to further check each profile. A list of the cruises checked by Parflox is stored at “H:\CTDDATA\1 Viðgerð”. Currently this has only been performed for all data sampled prior to 2015.

## 2.2 Chlorophyll-*a*

### 2.2.1 Sample collection

Field validation of fluorescence values by analytical determination of chl-*a* concentrations was carried out through the analysis of discrete water samples collected by Niskin bottles attached to a CTD rosette. Typically discrete samples were collected at depths of 5, 20 and 40m. A sample volume of 1-2 L of seawater was filtered onto glass fibre filters (nominal pore size of 0.7  $\mu\text{m}$ ) under a weak vacuum generated by flowing tap water. All samples were filtered on board R/V Magnus Heinason. Prior to filtration, GF/F filters were imbibed with several drops of a magnesium carbonate solution (1%  $\text{MgCO}_3$ ) to maintain alkaline pH during storage. Following filtration, filters were folded in half (sample material facing inwards) and wrapped in aluminium foil envelopes to protect them from light. Samples were then stored at  $-20^\circ\text{C}$  in a sealed container with silica gel until subsequent analysis in the laboratory.

### 2.2.2 Spectrophotometric determination of chl-*a*

Chl-*a* was measured spectrophotometrically according to the method of Parsons et al. (1984). In brief, folded filter samples were transferred to 12 mL glass ampoules, followed by 10 mL of 90% (V/V) acetone. The ampoules were capped and inverted several times to mix. The ampoules were covered in aluminium foil and placed in the fridge for an extraction period of 6-24 hours. Following the extraction period, the acetone solution was transferred into 10 mL polypropylene tubes and centrifuged for 10 minutes at 4000 rpm. The acetone extract was

transferred to a 1 cm Quartz cuvette and measured in Heyios spectrophotometer at multiple wavelengths of 750, 665, 647, and 630 nm. Fresh 90% acetone was used both as a reference and blank solution. A threshold of 0.005 absorbance units (1 cm cuvette) at 750 nm was used to assess turbidity interference. If sample values exceeded this threshold, the centrifugation step was repeated. The concentration of chl-*a* was determined according to Equation 3:

$$\text{Chl-}a \text{ (}\mu\text{g L}^{-1}\text{)} = [(11.85 \cdot D_{665}) - (1.54 \cdot D_{647}) - (0.08 \cdot D_{630}) \nu] / [V \cdot L] \quad \text{Eq. 3}$$

where D is absorbance at specified wavelength, following turbidity correction (absorbance at 750 nm),  $\nu$  is volume of acetone used for extraction (mL), V is volume of filtered seawater sample (L) and L is path length of cuvette (cm) (Jefferey and Humphrey, 1975).

Chl-*a* samples were typically taken as single replicates, and so, no quality check procedure has been in place. Duplicate analyses using the same method typically produce replicate values within 10% of each other. An overview of the chl-*a* data with matching fluorescence observations is summarised in Table 3.

### 2.3 Sampling area

The main sampling area was on and around the Faroe Plateau, including fjords, and a reduced small number of samples were collected in the Norwegian Sea (Table 3). All sampling was conducted onboard R/V Magnus Heinason.

**Table 3.** Summary of chl-*a* sample collection (2002-2019).

<b>Cruise Name</b>	<b>Area</b>	<b>Time of year</b>	<b>#Cruises</b>	<b>#Stations</b>	<b>#Chl-<i>a</i> samples</b>
Biological Oceanography	Faroe Plateau	April/May	17	346	1013
Herring survey and Section N	Norwegian Sea and Faroe Plateau	May	2	32	79
0-group survey	Faroe Plateau and Faroe Bank	June/July	16	370	1038
Fjords	Fjords	August/September	12	48	132
Section K	Faroe Plateau (West)	May/August	3	21	60
Hognaboði	Faroe Plateau (East)	2004-2005	19	20	47
Cod larvae	Faroe Plateau (East)	Spring 2019	3	5	13
<b>Total</b>			<b>72</b>	<b>842</b>	<b>2382</b>

In total, the dataset we have compiled for comparison includes 2382 paired  $F_{chl}$  and *chl-a* measurements, distributed across 842 stations and 72 cruises, carried out in the period 2002-2019. The majority of the data originate from the Biological Oceanography survey in April/May (42.5%) and the 0-group survey in June/July (43.6%). Plots from all cruises with sufficient data to perform a *chl-a* and fluorescence regression are included in Appendix 2.

## 2.4 Selecting data from the FAMRI database

All data from R/V Magnus Heinason are stored in the FAMRI database after quality check. For the purpose of this report, data have been selected from the database from the following tables:

1. KEMI\_KLA\_ALL: Chlorophyll-*a*. Collected during the upcast of the CTD.
2. CTD\_BOTL\_VIEW:  $F_{chl}$  observations (raw, not converted) concurrent to niskin bottle release (max  $F_{chl}$ , min  $F_{chl}$ , average  $F_{chl}$ , standard deviation of  $F_{chl}$ ). Collected during the upcast of the CTD.
3. CTD\_MVIEW: All CTD-profiles (downcast profiles) with a registered  $F_{chl} > 0$ . In this table, the fluorescence in the period 2002-2010 was converted to chlorophyll-*a* (QF\_FLU = 2, see also Appendix 1), whereas after 2010 the data have not been converted (QF\_FLU = 1).
4. EBBAM.CTD\_FLU\_RAW\_VIEW: Unconverted downcast fluorescence data (QF\_FLU = 1) from 2002-2010. A preliminary table, set up in order to access data from 2002-2010, stored in CTD\_MVIEW with OF\_FLU = 2.
5. KEMI\_SI\_ALL: Silicate
6. KEMI\_NI\_ALL: Nitrate

As a criteria for finding the mixed layer depth in CTD-profiles, we selected the uppermost depth at which the temperature difference from a surface reference (average of upper 10 m) exceeded 0.2 °C (Salter et al., 2015).

### 3 Results

The main objective of the present report is to assess the validity of field correction of in situ fluorescence data ( $F_{\text{chl}}$ ) with analytically-determined chl-*a* analysis. The ratio of measured  $F_{\text{chl}}$  to extracted chl-*a* is termed fluorescence yield per chl-*a* ( $F_{\text{chl}} \text{ chl-}a^{-1}$ ). In the present dataset,  $F_{\text{chl}} \text{ chl-}a^{-1}$  ranged from 0.06 to 13.3, with a mean of  $1.05 \pm 0.72$  and median of 0.94 ( $n = 2382$ ). Linear regression analyses of chl-*a* and  $F_{\text{chl}}$  exhibited a wide range of variability between years and for different surveys (Figure 1). The majority of the linear regressions (41 out of 45) exhibited statistically significant ( $P < 0.05$ ) regression coefficients (Table 4). However, the proportion of variance ( $R^2$ ) in chl-*a* explained by  $F_{\text{chl}}$  showed a broad range, with notably higher values observed for the Fjord survey (Figure 2). The data was subsequently subsetted by survey type (Table 3) to further examine variability in  $F_{\text{chl}} \text{ chl-}a^{-1}$  (Figure 3).

There is significant variability in the regression coefficients between  $F_{\text{chl}}$  and chl-*a*, with a range of 2.86 (Table 4; Figure 3). A maximum of 2.92 was recorded in spring of 2010 on the Biological Oceanography survey compared to a minimum of 0.06 in spring 2019. Arithmetic means ( $\pm 1\sigma$ ) for the different survey types were  $1.16 \pm 0.30$  (Fjords),  $0.73 \pm 0.70$  (0-group) and  $0.88 \pm 0.75$  (Biological Oceanography), corresponding to relative standard errors of 26, 96 and 86%, respectively. Standardized t-tests of the arithmetic means between different survey types showed that the regression coefficients from the fjord surveys were significantly higher than those from the 0-group survey ( $P < 0.05$ ), but not the Biological Oceanography survey. The mean regression coefficients from the 0-group and Biological Oceanography surveys were not significantly different from each other. In the majority of cases (9 out of the 14 paired comparisons) regression coefficients from the Biological Oceanography survey were higher than those from the 0-group survey (Figure 4). However, there was a notable shift from 2014 onwards in which summer 0-group regression coefficients were higher than those from the spring Biological Oceanography surveys (4 of the 5 cases). There was also evidence of strong inter-annual variability, with a notable increase in the regression coefficients from the spring Biological Oceanography survey during the period 2008-2010 (Fig. 4).

Fluorescent yield per chl-*a* was examined in relation to water column stratification (Fig. 5). During the Biological Oceanography surveys, the statistical distribution of  $F_{\text{chl}} \text{ chl-}a^{-1}$  is similar in both stratified and unstratified waters, with values  $< 2$  and a peak accounting for 35% of the data at values of 1 (Fig 5a and 5c). A similar distribution is observed for unstratified waters during summer (Fig. 5b). In contrast, stratified waters during the 0-group summer survey show a significant shift to a broader statistical distribution of  $F_{\text{chl}} \text{ chl-}a^{-1}$  with an increasing proportion of higher values (Fig. 5d).

We compared  $F_{\text{chl}} \text{ chl-}a^{-1}$  against several measured environmental factors on the 0-group survey (Fig. 6). The data were partitioned into two subsets, 2002-2015 and 2016-2019, depending on which version of the Seapoint Fluorometer was used to measure  $F_{\text{chl}}$  (Table 1). In the 2002-2015 dataset there is evidence of lower  $F_{\text{chl}} \text{ chl-}a^{-1}$  in association with decreased concentrations of silicate (Fig. 6c) and nitrate (Fig. 6e) and unstratified waters (Fig. 6a, 6g).

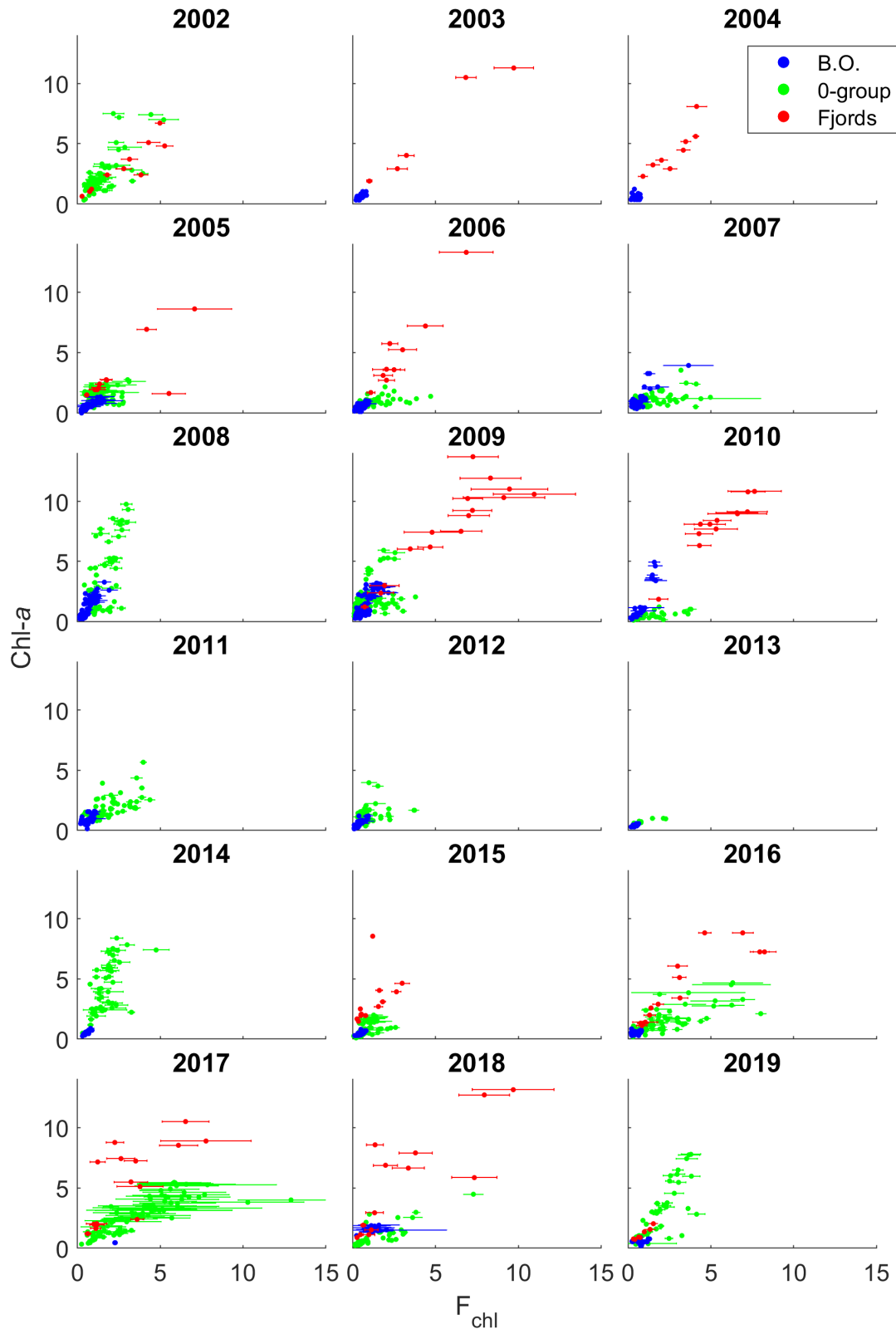


**Figure 1:** Linear regression models of in situ chl-*a* fluorescence ( $F_{\text{chl}}$ ) and extracted chlorophyll concentrations (chl-*a*) from the Biological Oceanography, 0-group and Fjord surveys conducted between 2002-2019. Horizontal bars indicate the standard deviation of the  $F_{\text{chl}}$  measurements calculated by the Seabird software during discrete bottle sampling events.  $F_{\text{chl}} \text{ chl-}a^{-1}$  is the amount of in situ fluorescence ( $F_{\text{chl}}$ ) for a given concentration of extracted chl-*a*, such that a large value of  $a$  (slope) in the linear equation  $y = ax + b$  corresponds to a low  $F_{\text{chl}} \text{ chl-}a^{-1}$ .

The lower fluorescent yield per chl-*a* in unstratified, compared to stratified, waters is also evident in 2016-2019, although to a slightly lesser extent (Fig. 6b, 6h). In contrast, the fluorescent yield per chlorophyll is slightly increased in 2016-2019 in association with higher silicate values (Fig. 6d) and lower nitrate values (Fig. 6f). To further investigate the apparent shifts in nutrient dynamics we subsetting the data to include only those stations from the 0-group survey stations originating from the well-mixed inner shelf (depth <100m). There were no 0-group survey data in 2003 and 2004 and no silicate data 2005-2010 and 2015-2016, resulting in available nitrate and silicate data for eight of the eighteen survey years. Since vertical gradients in nutrient concentrations in mixed waters are negligible, we averaged nutrient concentrations for the 0-group inner shelf stations by year and calculated the corresponding silicate:nitrate ratio. From the available data there is evidence of an increase in silicate:nitrate ratios on the inner shelf after 2014 (Fig. 7a). In 2002 and 2011-2014 silicate:nitrate ratios were always <0.5 (0.16-0.43), in 2017 onwards values were >0.5 (0.57-1.5). A similar averaging technique for  $F_{chl}$  and chl-*a* values was also carried out. There is a statistically significant relationship ( $R^2 = 0.74$ ,  $P=0.003$ ) between fluorescent yield per chl-*a* and silicate:nitrate ratios in the well-mixed shelf stations (Fig. 7b).

Changes in fluorometer sensitivity were addressed by examining fluorescent yield per chl-*a* within a constrained range of chlorophyll concentrations. We selected a range of 1-2  $\mu\text{g L}^{-1}$  which accounts for 26% of the total number of chl-*a* samples.  $F_{chl}$  was normalised to chl-*a* in this range and subsetting by year (Fig. 8). The highest median value of 2.00 was recorded in 2014. The fluorescence yield per chl-*a* is generally higher from the newer sensor (HFSPC) than the old sensor (HFSPA), although high and low values are evident from both sensors. There was no significant relationship between fluorometer sensitivity and age.

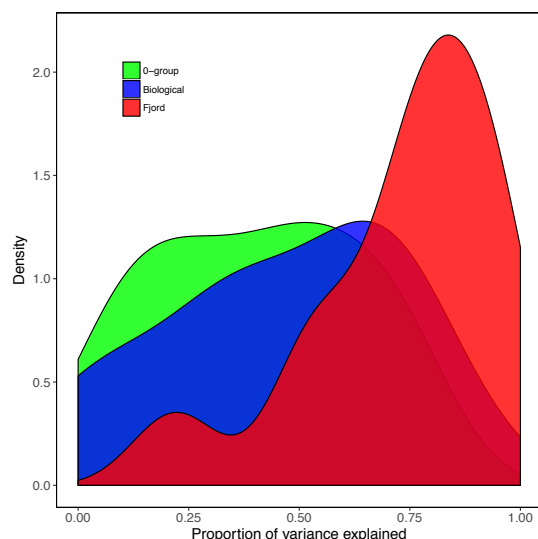


**Figure 2:** Density plot of regression variance ( $R^2$ ) for each of the survey types carried out during the period 2002-2019 (Table 4). Biological Survey ( $n=17$ ), 0-group survey ( $n=16$ ), Fjord survey ( $n=12$ ) (Table 3).

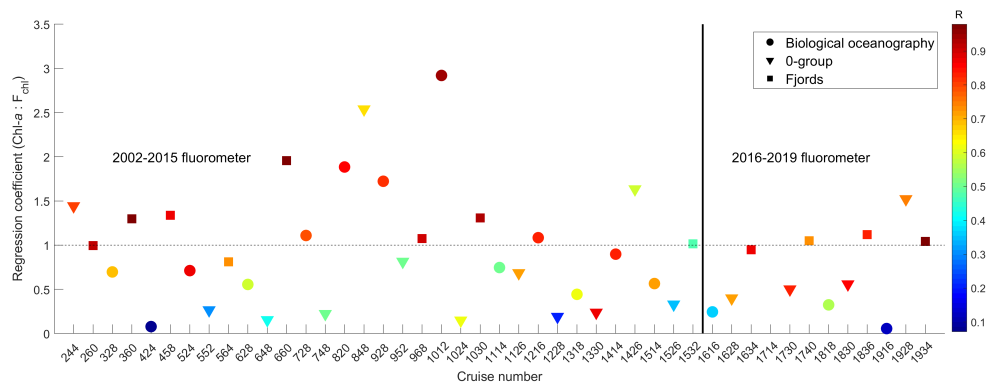


**Figure 3:** Temporal variability in regression coefficients ( $a$  in  $y = ax + b$ ) from the individual linear regression models derived from each survey. Symbols correspond to the different survey types and fill value denotes the proportion of explained variance ( $R^2$ ), cf Table 4

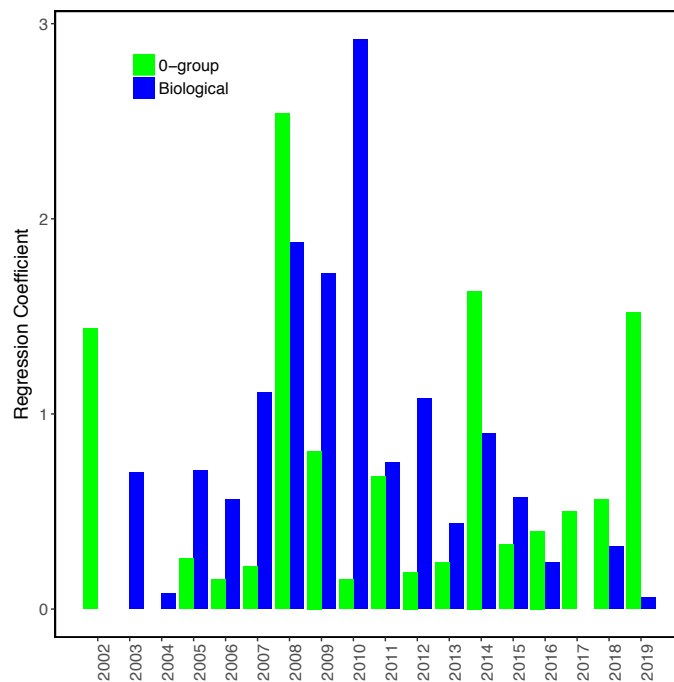


**Figure 4:** Regression coefficients ( $a$  in  $y = ax + b$ ) for the Biological Oceanography and 0-group surveys during the period 2002-2019. Different Seapoint fluorometers were in use 2002-2015 and 2016-2019 (see Table 1). Fluorescent yield per chlorophyll is the amount of in situ fluorescence for a given amount of chlorophyll, such that a large value of  $a$  (slope) corresponds to a low fluorescent yield.

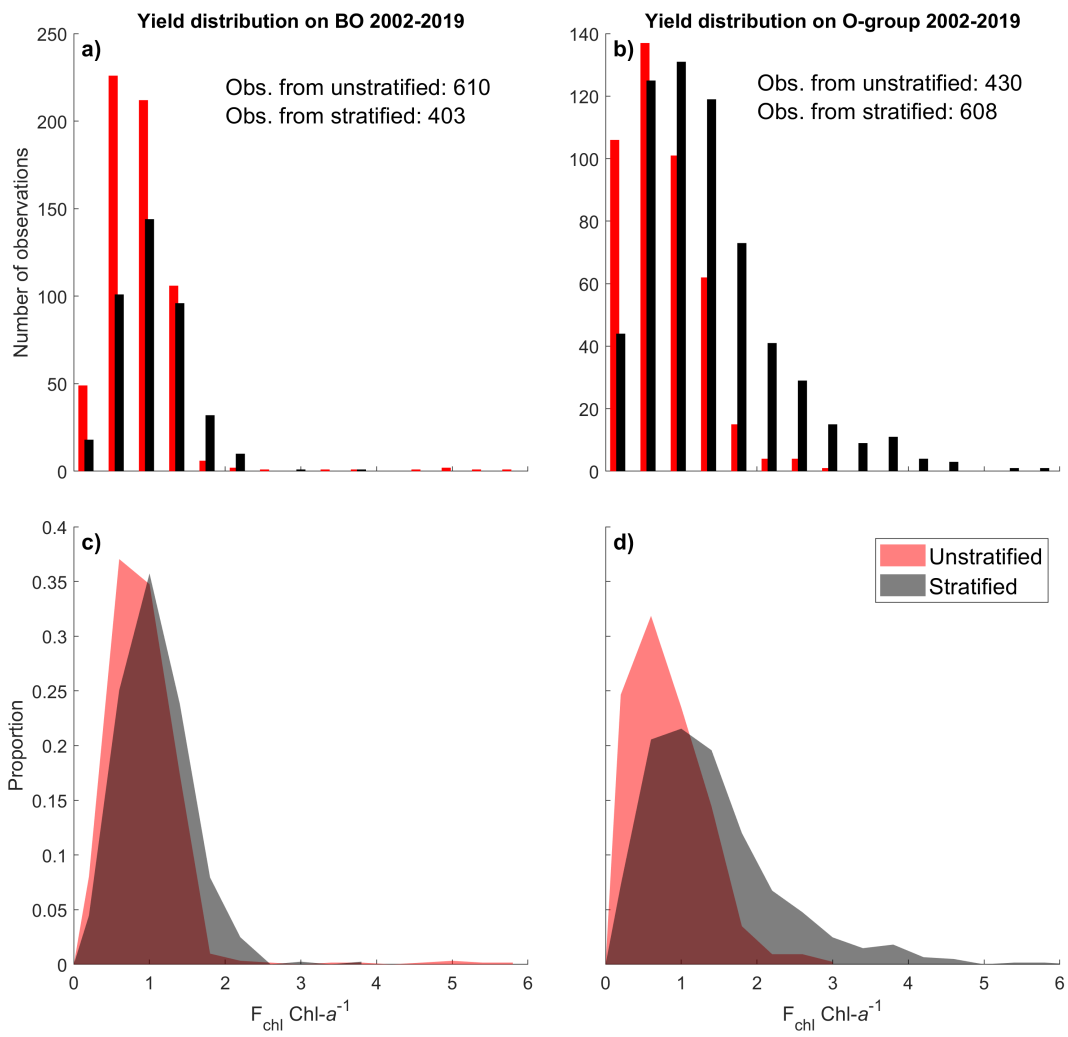


**Figure 5** Number of observations and statistical distribution of fluorescent yield per chl-*a* ( $F_{chl} \text{ chl-}a^{-1}$ ) values on the Biological Oceanography survey (panels a and b) and O-group survey (panels c and d).

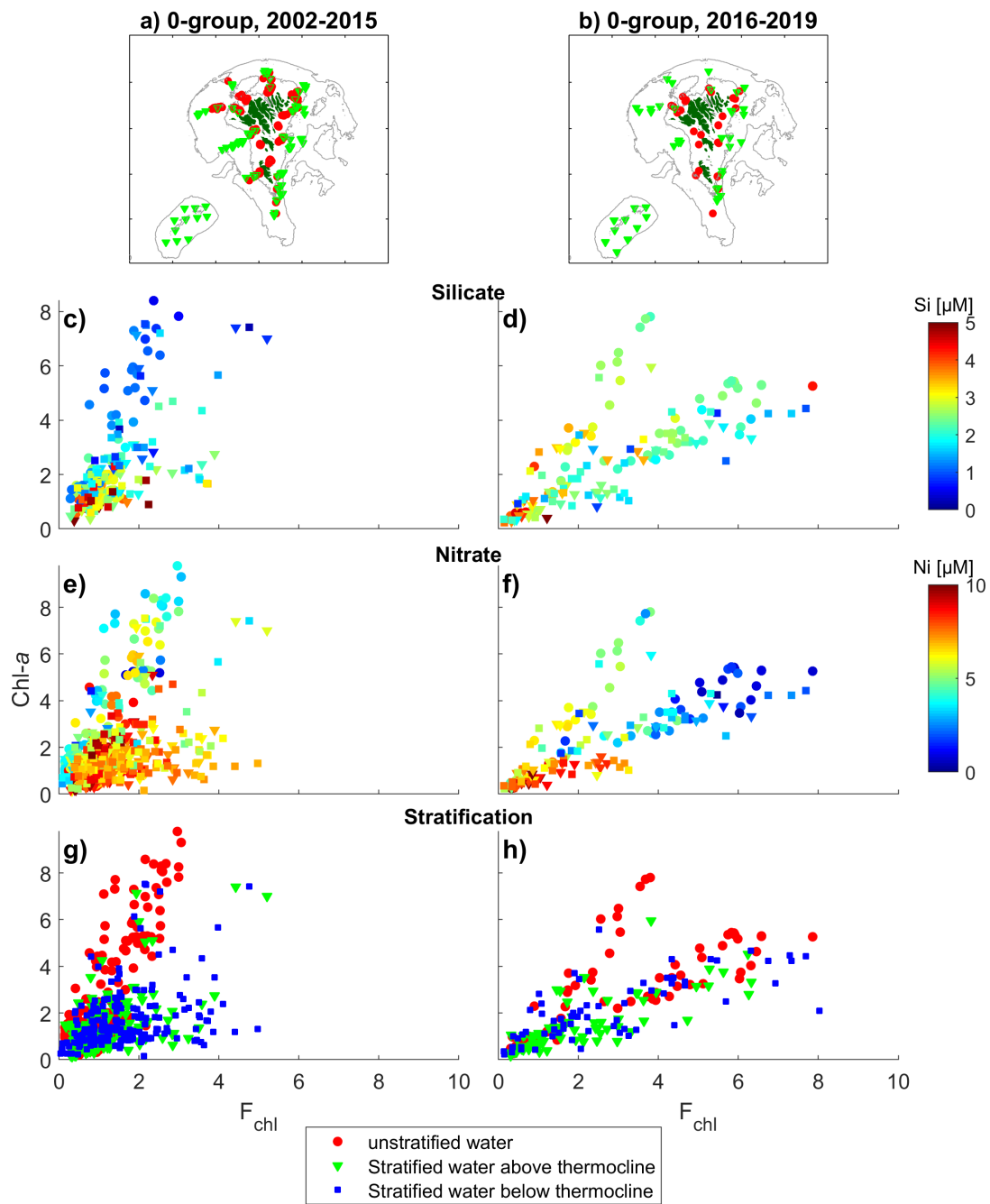


**Figure 6:** Regression models between  $F_{chl}$  and  $chl-a$  from the 0-group survey in relation to concentrations of silicate (panels a-b), nitrate (c-d) and water-column stratification (panels d-h). Panels are separated based on the survey periods that the old (2002-2015) and new (2016-2019) fluorimeters were in use.

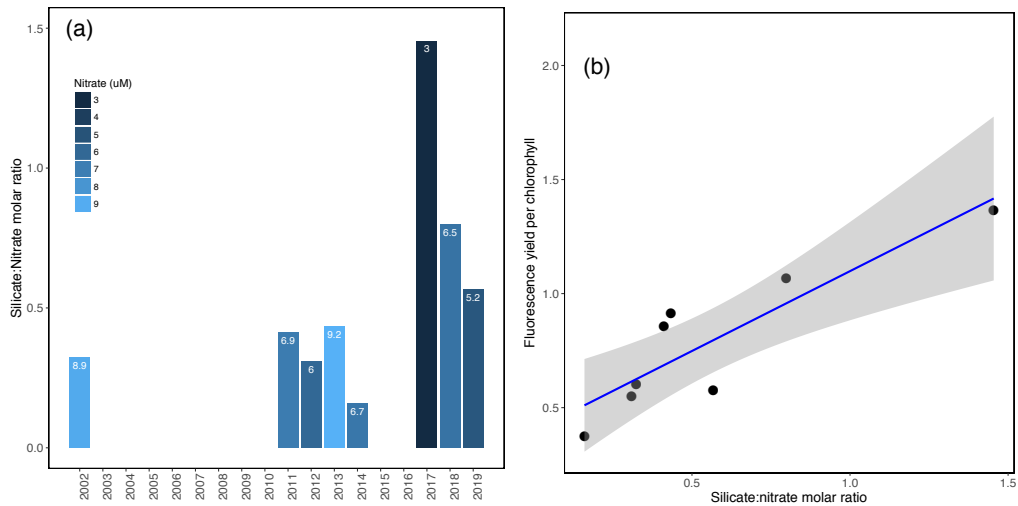


**Figure 7** (a) Inter-annual variability in residual silicate:nitrate concentrations on the inner shelf (<100m) from summer 0-group survey. Values represent means from all depths and stations occupied within a particular survey year. Averaging was carried out after confirming there was no pattern in the vertical distribution of silicate and nitrate, which were fully mixed over the upper 40m. (b) Linear regression model between silicate:nitrate ratios and fluorescence yield per chlorophyll from inner shelf waters occupied during summer 0-group surveys ( $R^2 = 0.74$ ,  $P = 0.003$ ). Molar ratios were calculated from station averages of nutrient concentrations in the upper 40m for a given survey year. Fluorescence yield per chlorophyll is the measured  $F_{chl}$  normalised to extracted chl-*a* concentrations. Values represent station averages from the upper 40m for a given survey year.

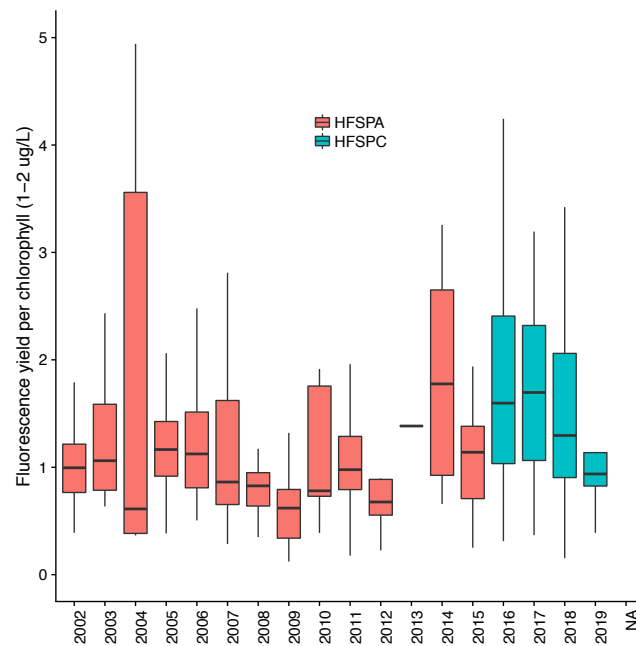


**Figure 8:** Box plot of fluorometer sensitivity as a function of time.  $F_{chl}$  was normalised to extracted chlorophyll-*a* concentrations in the range of 1-2  $\mu\text{g L}^{-1}$ . The median (Q2) is used to describe central tendency and is denoted by the horizontal bar. The upper and lower hinges represent the 75% (Q3) and 25% (Q1) percentiles, respectively. Interquartile range (IQR) is defined as the difference between the 75 and 25% percentiles (Q3-Q1). The lower whisker is the smallest observation  $\geq Q1 - (1.5 * IQR)$ . The upper whisker is the largest observation  $\leq Q3 + (1.5 * IQR)$

**Table 4.** Results from linear regression analyses between Fluorescence and Chlorophyll-*a* from extracted samples. The regression coefficients (*a*), intercept (*b*), sample size (*n*) and proportion of variance explained ( $R^2$ ) are given together with their respective significance levels (*p*). *p*-values >0.05 are printed in red.

Cruise	Survey Type	Season	a	b	n	R <sup>2</sup>	p-value
328	Biological Oceanography	Spring	0.70	0.29	57	0.48	0.00000
424	Biological Oceanography	Spring	0.08	0.48	57	0.01	0.59879
524	Biological Oceanography	Spring	0.71	0.08	71	0.75	0.00000
628	Biological Oceanography	Spring	0.56	0.21	119	0.35	0.00000
728	Biological Oceanography	Spring	1.11	0.19	73	0.61	0.00000
820	Biological Oceanography	Spring	1.88	-0.08	107	0.74	0.00000
928	Biological Oceanography	Spring	1.72	-0.03	114	0.66	0.00000
1012	Biological Oceanography	Spring	2.92	-0.86	31	0.88	0.00000
1114	Biological Oceanography	Spring	0.75	0.42	50	0.26	0.00018
1216	Biological Oceanography	Spring	1.08	0.11	32	0.68	0.00000
1318	Biological Oceanography	Spring	0.44	0.20	19	0.38	0.00502
1414	Biological Oceanography	Spring	0.90	0.01	24	0.69	0.00000
1514	Biological Oceanography	Spring	0.57	0.19	35	0.51	0.00000
1616	Biological Oceanography	Spring	0.24	0.37	47	0.13	0.01256
1818	Biological Oceanography	Spring	0.32	1.16	18	0.32	0.01513
1916	Biological Oceanography	Spring	0.06	0.52	31	0.01	0.52674
244	0-group	Summer	1.44	0.28	63	0.63	0.00000
552	0-group	Summer	0.26	1.09	70	0.09	0.01183
648	0-group	Summer	0.15	0.74	77	0.17	0.00019
748	0-group	Summer	0.22	0.75	90	0.25	0.00000
848	0-group	Summer	2.54	-0.13	56	0.44	0.00000
952	0-group	Summer	0.81	1.23	95	0.25	0.00000
1024	0-group	Summer	0.15	0.26	50	0.38	0.00000
1126	0-group	Summer	0.68	0.61	71	0.51	0.00000

1228	0-group	Summer	0.19	1.10	42	0.04	0.20564
1330	0-group	Summer	0.24	0.46	8	0.76	0.00470
1426	0-group	Summer	1.63	1.48	48	0.34	0.00001
1526	0-group	Summer	0.33	0.70	48	0.12	0.01597
1628	0-group	Summer	0.40	0.62	63	0.52	0.00000
1730	0-group	Summer	0.50	0.91	92	0.69	0.00000
1830	0-group	Summer	0.56	0.26	47	0.73	0.00000
1928	0-group	Summer	1.52	0.06	36	0.56	0.00000
260	Fjords	Autumn	0.99	0.28	11	0.83	0.00010
360	Fjords	Autumn	1.30	0.16	6	0.96	0.00067
458	Fjords	Autumn	1.34	0.74	8	0.75	0.00537
564	Fjords	Autumn	0.81	1.17	10	0.54	0.01585
660	Fjords	Autumn	1.96	-0.51	9	0.94	0.00001
968	Fjords	Autumn	1.07	1.52	15	0.80	0.00001
1030	Fjords	Autumn	1.31	0.90	12	0.87	0.00001
1532	Fjords	Autumn	1.02	1.97	12	0.22	0.11998
1634	Fjords	Autumn	0.95	1.19	14	0.77	0.00004
1740	Fjords	Autumn	1.05	2.16	15	0.53	0.00213
1836	Fjords	Autumn	1.12	2.02	13	0.69	0.00048
1934	Fjords	Autumn	1.04	0.31	7	0.93	0.00039

## 4 Discussion

### 4.1 Recommendations for storage of $F_{chl}$ and extracted chl-*a* values in the FAMRI database.

The principal objective of this technical report was to examine variability of the fluorescent yield per chl-*a* in Faroese waters and provide recommendations for the FAMRI internal database. There is a first order relationship between the concentration of chl-*a* and in situ fluorescence ( $F_{chl}$ ), that is to say that any increase in chl-*a* will result in a corresponding increase in  $F_{chl}$ . However, reliable “field calibration” of fluorometer output with the extracted chl-*a* values requires a fixed fluorescent yield per chl-*a* for a particular dataset. In practice that means that any increases in chl-*a* will result in a proportional increase in  $F_{chl}$  according to an empirical conversion derived from a statistically robust model. Typically such models are assumed to be linear and thus take the form  $y = ax + b$ , where  $y$  is extracted chl-*a* ( $\mu\text{g L}^{-1}$ ) and  $x$  is fluorometer output  $F_{chl}$ . Previous work by FAMRI based on 1204 samples obtained from 37 cruises (2002-2010) established this relationship to be  $\text{chl-}a \text{ } (\mu\text{g L}^{-1}) = 1.23 \cdot (F_{chl}) + 0$  (intercept forced through zero) (Appendix 1).

At the time of writing this technical report we established that the relationship described above has been applied to correct 59% (2002-2010,  $n = 1427$  of 2382) of the  $F_{chl}$  values stored in the FAMRI database. Associated quality codes of QF 1 or 2 have been used, where 1 = raw data and 2 = field-calibrated data. Data entries for the period 2002-2010 were thus stored in one of the following ways: (i) raw  $F_{chl}$  values (OKALFLU) assigned a quality code of 1 (OKALQF = 1), or (ii) field-corrected  $F_{chl}$  values (FLU), equivalent to OKALFLU multiplied by 1.23, assigned a quality code of 2 (QF\_FLU = 2). The remaining 41% (2011-2019) of the  $F_{chl}$  values in the FAMRI database were stored as follows: no values or quality code assignments for raw  $F_{chl}$  (OKALFLU), all values stored as field-corrected  $F_{chl}$  values (FLU) with the raw data quality code (QF\_FLU = 1), i.e. no field correction.

Due to this discrepancy in the database in storing raw data values as either as FLU with QF\_FLU = 1, or OKALFLU with OKALQF = 1, we re-examined the relationships between chl-*a* and  $F_{chl}$  for the entire observation period (2002-2019) in order to assess the validity of field-correcting all data entries. However, our analysis revealed that there is large variation in the regression coefficients of  $F_{chl}$  and chl-*a* between surveys and years that varies by up to one order of magnitude. We conclude from this variation in fluorescent yield per chl-*a* that it is not possible to apply a single empirical conversion factor to generate field-corrected  $F_{chl}$  values in Faroese waters. Based on our findings and recommendations, the FAMRI database has been modified as follows: All field-corrected  $F_{chl}$  values (FLU) collected from 2002-2010 have been replaced with raw  $F_{chl}$  values and assigned a quality code 1 (QF\_FLU = 1). All  $F_{chl}$  values collected from 2011-2019 are maintained as raw  $F_{chl}$  (FLU) with quality code 1 (QF\_FLU = 1). We have recommended that all future  $F_{chl}$  values collected (2020 onwards) should be also be stored as raw  $F_{chl}$  (FLU) and assigned a quality code 1 (QF\_FLU = 1).

It is important to emphasise that these recommendations and actions are primarily designed to preserve traceability in FAMRI’s internal database. We acknowledge that in certain circumstances empirical corrections of raw  $F_{chl}$  with extracted chl-*a* may yield satisfactory results that serve specific research questions. However, as database curators we are unable to

fully envisage the diverse range of scenarios and assumptions encompassing how these datasets might be used in the future. Individual users are able to download both raw  $F_{chl}$  and extracted chl-*a* values, now independently stored in the FAMRI database as FLU and KL\_A, respectively, and apply empirical conversions that address the assumptions and caveats of variable fluorescent yields per chl-*a*.

#### **4.2 Possible explanations for variable fluorescent yields per chl-*a* in Faroese waters**

We observed significant variability in fluorescent yields per chl-*a* in different seasons, e.g. the spring Biological Oceanography survey and summer 0-group survey, that cover similar geographical areas (Appendix 2). In over two-thirds of the cases, fluorescent yields per chl-*a* are lower (higher regression coefficients) in spring than summer. In addition, there is evidence of significant inter-annual variation for a given season, notably a reduction in fluorescent yields per chl-*a* in spring during the period 2007-2010. These seasonal and inter-annual variations can likely be attributed to different phytoplankton communities. It is well established that certain phytoplankton species exhibit different fluorescent yields (Vincent, 1983; Proctor and Roesler, 2010). Taxonomic variability arises in part due to differential pigment-protein complexes in photosynthetic structures (photosystems I and II). The majority of chlorophyll fluorescence from phytoplankton cells originates from chl-*a* bound to protein complexes in photosystem II (Falkowski and Raven, 1997). In contrast, chl-*a* bound in photosystem I exhibits minimal in situ fluorescence. The proportion of “fluorescently-inactive” chl-*a* contained in photosystem I varies between taxonomic groups. Diatoms are observed to have comparatively low fluorescent yields (Vincent, 1983), suggesting that the increase in the slope of fluorescence versus chl-*a* observed during 2007-2010 could be indicative of enhanced diatom-derived biomass during the Biological Oceanography survey in spring.

Although we do not have supporting phytoplankton count data to validate the suggestion that lower fluorescent yields can be linked to diatom biomass, corresponding nutrient concentrations appear to support this conclusion since lower fluorescent yields are associated with enhanced drawdown of silicate in summer. Interestingly, we observed a switch in 2014 in the seasonal differences between fluorescent yields. From 2005-2013, the fluorescent yield was lower in spring than summer (90% of cases), whereas from 2014-2019 fluorescent yields were lower in summer (80% of the cases). This switch appears to be associated with changes in nutrient stoichiometry as there is a notable increase in the silicate:nitrate ratio during the same period. For those years where data is available, there is a positive correlation between silicate:nitrate ratios and fluorescent yield. These results further demonstrate the potential impact of phytoplankton community structure, and in particular diatom biomass, on fluorescent yields. Additionally, the available data appears to indicate a recent regime shift towards phytoplankton communities comprised of a greater proportion of non-diatom biomass. It is worth stressing these results remain somewhat speculative in the absence of corresponding phytoplankton count data and full calibration history of the fluorometers. Nevertheless, these findings highlight the potential for shifts in phytoplankton community dynamics that can partly explain the observed variability in fluorescent yields.

We also examined the degree of water-column stratification as a potential factor controlling the variability of fluorescent yield within the dataset. Samples originating from unstratified shelf waters are characterised by a lower fluorescent yield than those from stratified waters. Stratification has important implications for the ambient light environment experienced by phytoplankton cells. Since photosynthetically active radiation (PAR) attenuates over depth, phytoplankton constrained in a shallow stratified layer at the surface will experience higher average irradiance than those in waters mixed over greater depths. Photophysiological mechanisms in phytoplankton, including both photochemical quenching and non-photochemical quenching (NPQ), have evolved to deal with rapidly fluctuating light conditions (Falkowski and Kiefer, 1985; Müller et al., 2001), with NPQ exerting a particularly strong effect on the degree of absorbed photon energy resulting in fluorescence (Babin, 2008). In field studies, the impact of variations in NPQ on fluorescent yield have been observed over a wide range of spatial scales (Browning et al., 2014; Carberry et al., 2019; Moiseeva et al., 2019). Vertical patterns are also evident with maximal quenching of  $F_{chl}$  typically observed at the surface and decreasing exponentially with depth as a function of irradiance (Cullen et al., 1992; Sackmann et al., 2008). Strong diurnal patterns of enhanced NPQ and associated reductions in  $F_{chl}$  are consistently observed, with highest NPQ occurring at noon in line with maximum irradiance (Falkowski and Kolber, 1995; Xing et al., 2012). This could imply some of the observed variability in fluorescent yield may simply derive from the time of day sampling is conducted. However, interpreting the net impact of NPQ on fluorescent yield per chl-*a* as a direct consequence of stratification is challenging. Nutrient dynamics and phytoplankton community structure are also influenced by stratification and may impact fluorescent yield (as previously described) independent of the photophysiological response of individual cells.

The discussion above highlights the potential pitfalls in the application of a single empirical conversion for fluorescence-derived estimates of phytoplankton-derived chlorophyll.

### **4.3 Fluorometer performance**

During the preparation of this technical report we attempted to document the calibration history of the two different fluorometers used by FAMRI. We ascertained that the “old fluorometer” (HFSPA #2348), in use from 2002-2015, was calibrated once at the factory upon delivery in 2002. The “new fluorometer” (HFSPC #SCF3737) has been factory calibrated at the point of delivery (2016) and again in December 2019. The second factory calibration did not reveal any offset. The manufacturers (Seapoint) state that time-dependent reductions in fluorometer sensitivity can occur due to scratched optical surfaces and reductions in LED efficiency. It is reasonable to assume therefore that observed changes in fluorescent yield could also be linked to variable fluorometer performance as a function of age. We examined time-dependent changes in fluorescent output for a given chlorophyll range (1-2  $\mu\text{g L}^{-1}$ ), but did not observe any notable reduction in sensitivity. Although the new fluorometer (2016 onwards) is characterised by comparatively higher fluorescent yields (Figure 8) this increase was already evident in 2014 and 2015. Since these increases were observed at the end of the lifetime of the old fluorometer, it would suggest that the differences are primarily related to changing field conditions described in section 4.2, rather than a stepwise improvement in sensitivity associated with the new fluorometer. However, changes

in the sensitivity of fluorometers could clearly impact variability in fluorescent yields and regular factory calibrations are necessary to avoid these potential artefacts.

We recommend that from 2020 onwards, the fluorometers used by Havstovan are returned to the factory for calibration every third year. The purpose of this calibration is to ensure that there are no major problems associated with scratched sensor surfaces and LED output. We do not believe it is necessary to calibrate more frequently than this due to the challenges in finding appropriate primary standards for fluorescence sensors (see Introduction) and the considerable challenges linking fluorescence to chlorophyll-derived biomass.

One issue that remains unresolved at the time of writing is an understanding of the factors that govern the degree of standard deviation on fluorescence measurements. The continuous fluorescence profiles archived in the FAMRI database originate mainly from the downcast of the CTD. However, the fluorescence values used for comparison with extracted chlorophyll-*a* samples are taken from the upcast when Niskin bottles are closed. The Seabird software averages hundreds of fluorescence measurements at a discrete depth around the time the Niskin bottle is closed for collecting water samples, resulting in multiple measurements at the “bottle-depth” and an associated standard deviation. There are large and unexplained differences in the magnitude of this standard deviation between years (cf. 2017 and 2019 in Fig. 1). It is possible that higher values are associated with fine-scale variations in phytoplankton biomass encountered at transition layers, or due to physical disturbance caused by the rosette itself. Although the causes of this variation remain unclear, it is something that will be observed carefully during future deployments.

## **5 Conclusions**

The main objective of this report was to examine the variability in fluorescent yield per chl-*a* from the biological surveys conducted in Faroese waters during the period 2002-2019. We observed significant variability in fluorescent yield covering several orders of magnitude (0.06 - 13.3), manifested in regression coefficients that ranged from 0.06 – 2.92. Based on this variability we conclude that it is ill-advised to use a single empirical conversion to produce field-corrected fluorescence datasets. Consequently, the FAMRI database has been modified to store all fluorescence data as raw in situ fluorescence values. We recommend that all future fluorescence data should be stored in a similar way. Furthermore we suggest that fluorometers should be returned to the manufacturer (Seapoint) for factory calibration every third year to carefully monitor variations in sensitivity and analytical performance of the fluorometers

## 6. References

- Álvarez, E., Nogueira, E., and López-Urrutia, Á. (2017). In vivo single-cell fluorescence and size scaling of phytoplankton chlorophyll content. *Appl. Environ. Microbiol.* 83. doi:10.1128/AEM.03317-16.
- Babin, M. (2008). “Phytoplankton Fluorescence: Theory, Current Literature and in situ Measurement,” in *Real-Time Coastal Observing Systems for Marine Ecosystem Dynamics and Harmful Algal Blooms: Theory, Instrumentation and Modelling*, eds. M. Babin, C. S. Roesler, and J. J. Cullen (Paris: UNESCO), 237–280.
- Behrenfeld, M. J., O’Malley, R. T., Siegel, D. A., McClain, C. R., Sarmiento, J. L., Feldman, G. C., et al. (2006). Climate-driven trends in contemporary ocean productivity. *Nature* 444, 752–755.
- Billet, D. S., Bett, B. J., Rice, A. L., Thurston, M. H., Galéron, J., Sibuet, M., et al. (2001). Long-term change in the megabenthos of the Porcupine Abyssal Plain (NE Atlantic), High resolution temporal and spatial study of the benthic biology and geochemistry of a North-Eastern Atlantic abyssal locality (BENGAL). *Prog. Oceanogr.* 50, 325–348.
- Browning, T. J., Bouman, H. A., and Moore, C. M. (2014). Satellite-detected fluorescence: Decoupling nonphotochemical quenching from iron stress signals in the South Atlantic and Southern Ocean. *Global Biogeochem. Cycles* 28, 510–524.
- Carberry, L., Roesler, C., and Drapeau, S. (2019). Correcting in situ chlorophyll fluorescence time-series observations for nonphotochemical quenching and tidal variability reveals nonconservative phytoplankton variability in coastal waters. *Limnol. Oceanogr. Methods* 17, 462–473. doi:10.1002/lom3.10325.
- Collins, D. J., Kiefer, D. A., Soohoo, J. B., and McDermid, I. S. (1985). The role of reabsorption in the spectral distribution of phytoplankton fluorescence emission. *Deep Sea Res.* 32, 983–1003.
- Cullen, J. J., Yang, X., and MacIntyre, H. L. (1992). “Nutrient limitation of marine photosynthesis,” in *Primary productivity and biogeochemical cycles in the sea.*, eds. P. G. Falkowski and A. D. Woodhead (New York), 70–88.
- Debes, H. H., and Eliassen, K. (2006). Seasonal abundance, reproduction and development of four key copepod species on the Faroe shelf. *Mar. Biol. Res.* 2, 249–259.
- Debes, H. H., Eliassen, K., and Gaard, E. (2008). Seasonal variability in copepod ingestion and egg production on the Faroe shelf. *Hydrobiologia* 600, 247–265.
- Falkowski, P. G., and Kolber, Z. A. (1995). Variations in chlorophyll fluorescence yields in phytoplankton in the world oceans. *Funct. Plant Biol.* 22, 341–355.
- Falkowski, P. G., and Raven, J. A. (1997). *Aquatic Photosynthesis*. Malden, Massachusetts: Blackwell Sciences.
- Falkowski, P., and Kiefer, D. A. (1985). Chlorophyll a fluorescence in phytoplankton: relationship to photosynthesis and biomass. *J. Plankton Res.* 7, 715–731.
- Field, C. B., Behrenfeld, M. J., Randerson, J. T., and Falkowski, P. G. (1998). Primary production of the biosphere: Integrating terrestrial and oceanic components. *Science* (80-. ). 281, 237–240.
- Gaard, E. (1999). Zooplankton community structure in relation to its biological and physical

- environment on the Faroe Shelf, 1989-1997. *J. Plankton Res.* 21, 1133–1152.
- Gaard, E. (2000). Seasonal abundance and development of *Calanus finmarchicus* in relation to phytoplankton and hydrography on the Faroe Shelf. *ICES J. Mar. Sci.* 57, 1605–1611.
- Gaard, E., Hansen, B., Olsen, B., and Reinaert, J. (2002). “Ecological Features and Recent Trends in the Physical Environment, Plankton, Fish Stocks, and Seabirds in the Faroe Shelf Ecosystem,” in *Large Marine Ecosystems in the North Atlantic*, eds. K. Sherman and H. R. Skjoldal (Amsterdam: Elsevier), 245–265.
- Gaard, E., and Steingrund, P. (2001). Reproduction of Faroe Plateau Cod: Spawning Grounds, Egg Advection and Larval Feeding. *Fróðskaparrit* 48, 87–103.
- Geider, R. J. (1987). Light and temperature dependence of the carbon to chlorophyll a ration in microalgae and cyanobacteria: Implications for physiology and growth of phytoplankton. *New Phytol.* 106, 1–34. doi:<https://doi.org/10.1111/j.1469-8137.1987.tb04788.x>.
- Geider, R. J., Greene, R. M., Kolber, Z., Macintyre, H.L., and Falkowski, P. G. (1993a). Fluorescence assessment of the maximum quantum efficiency of photosynthesis in the western North Atlantic. *Deep Sea Res. Part I* 40, 1205–1224.
- Geider, R. J., La Roche, J., Greene, R. M., and Olaizola, M. (1993b). Response of the photosynthetic apparatus of *phaeodactylum-tricornutum* (bacillariophyceae) to nitrate, phosphate, or iron starvation. *J. Phycol.* 29, 755–766.
- Geider, R. J., MacIntyre, H. L., and Kana, T. M. (1998). A dynamic regulatory model of phytoplanktonic acclimation to light, nutrients, and temperature. *Limnol. Oceanogr.* 43, 679–694. doi:<https://doi.org/10.4319/lo.1998.43.4.0679>.
- Horton, P., Ruban, A. V., and Walters, R. G. (1996). Regulation of light harvesting in green plants. *Annu. Rev. Plant Physiol.* 47, 655–684.
- Huot, Y., and Babin, M. (2010). “Overview of fluorescence protocols: Theory, basic concepts and practice,” in *Chlorophyll a fluorescence in aquatic sciences: Methods and applications*, eds. D. J. Suggett, M. A. Borowitzka, and O. Prášil (Springer Netherlands), 31–74.
- Jacobsen, S., Gaard, E., Hátun, H., Steingrund, P., Larsen, K. M. H., Reinert, J., et al. (2019). Environmentally Driven Ecological Fluctuations on the Faroe Shelf Revealed by Fish Juvenile Surveys. *Front. Mar. Sci.* doi:<https://doi.org/10.3389/fmars.2019.00559>.
- Jeffrey, S. W., and Humphrey, G. F. (1975). New spectrophotometric equations for determining chlorophyll a, b, c1 and c2 in higher plants, algae and natural phytoplankton. *Biochem. und Physiol. der Pflanze* 176, 191–194.
- Kirk, J. T. . (1994). *Light and Photosynthesis in Aquatic Ecosystems*. 2nd Edition. Cambridge: Cambridge University Press.
- Kolber, Z., Zehr, J., and Falkowski, P. (1988). Effects of growth irradiance and nitrogen limitation on photosynthetic energy conversion in photosystem II. *Plant Physiol.* 88, 923–929.
- Kruskopf, M., and Flynn, K. J. (2006). Chlorophyll content and fluorescence responses cannot be used to gauge reliably phytoplankton biomass, nutrient status or growth rate. *New Phytol.* 169, 525–536.
- Lima, I. D., Lam, P. J., and Doney, S. C. (2014). Dynamics of particulate organic carbon flux

- in a global ocean model. *Biogeosciences* 11, 1177–1198.
- López-Sandoval, D. C., Fernández, A., and Marañón, E. (2011). Dissolved and particulate primary production along a longitudinal gradient in the Mediterranean Sea. *Biogeosciences* 8, 815–825. doi:10.5194/bg-8-815-2011.
- Lorenzen, C. J. (1966). A method for the continuous measurement of in vivo chlorophyll concentration. *Deep Sea Res. Oceanogr. Abstr.* 13, 223–227.
- Moiseeva, N. A., Churilova, T. Y., Efimova, T. V., Krivenko, O. V., and Matorin, D. N. (2019). Fluorescence of Chlorophyll a during Seasonal Water Stratification in the Black Sea. *Phys. Oceanogr.* 26, 425–437.
- Moore, C. M., Suggett, D. J., Hickman, A. E., Kim, Y. N., Tweddle, J. F., Sharples, J., et al. (2006). Phytoplankton photoacclimation and photoadaptation in response to environmental gradients in a shelf sea. *Limnol. Oceanogr.* 51, 936–949.
- Müller, P., Li, X. P., and Niyogi, K. K. (2001). Non-Photochemical Quenching: A Response to Excess Light Energy. *Plant Physiol.* 125, 1558–1556.
- Parsons, T. R., Maita, Y., and Lalli, C. M. (1984). *A Manual of Chemical and Biological Methods of Seawater Analysis*. 1st edition. Oxford: Pergamon Press.
- Proctor, C. W., and Roesler, C. S. (2010). New insights on obtaining phytoplankton concentration and composition from in-situ multispectral Chlorophyll fluorescence. *Limnol. Oceanogr. Methods* 8, 695–708.
- Rembauville, M., Blain, S., Caparros, J., and Salter, I. (2016). Particulate matter stoichiometry driven by microplankton community structure in summer in the Indian sector of the Southern Ocean. *Limnol. Oceanogr.* doi:10.1002/lno.10291.
- Riemann, B., Simonsen, P., and Stensgaard, L. (1989). The carbon and chlorophyll content of phytoplankton from various nutrient regimes. *J. Plankton Res.* 11, 1037–1045. doi:https://doi.org/10.1093/plankt/11.5.1037.
- Ruhl, H. A., and Smith, K. L. (2004). Shifts in Deep-Sea Community Structure Linked to Climate and Food Supply. *Science (80-. )*. 305, 513–515.
- Sackmann, B., Perry, B. M., and Eriksen, C. (2008). Seaglider observations of variability in daytime fluorescence quenching of chlorophyll-a in Northeastern Pacific coastal waters. *Biogeosciences* 5, 2839–2865.
- Salter, I., Galand, P. E., Fagervold, S. K., Lebaron, P., Obernosterer, I., Oliver, M. J., et al. (2015). Seasonal dynamics of active SAR11 ecotypes in the oligotrophic Northwest Mediterranean Sea. *ISME J.* 9, 347–360. doi:10.1038/ismej.2014.129.
- Sarmiento, J. L., Toggweiler, J. R., Najjar, R., Webb, D. J., Jenkins, W. J., Wunsch, C., et al. (1988). Ocean Carbon-Cycle Dynamics and Atmospheric pCO<sub>2</sub>. *Philos. Trans. R. Soc. London A Math. Phys. Eng. Sci.* 325, 3–21.
- Sarmiento, J. L., and Toggweiler, J. R. (1984). A new model for the role of oceans in determining atmospheric pCO<sub>2</sub>. *Nature* 308, 621–624.
- Schrader, P. S., Milligan, A. J., and Behrenfeld, M. J. (2011). Surplus photosynthetic antennae complexes underlie diagnostics of iron limitation in a cyanobacterium. *PLoS One* 6, e18753.
- Sosik, H. M., and Mitchell, B. G. (1991). Absorption, fluorescence, and quantum yield for

- growth in nitrogen limited *Dunaliella tertiolecta*. *Limnol. Oceanogr.* 36, 910–921.
- Steingrund, P., and Gaard, E. (2005). Relationship between phytoplankton production and cod production on the Faroe Shelf. *ICES J. Mar. Sci.* 62, 163–176.
- Strzepek, R. F., and Harrison, P. J. (2004). Photosynthetic architecture differs in coastal and oceanic diatoms. *Nature* 431, 689–692.
- Vincent, W. F. (1983). Fluorescence properties of the freshwater phytoplankton: Three algal classes compared. *Br. Phycol. J.* 18, 5–21.
- Xing, X., Claustre, H., Blain, S., D’Ortenzio, F., Antoine, D., Ras, J., et al. (2012). Quenching correction for in vivo chlorophyll fluorescence acquired by autonomous platforms: A case study with instrumented elephant seals in the Kerguelen region (Southern Ocean). *Limnol. Oceanogr. Methods* 10, 483–495.
- Yacobi, Y. Z., and Zohary, T. (2010). Carbon:chlorophyll a ratio, assimilation numbers and turnover times of Lake Kinneret phytoplankton. *Hydrobiologia* 639, 185–196.

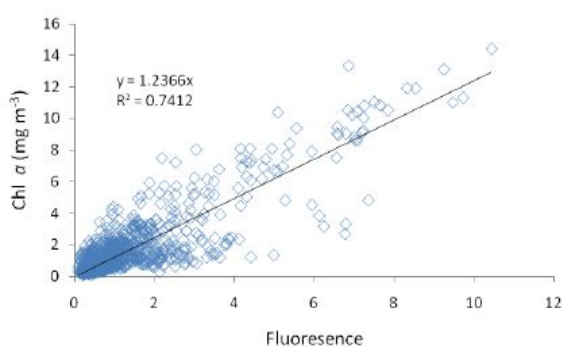
## Appendix 1

### CTD fluorescence calibration for 2002 – 2010

The Seapoint Chlorophyll Fluorometer was calibrated from the linear relation between observed fluorescence and Chl *a* concentration in a total of 1204 samples obtained on 37 cruises from 2002 to 2011 (Fig. 1), giving the relation:

$$\text{Chl. A } (\mu\text{g/l}) = 1.2 \times \text{fluorescence}$$

The instrument description states that the fluoremeter is very stable, with very little change in sensitivity over time. Some decrease in sensitivity can be expected after extended use due to decreased output of the lamps (about a 10% decrease in output after 5000 hours of operation) and scratched window surfaces. Furthermore we did not observe a trend in the calibration constant over time.



Year	n	a	r <sup>2</sup>
2010	101	1.2876	0.8115
2009	267	1.3847	0.6484
2008	115	1.7787	0.7494
2007	188	1.1993	0.8033
2006	140	1.2757	0.7404
2005	124	1.0319	0.6828
2004	66	1.4804	0.8769
2003	124	1.0806	0.7526
2002	79	1.3122	0.5154
All years	1204	1.2366	0.7412

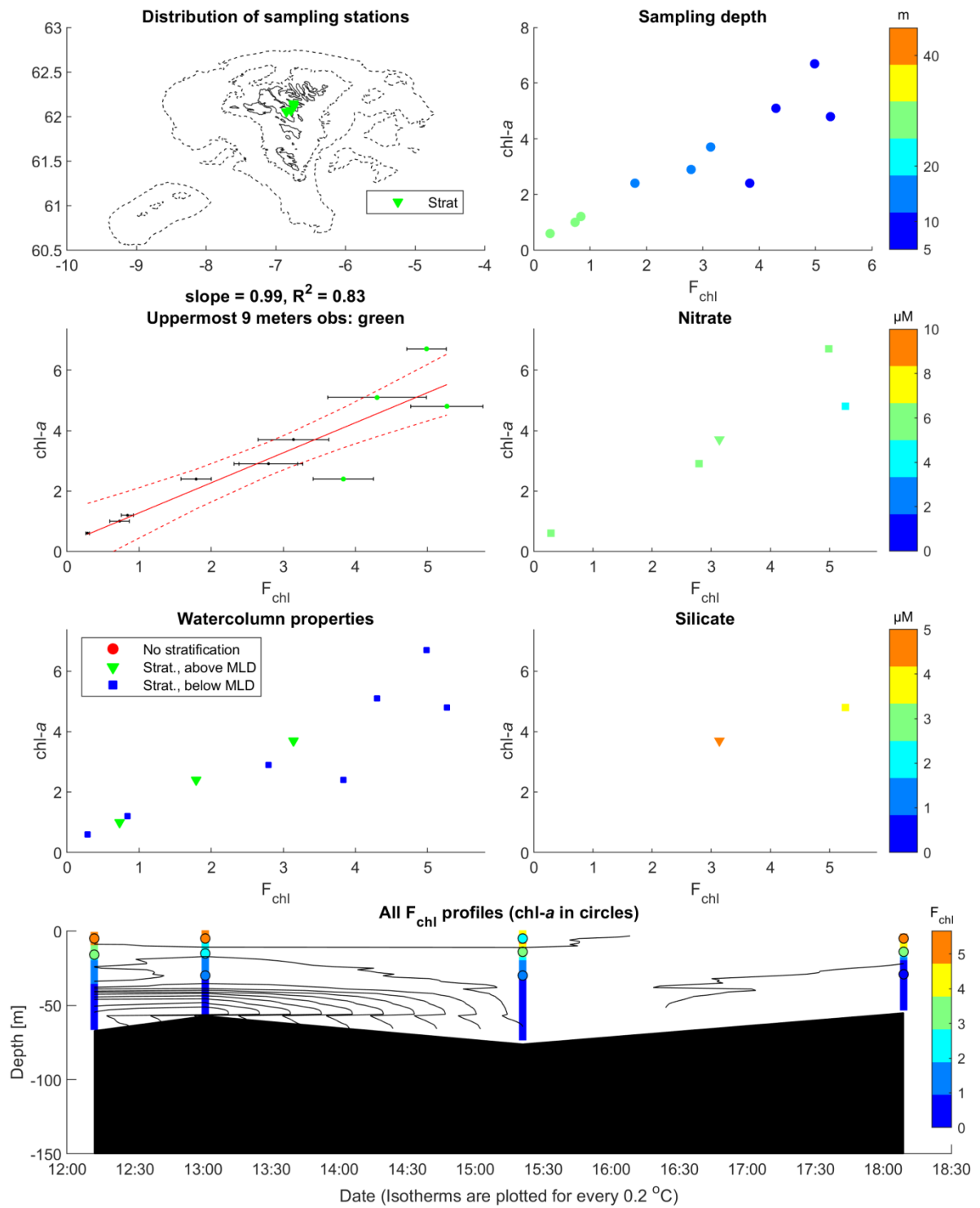
However, the amount of light emitted as fluorescence by the phytoplankton is dependent on the photo-physiological characteristics of the plankton. Thus there most probably is some variation in the relation between emitted fluorescence and the Chl *a* concentration, in time and space.

In addition there are various substances (e.g. colored dissolved organic matter, sand and bubbles) in seawater which influence the fluorescence measurements. Thus calculated Chl *a* concentrations from fluorescence measurements should be treated with caution.

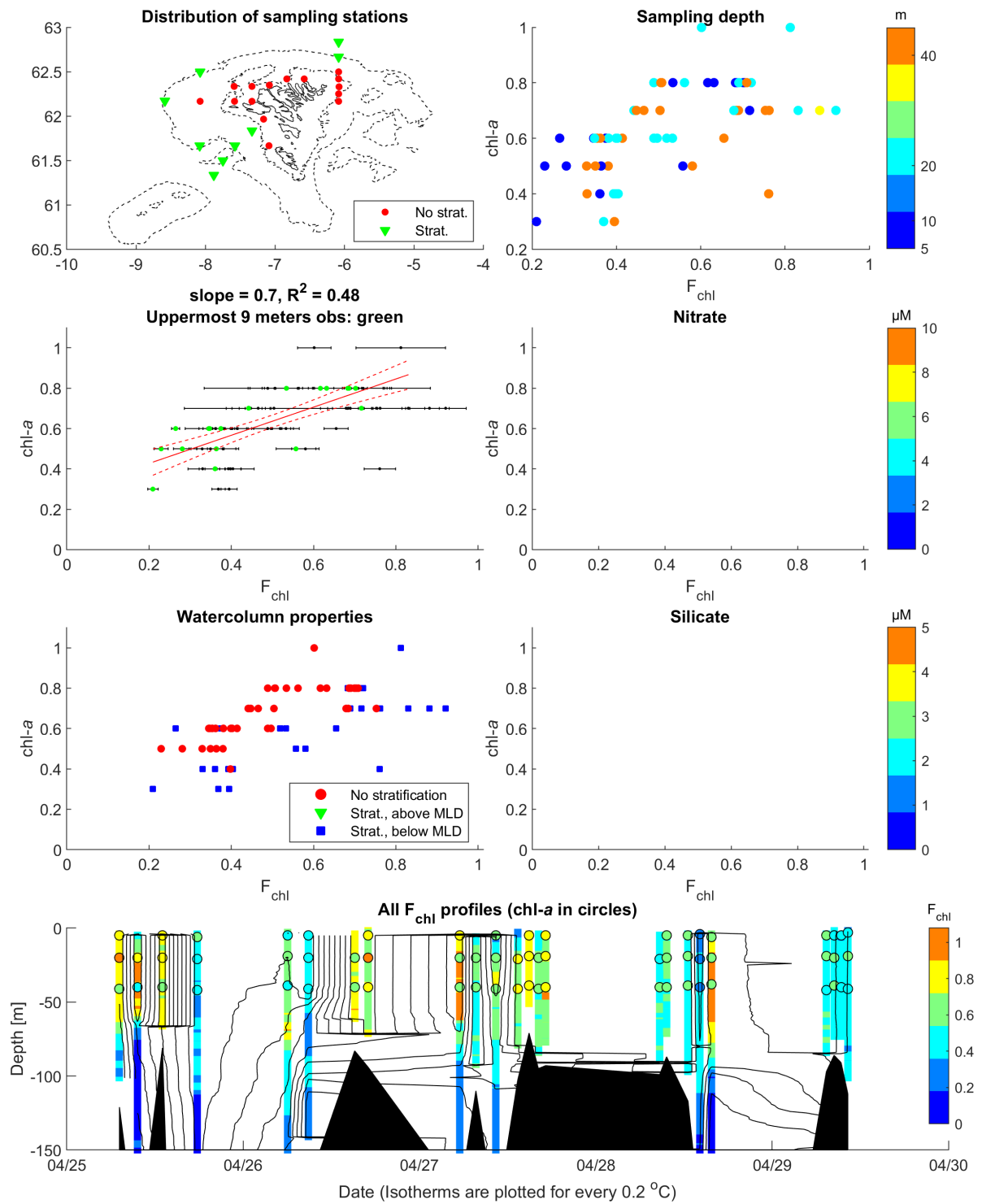
Gunnvør á Norði, Maj 2011



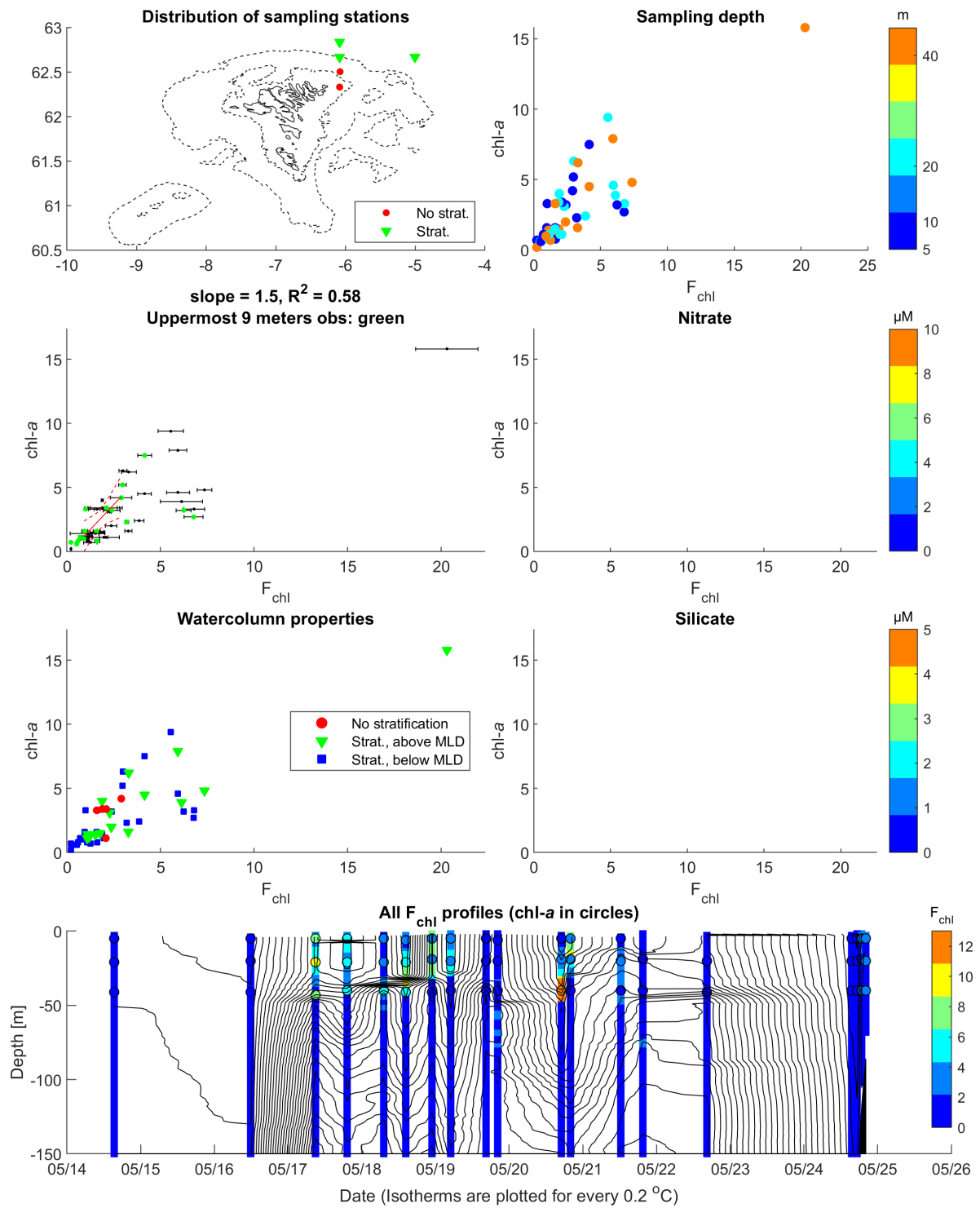
**Cruise 260, Fjords, 3/9-2002**



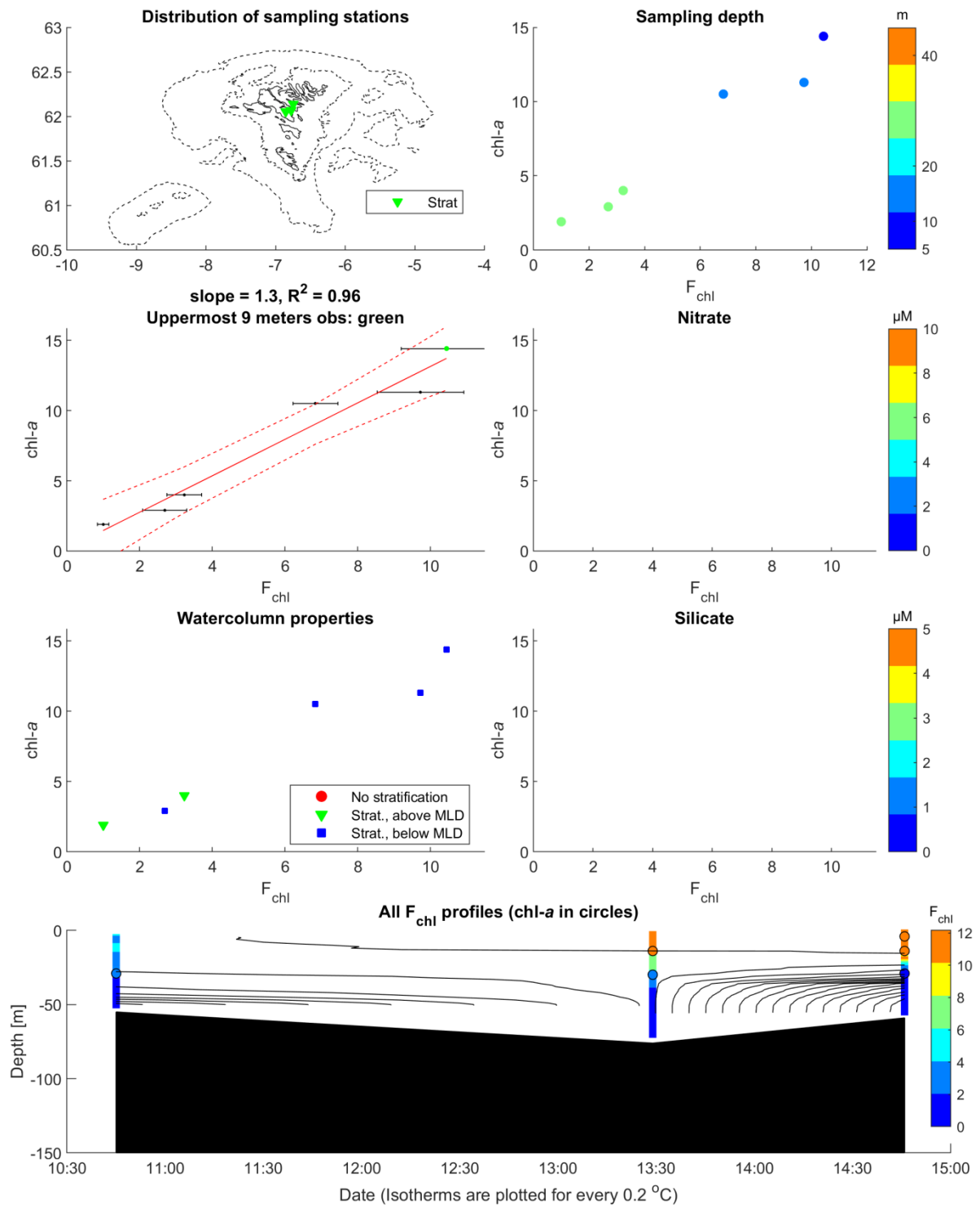
Cruise 328, Biological oceanography and section N, 25/4-29/4, 2003



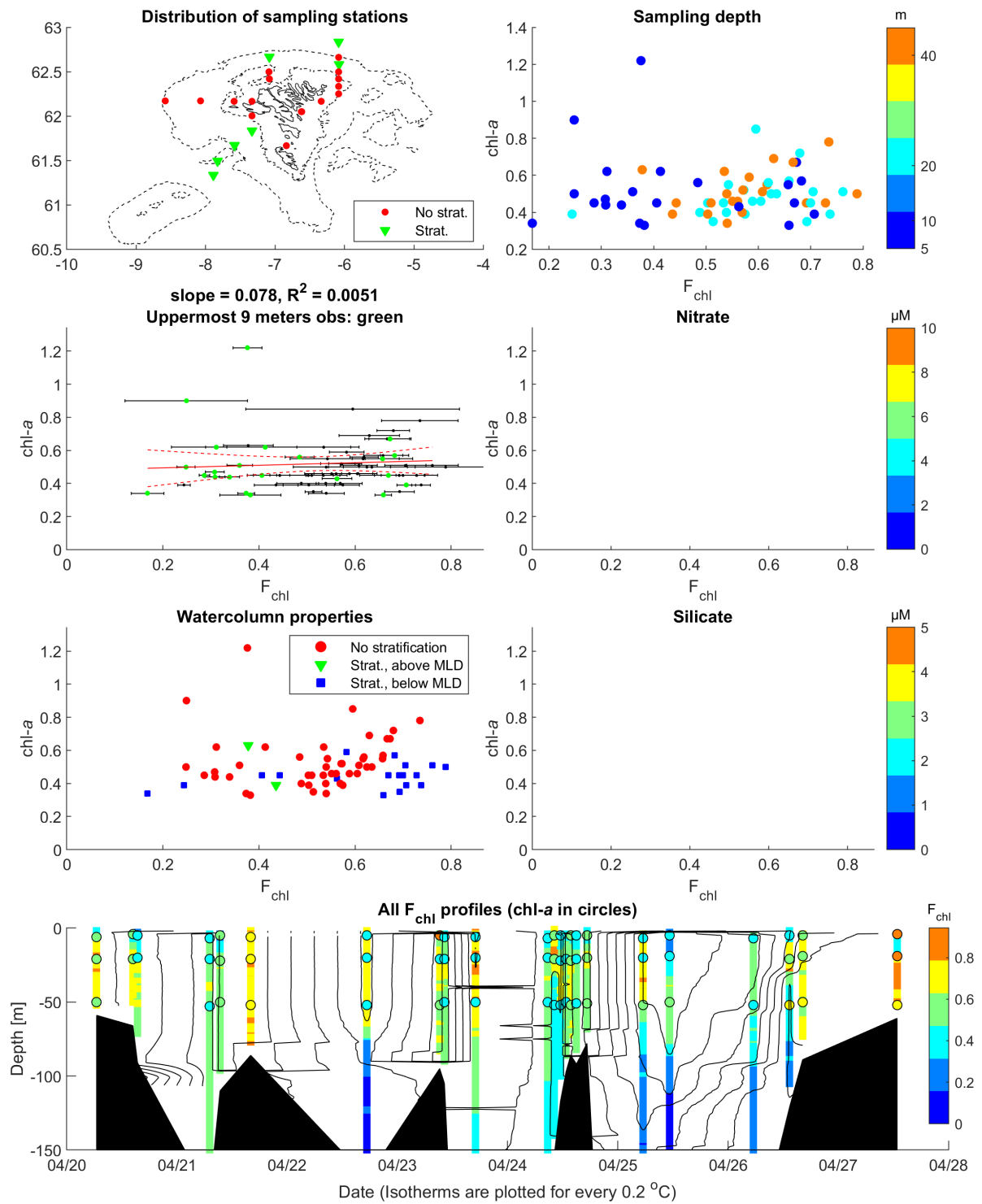
Cruise 332, Herring and section N, 14/5-24/5, 2003



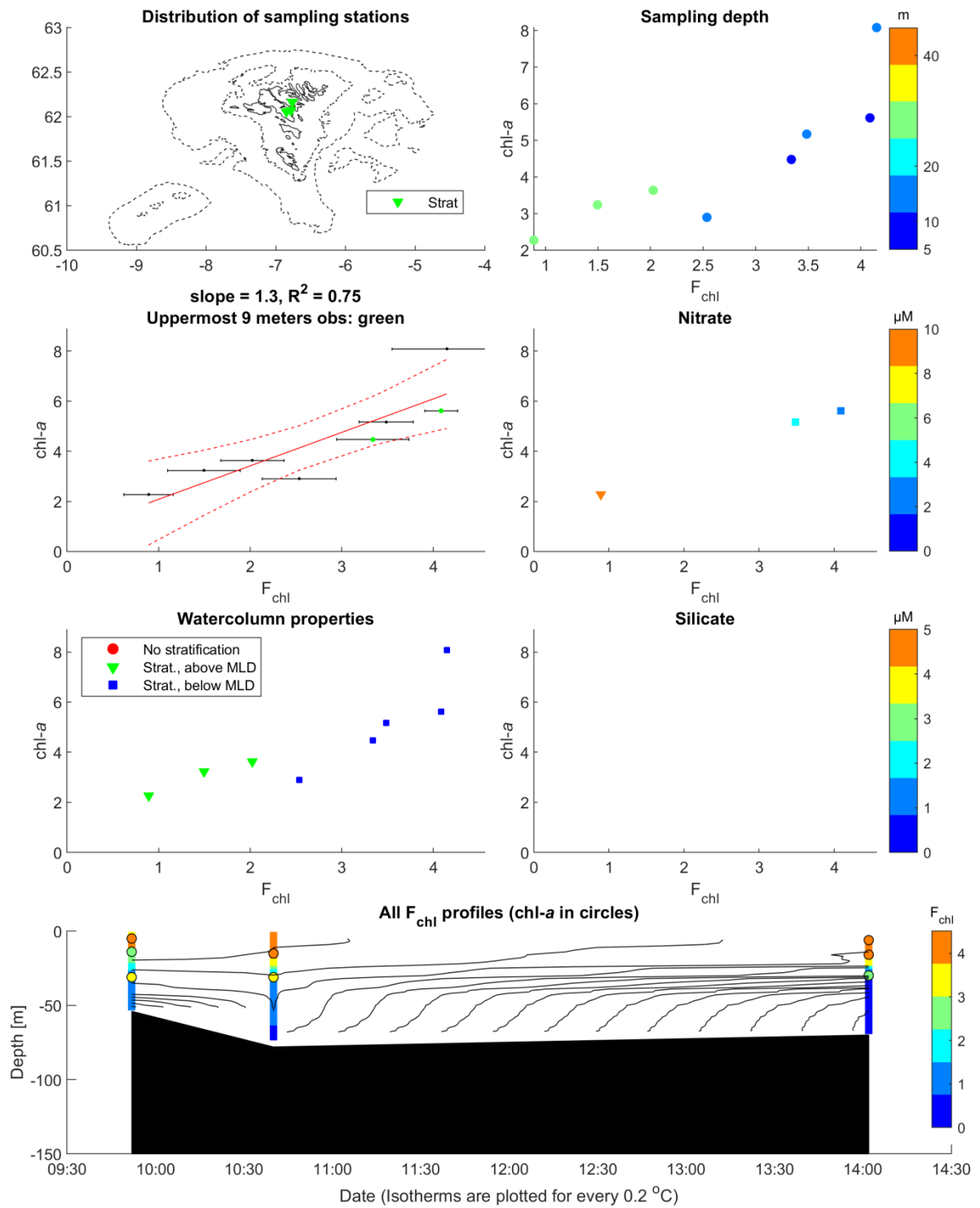
**Cruise 360, Fjords, 2/9-2003**



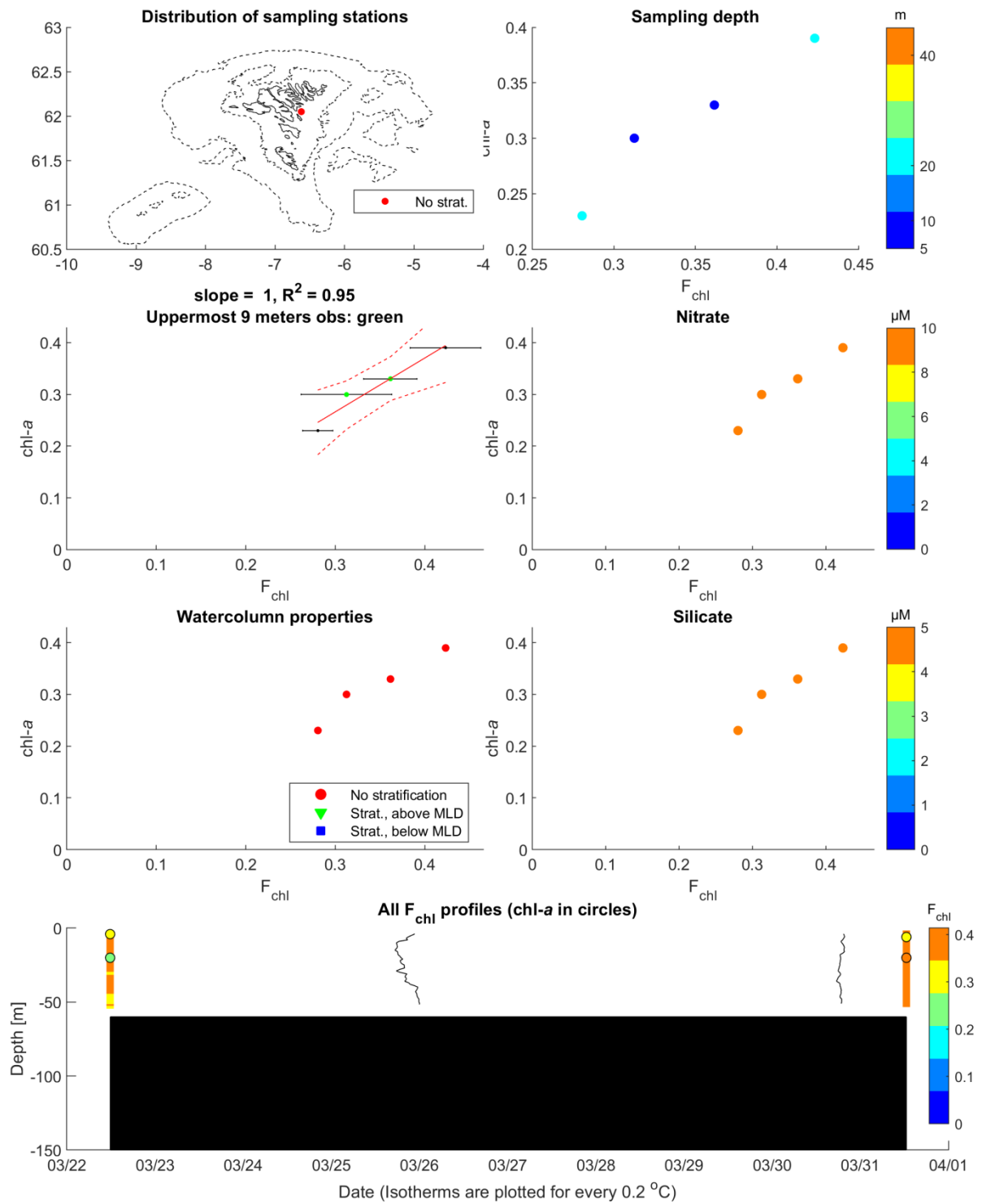
Cruise 424, Biological oceanography and section N, 20/4-27/4, 2004



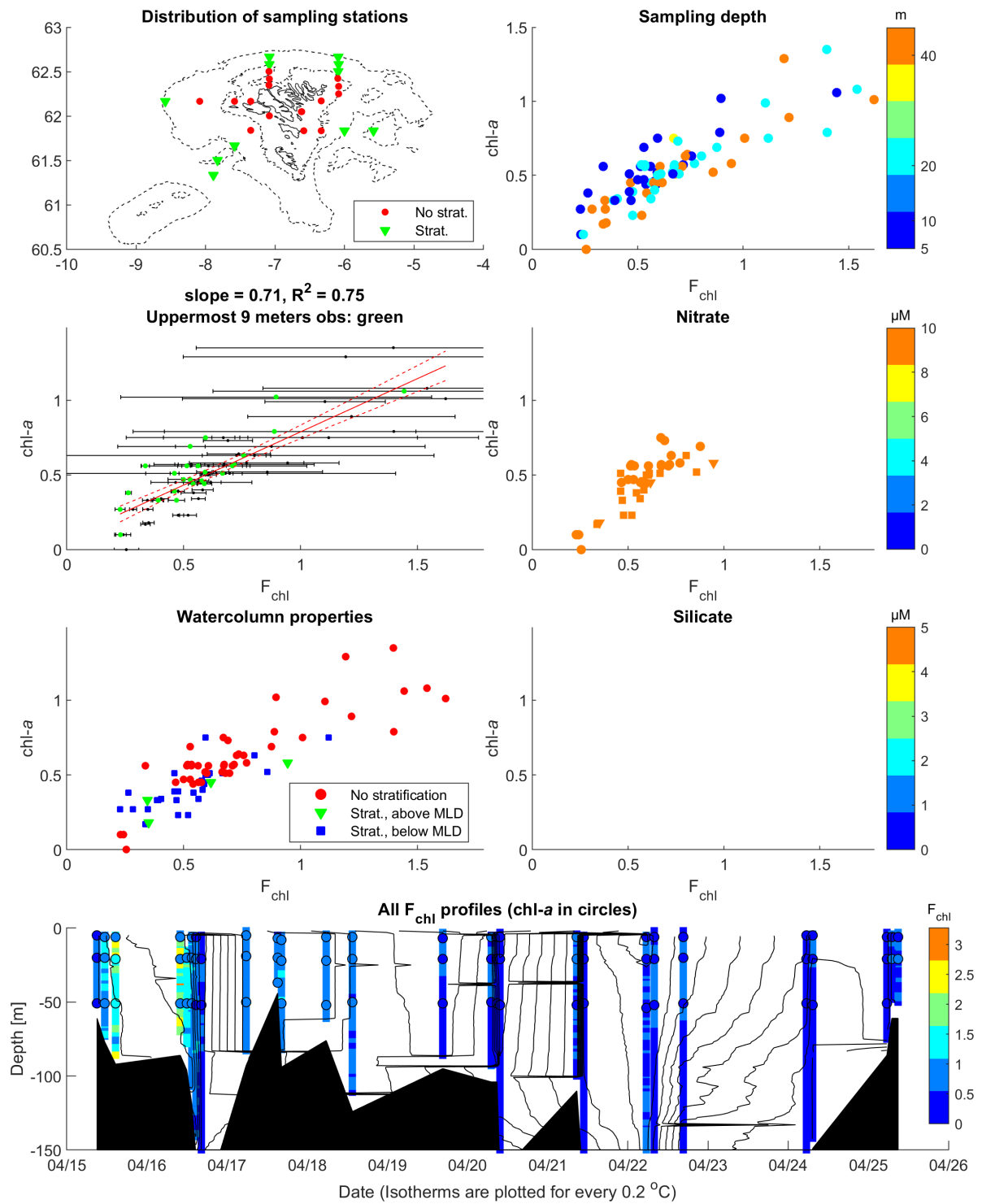
**Cruise 458, Fjords, 30/8-2004**



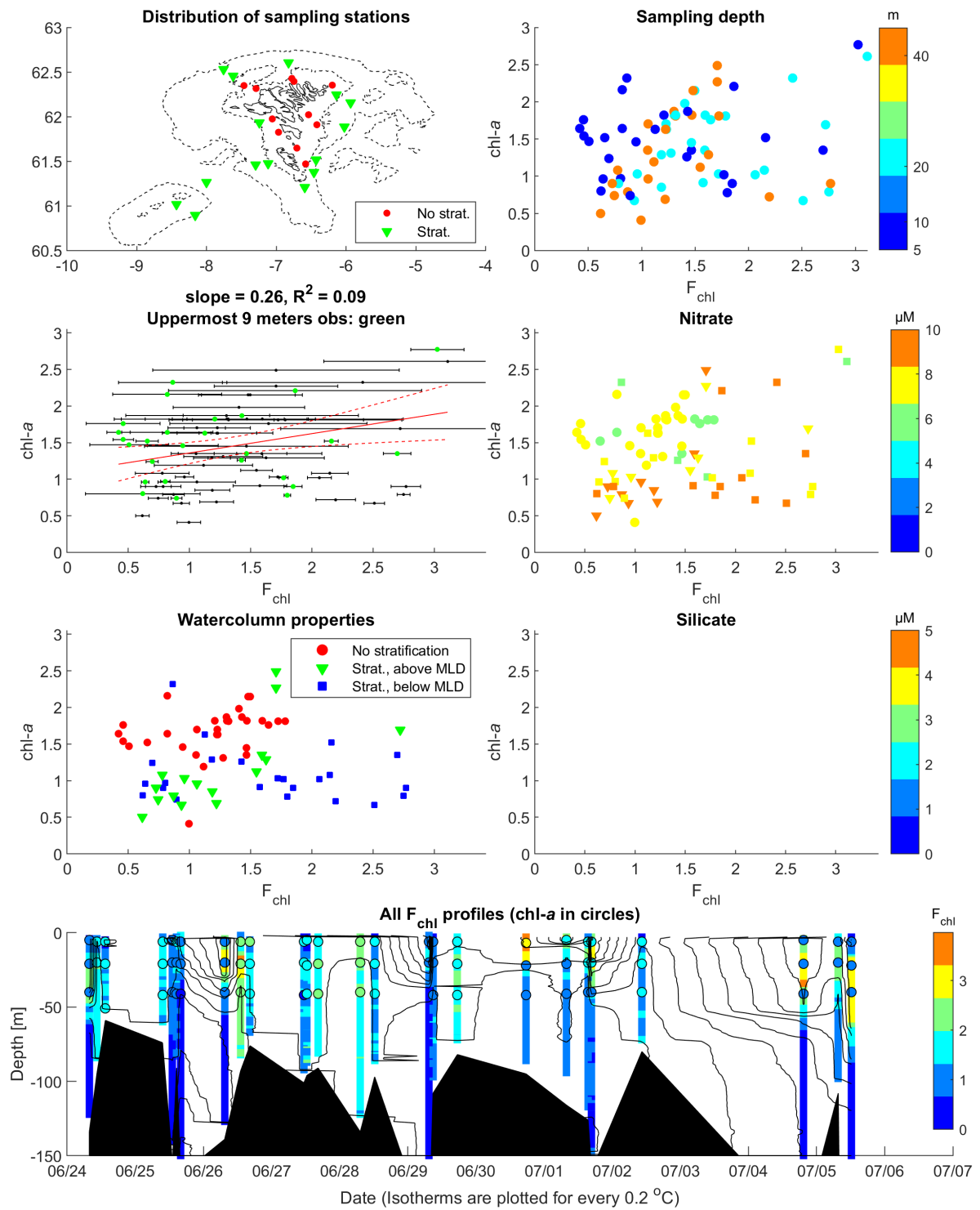
**Cruise 519, Hognabodi, 22/3-31/3, 2005**



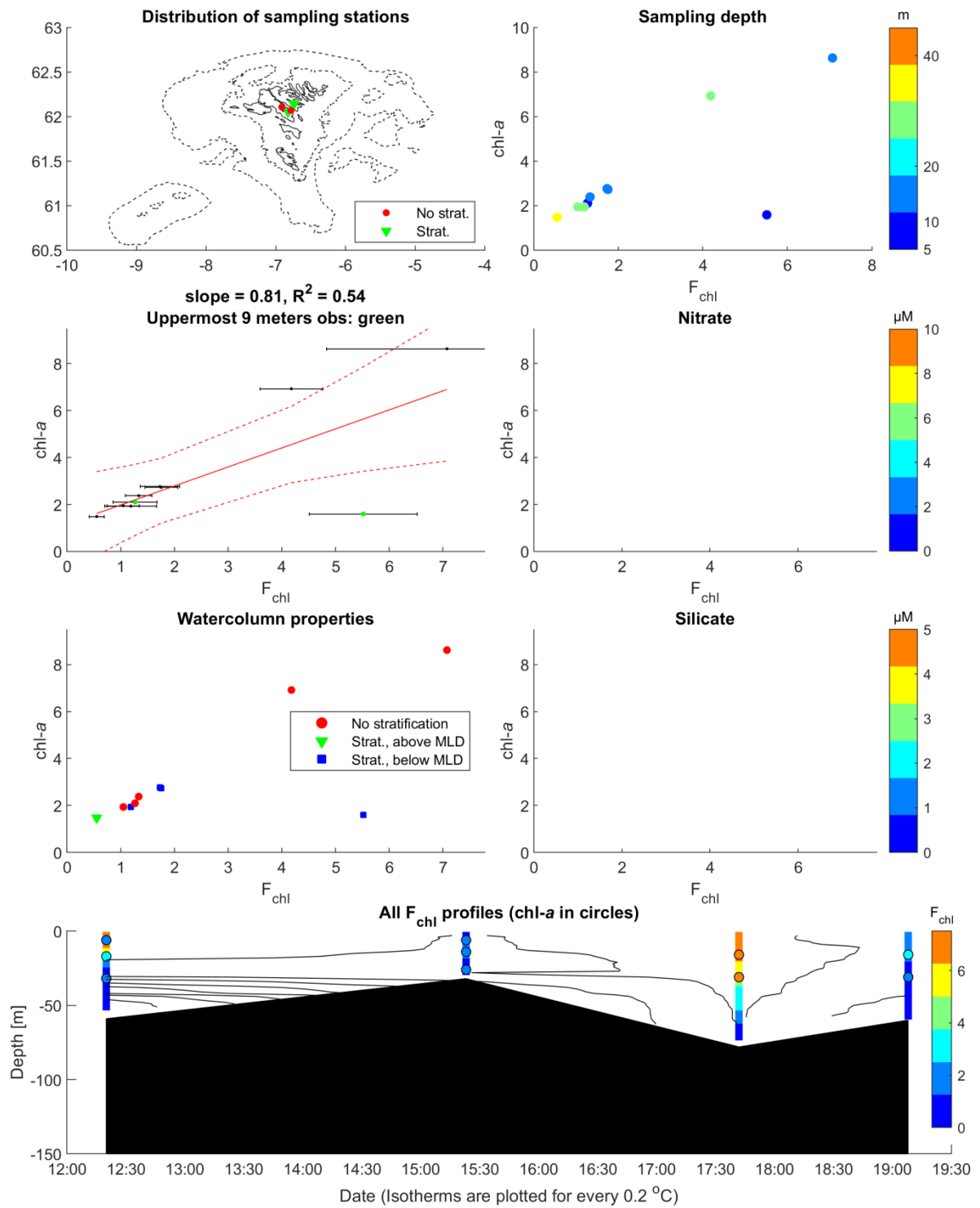
**Cruise 524, Biological oceanography and section N, 15/4-25/4, 2005**



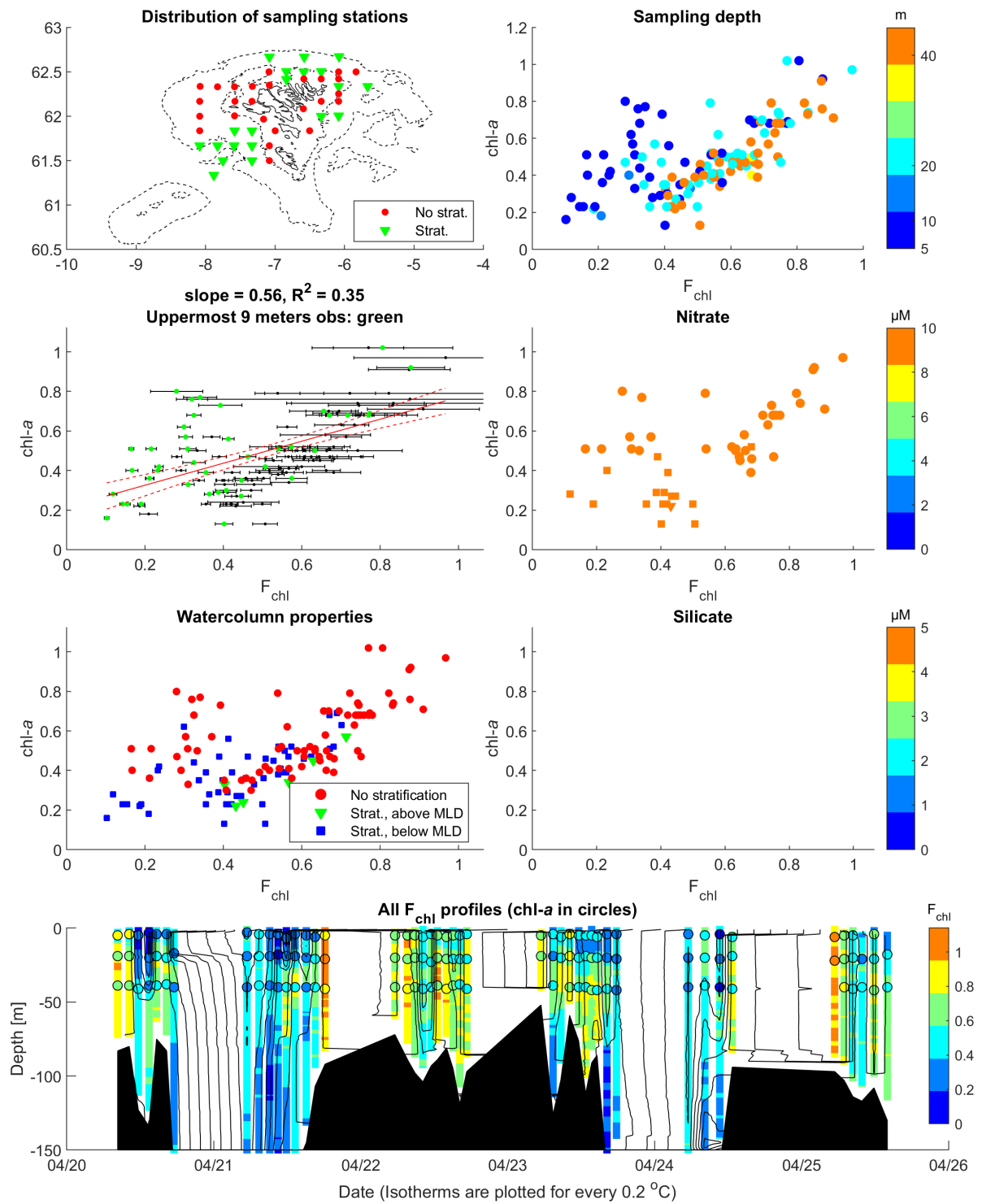
Cruise 552, 0-group, 24/6-5/7, 2005



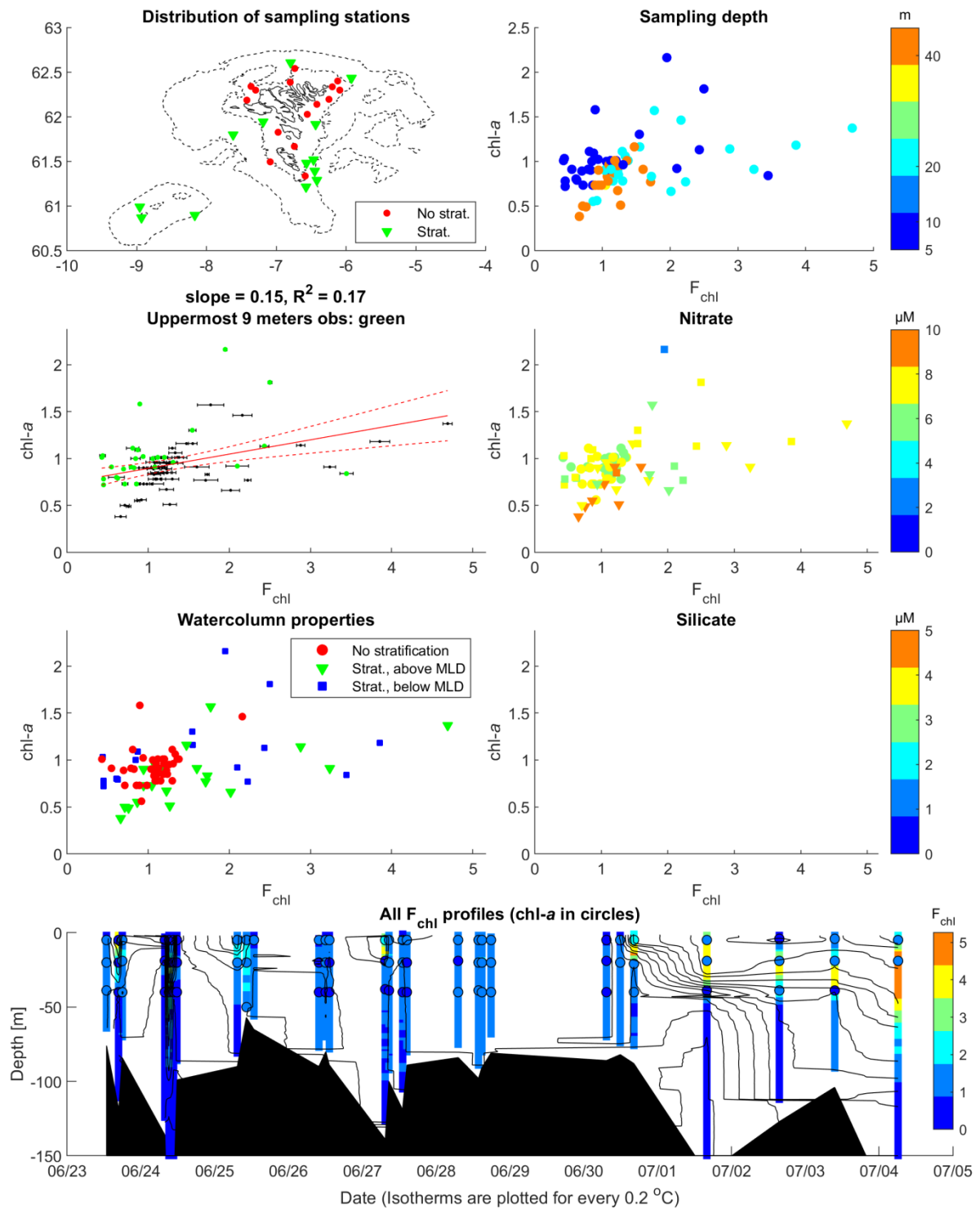
Cruise 564, Fjords, 29/8-2005



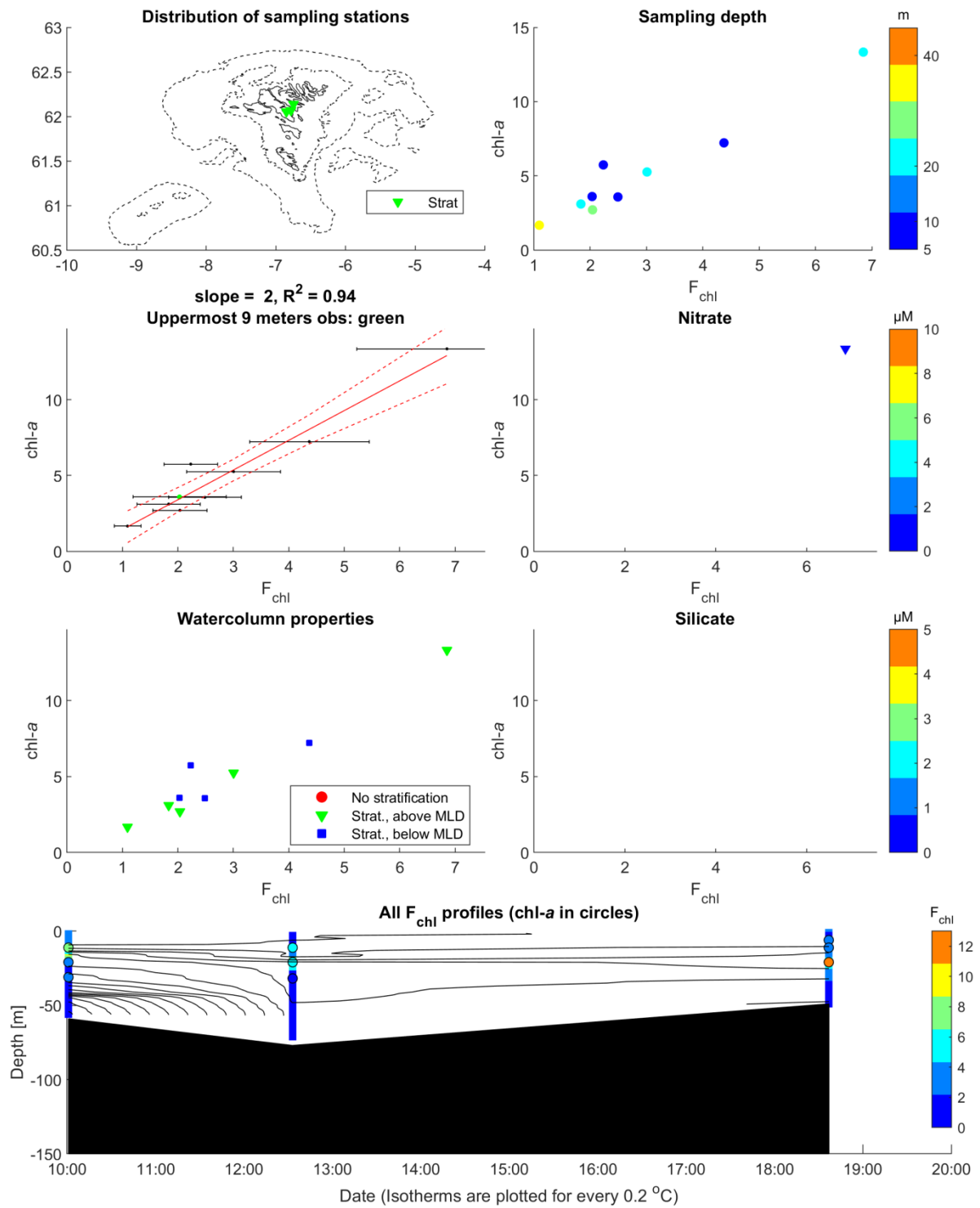
Cruise 628, Biological oceanography, 20/4-25/4, 2006



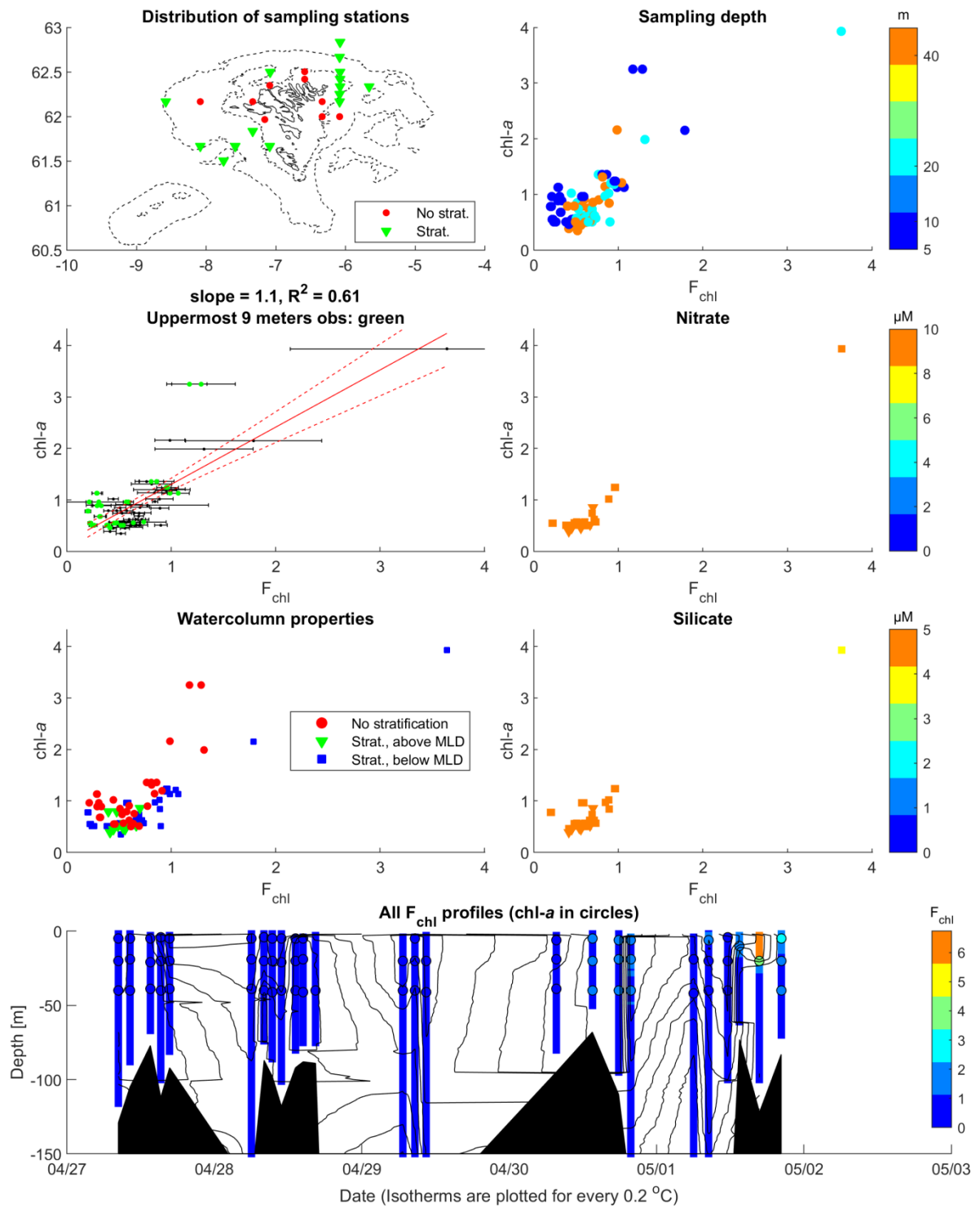
Cruise 648, 0-group, 23/6-4/7, 2006



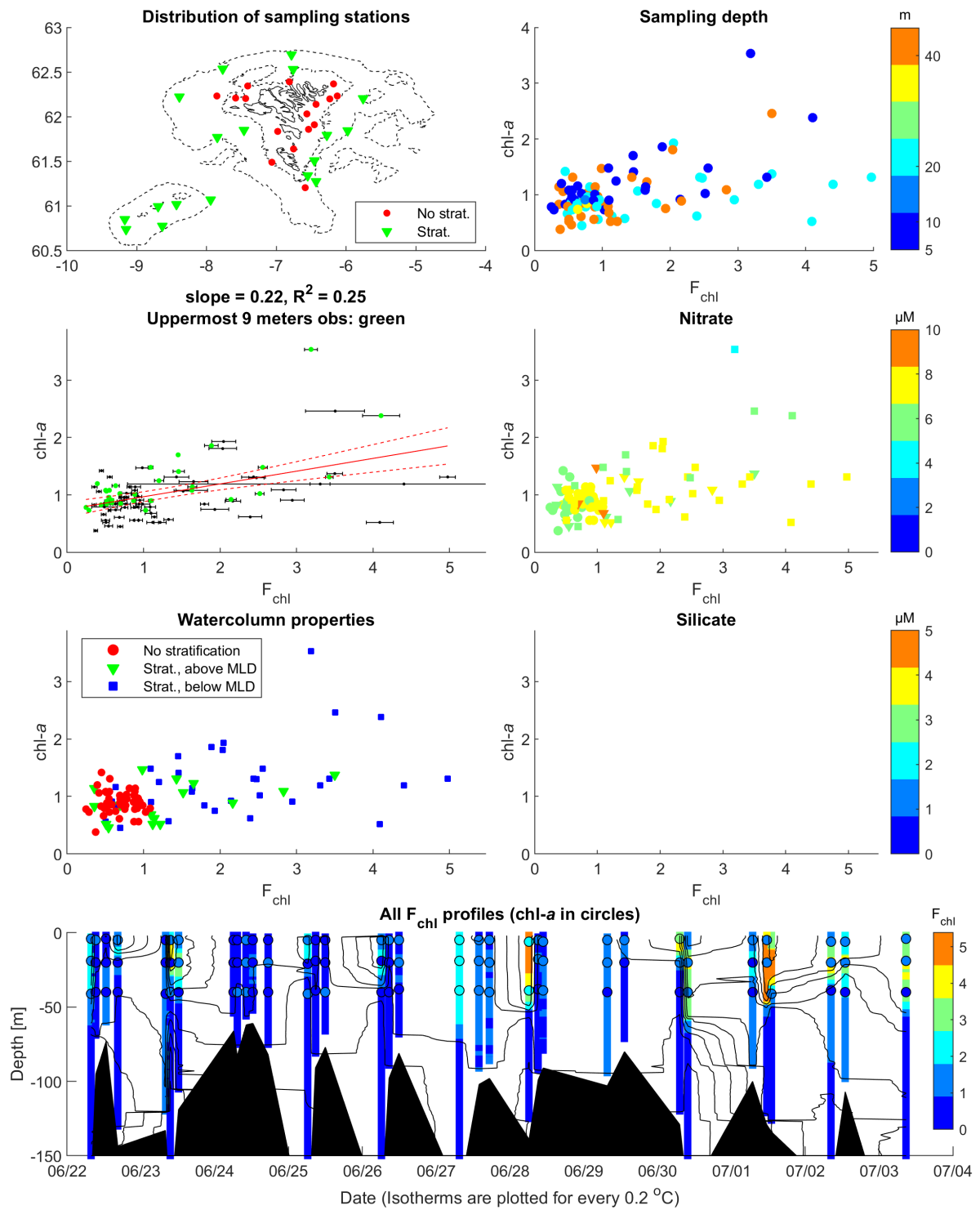
**Cruise 660, Fjords, 29/8-2006**



Cruise 728, Biological oceanography and section N, 27/4-1/5, 2007

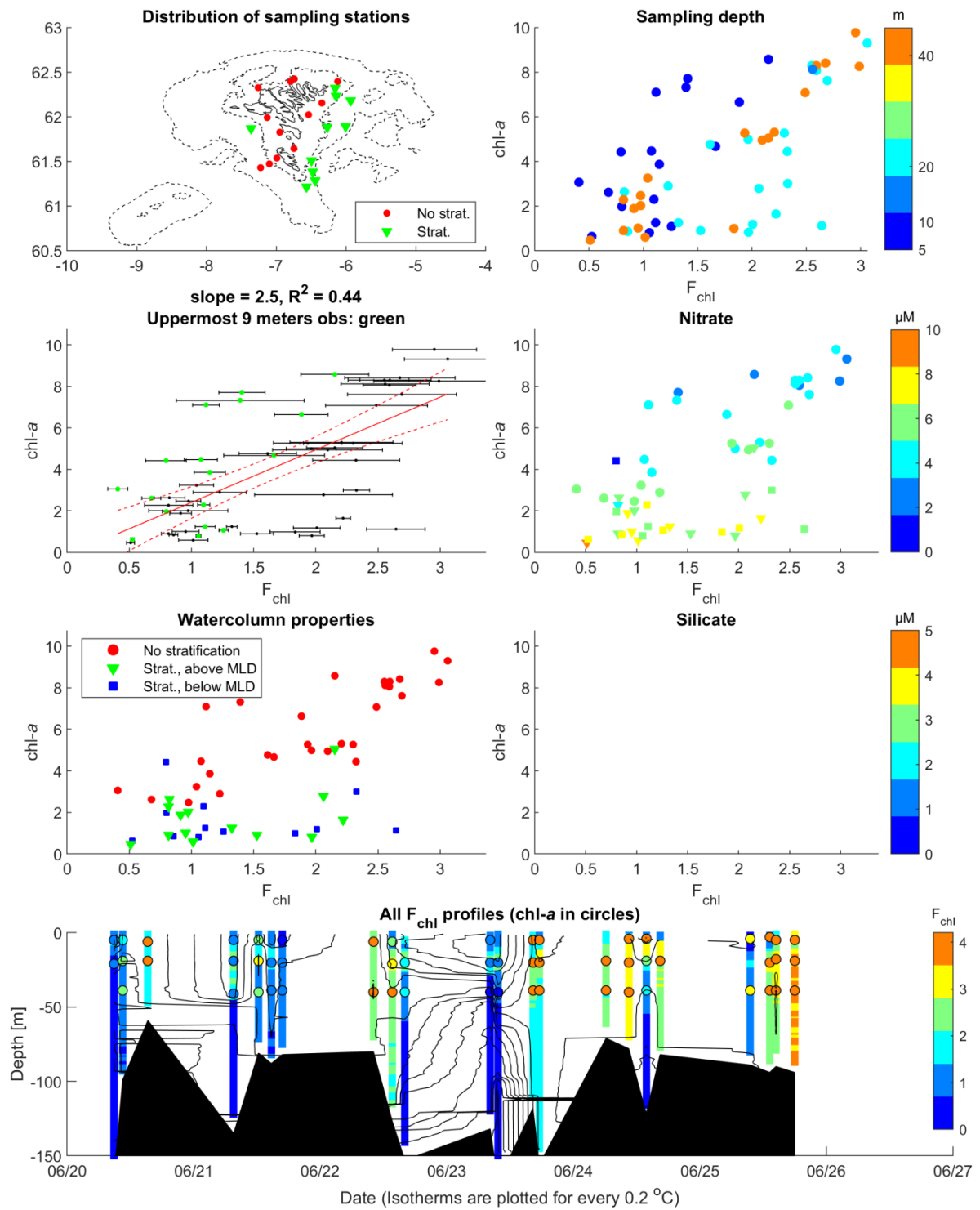


Cruise 748, 0-group, 22/6-3/7, 2007

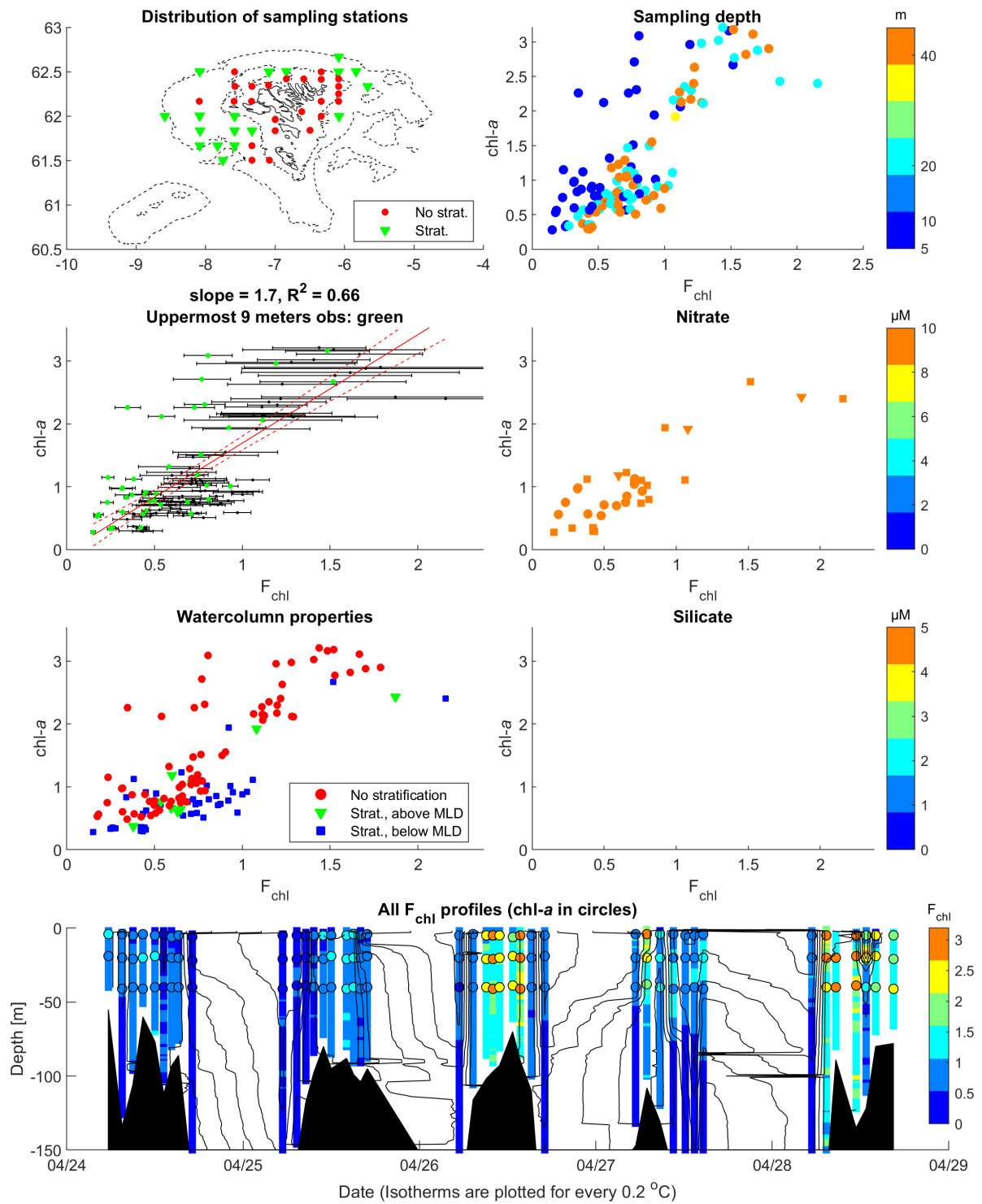




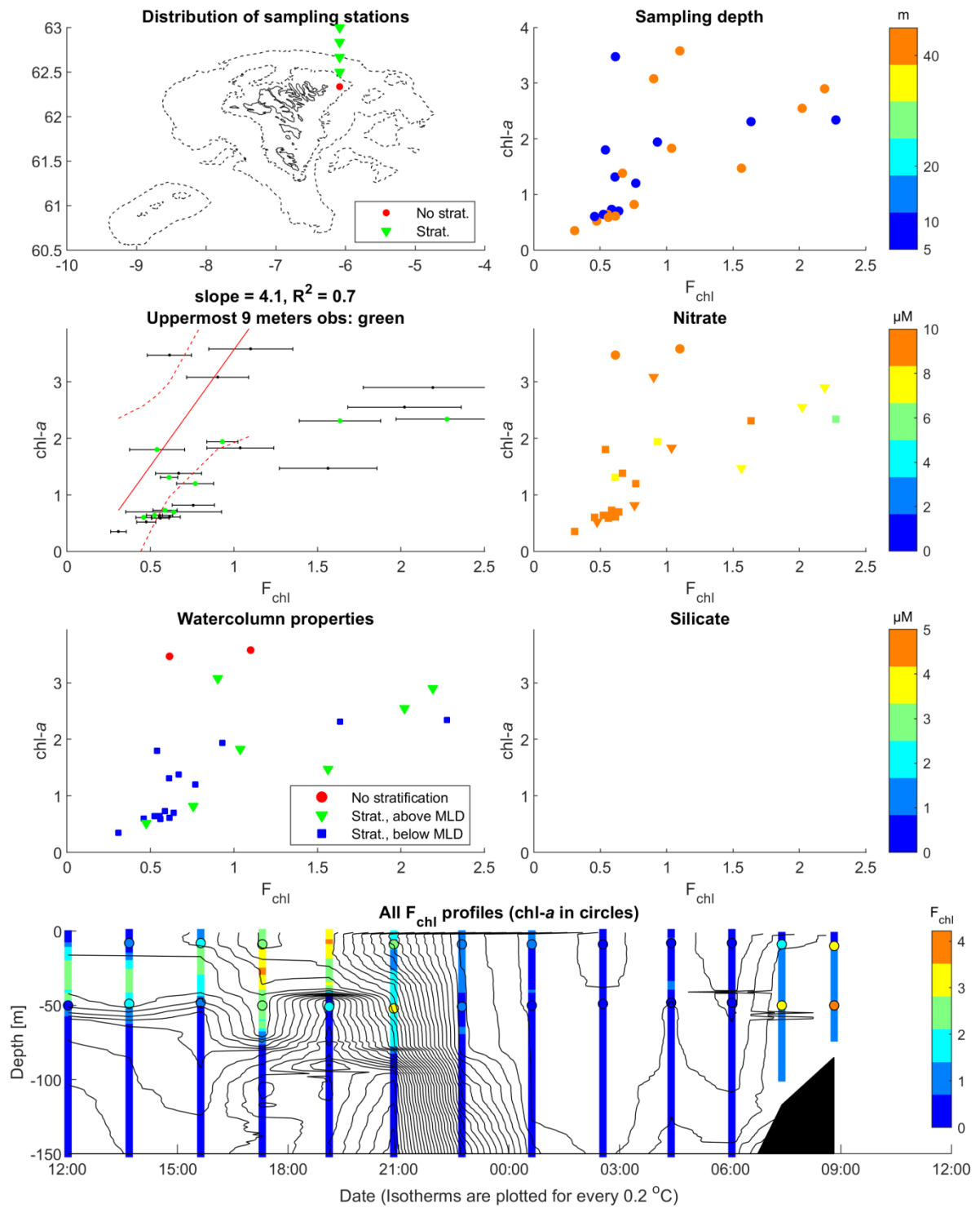
Cruise 848, 0-group, 20/6-25/6, 2008



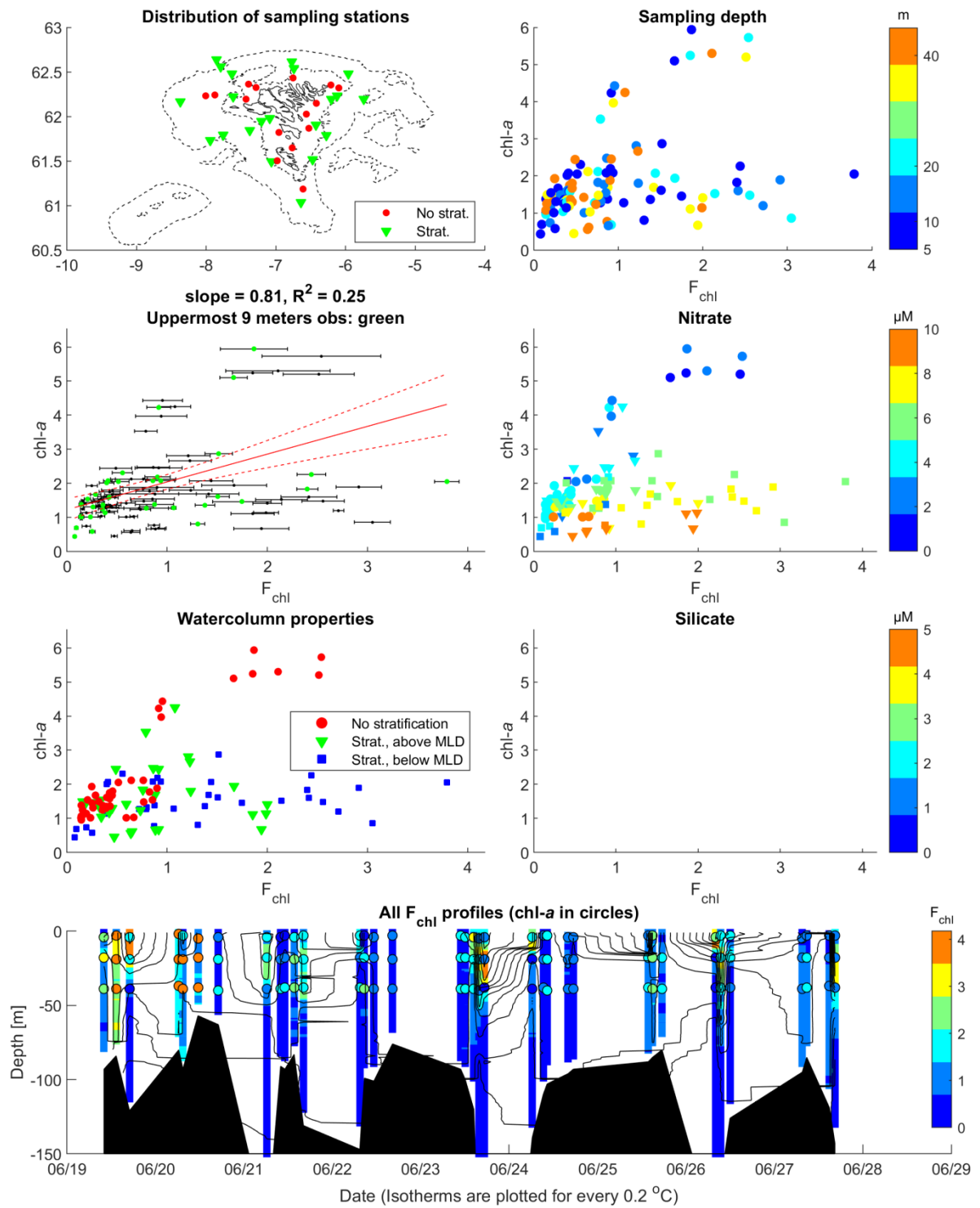
Cruise 928, Biological oceanography, 24/4-28/4, 2009



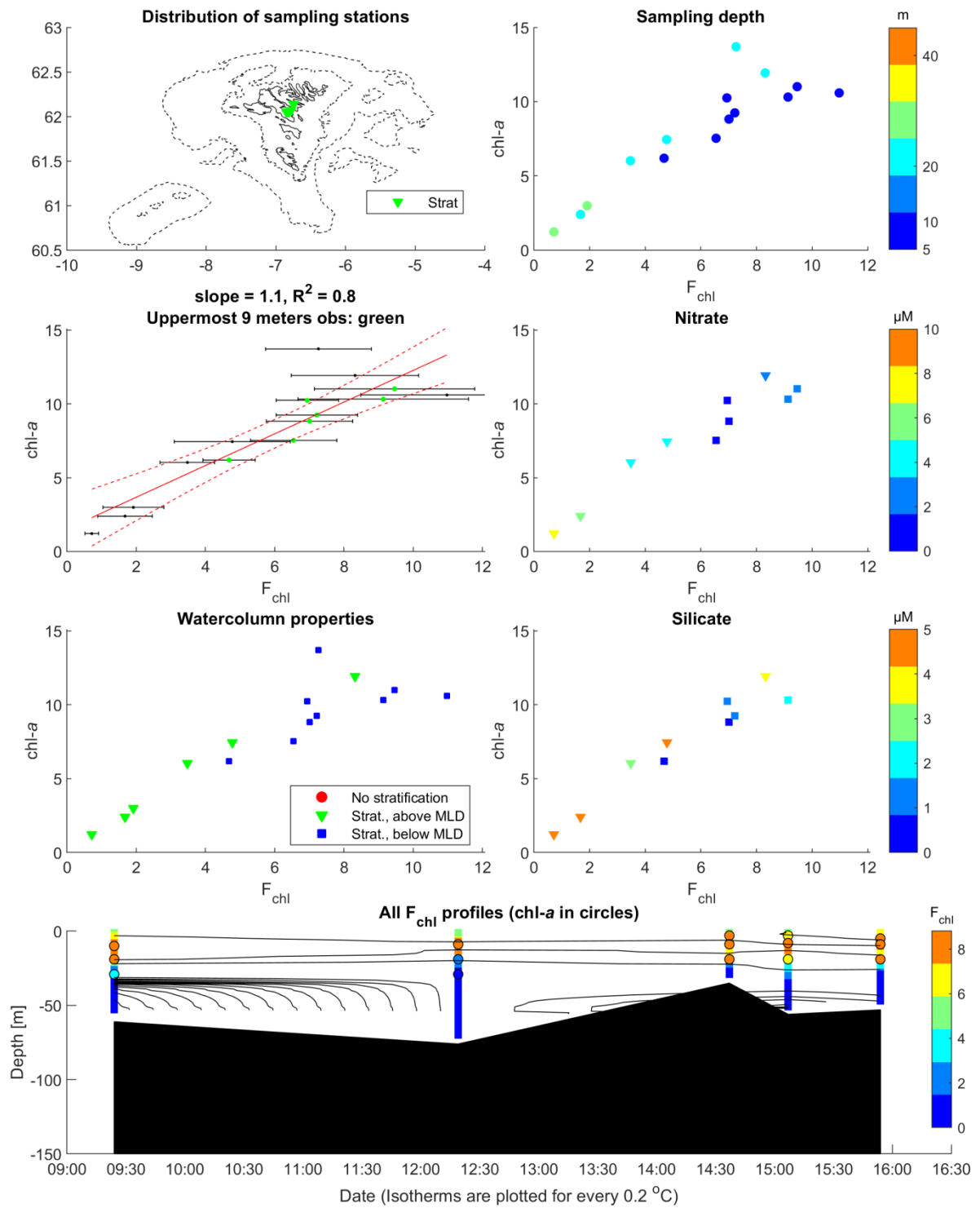
**Cruise 932, Section N, 11/5-12/5, 2009**



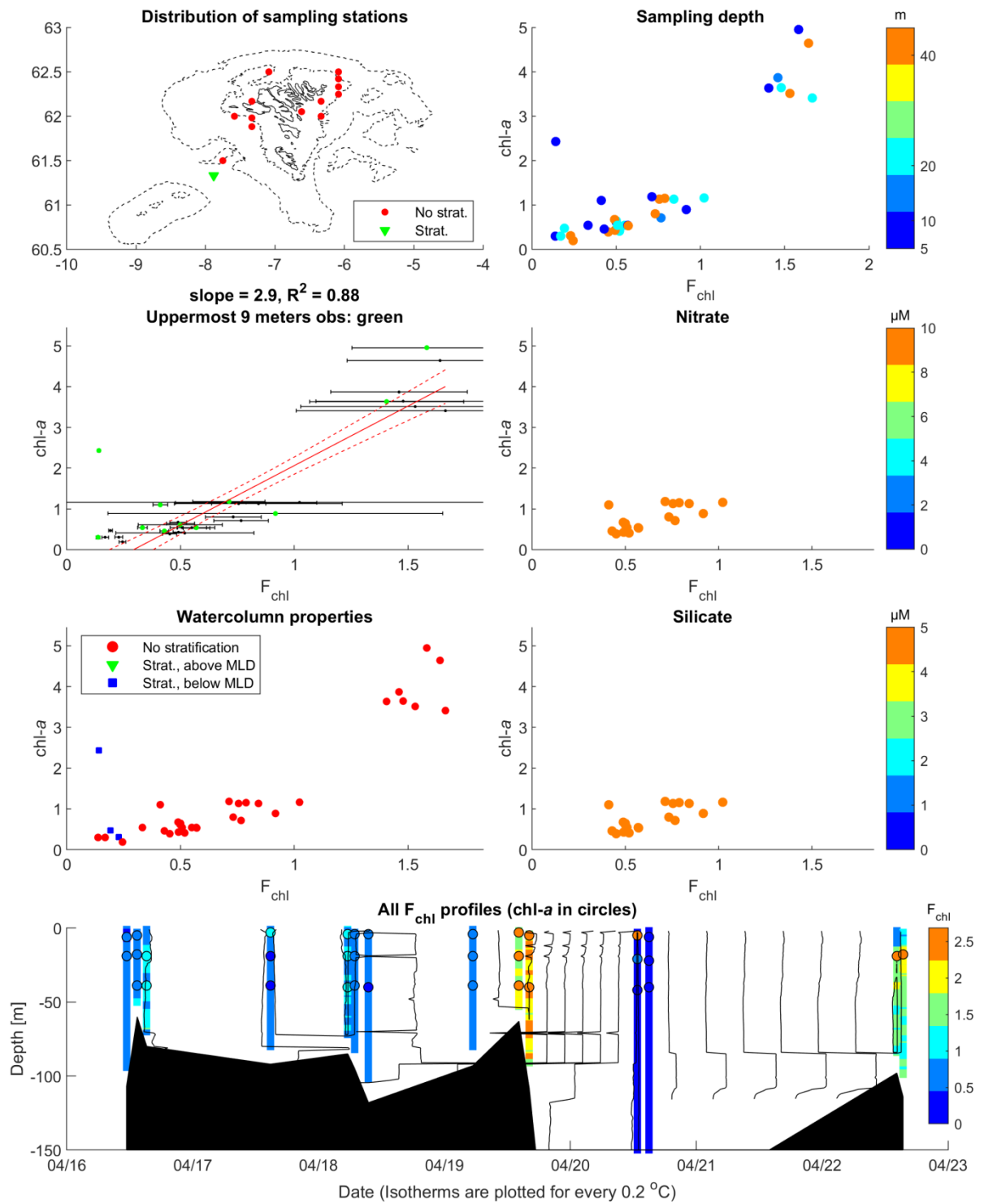
**Cruise 952, 0-group, 19/6-27/6, 2009**



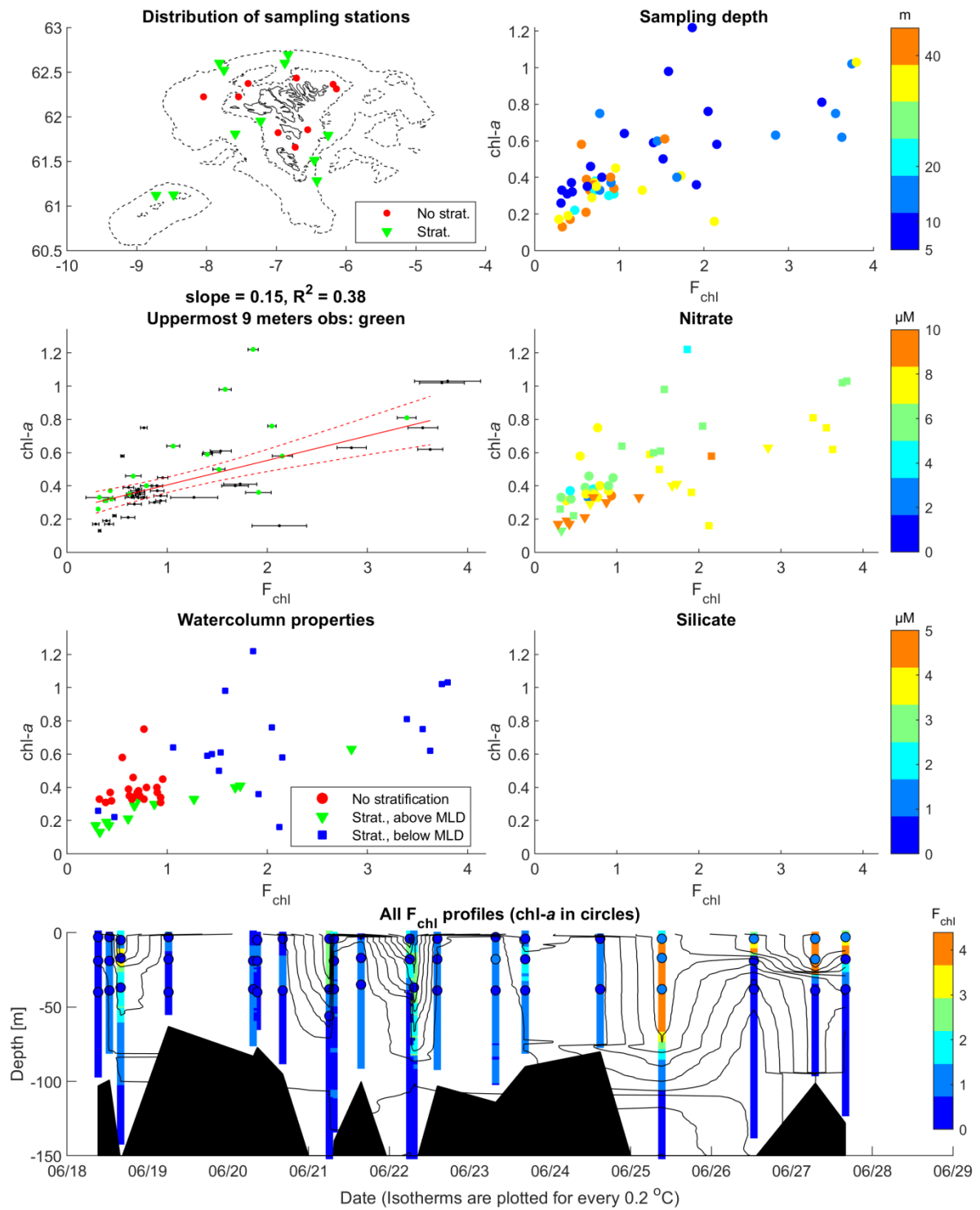
**Cruise 968, Fjords, 25/8-2009**



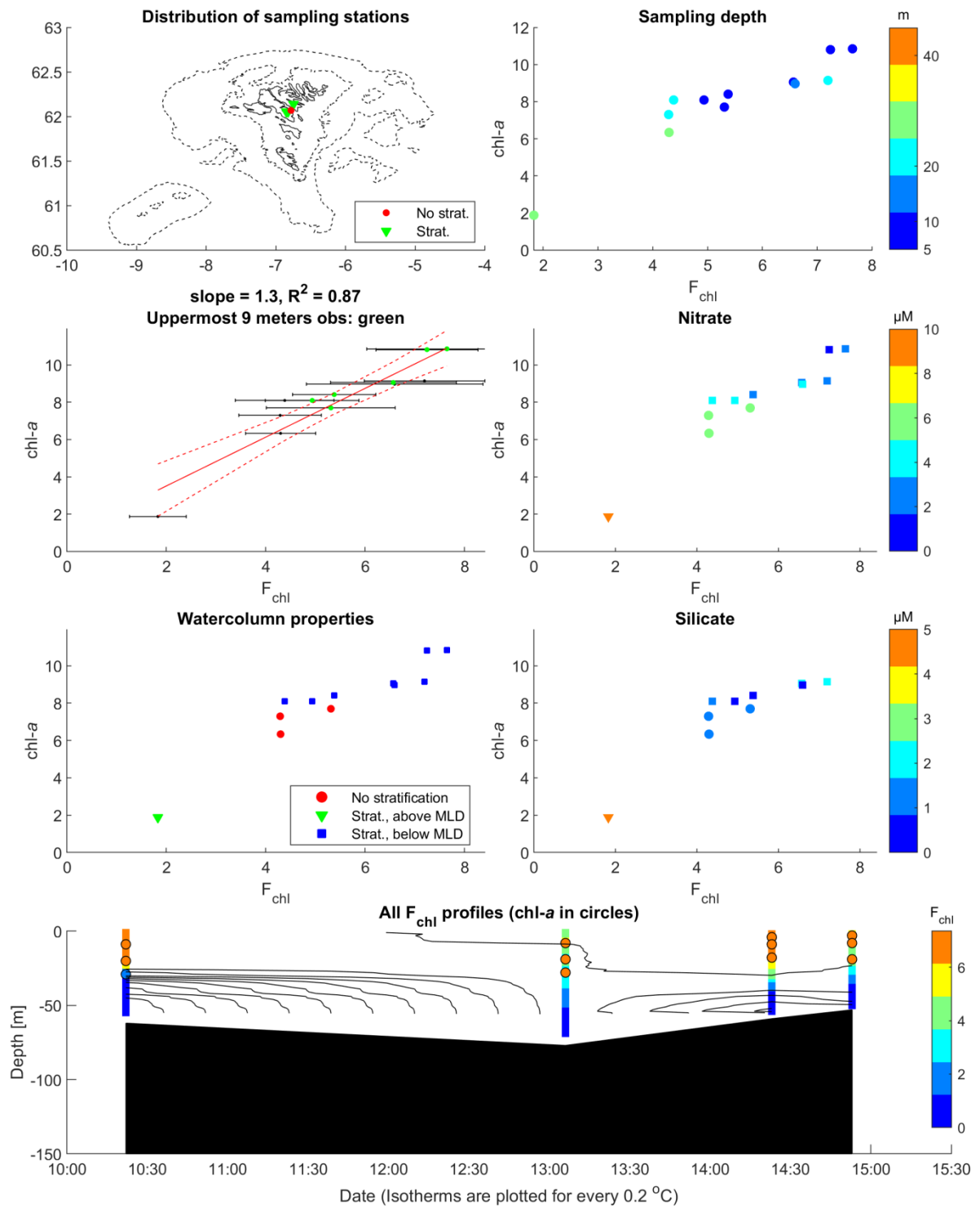
Cruise 1012, Biological oceanography, 16/4-22/4, 2010



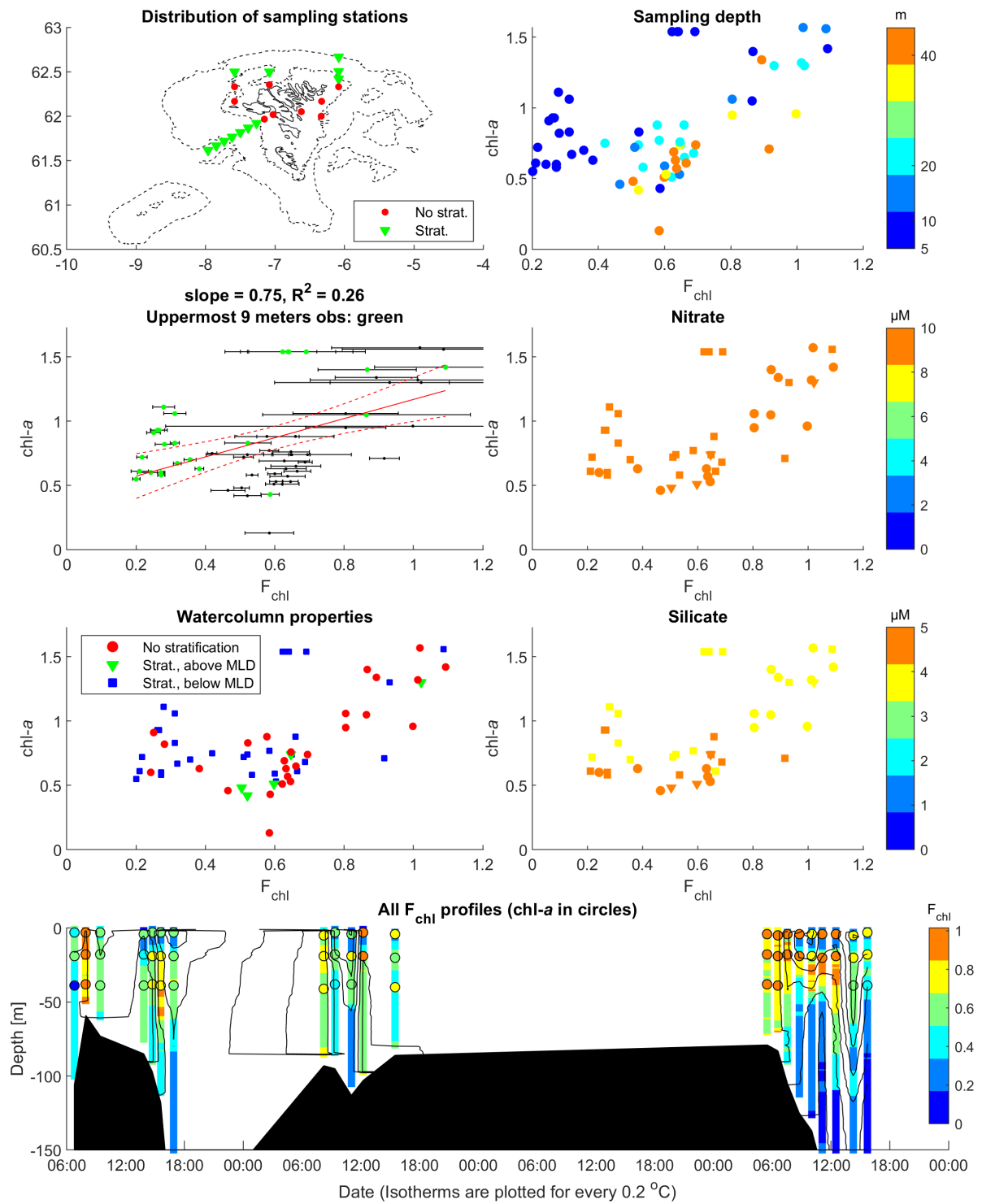
Cruise 1024, 0-group, 18/6-27/6, 2010



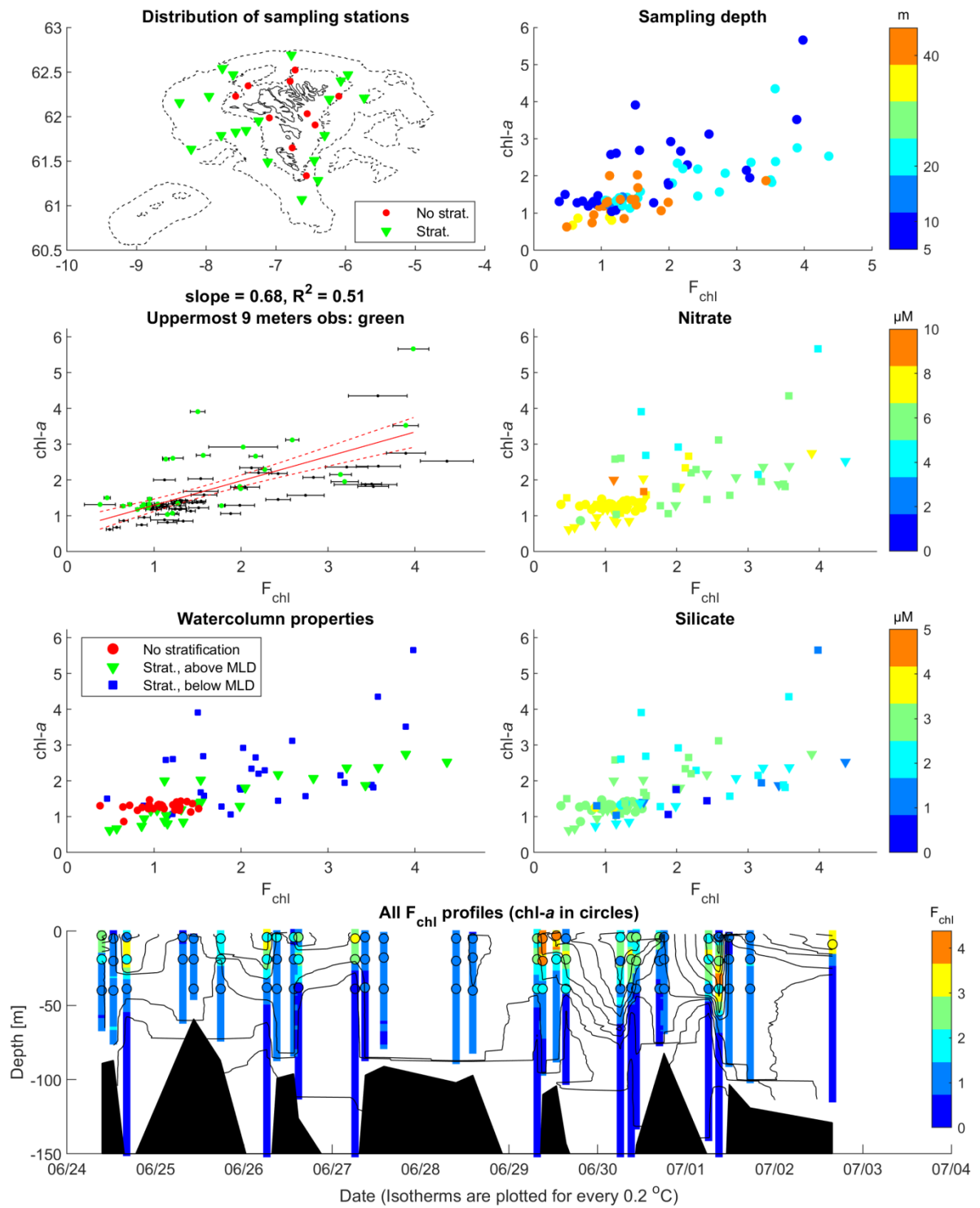
Cruise 1030, Fjords, 31/8-2010



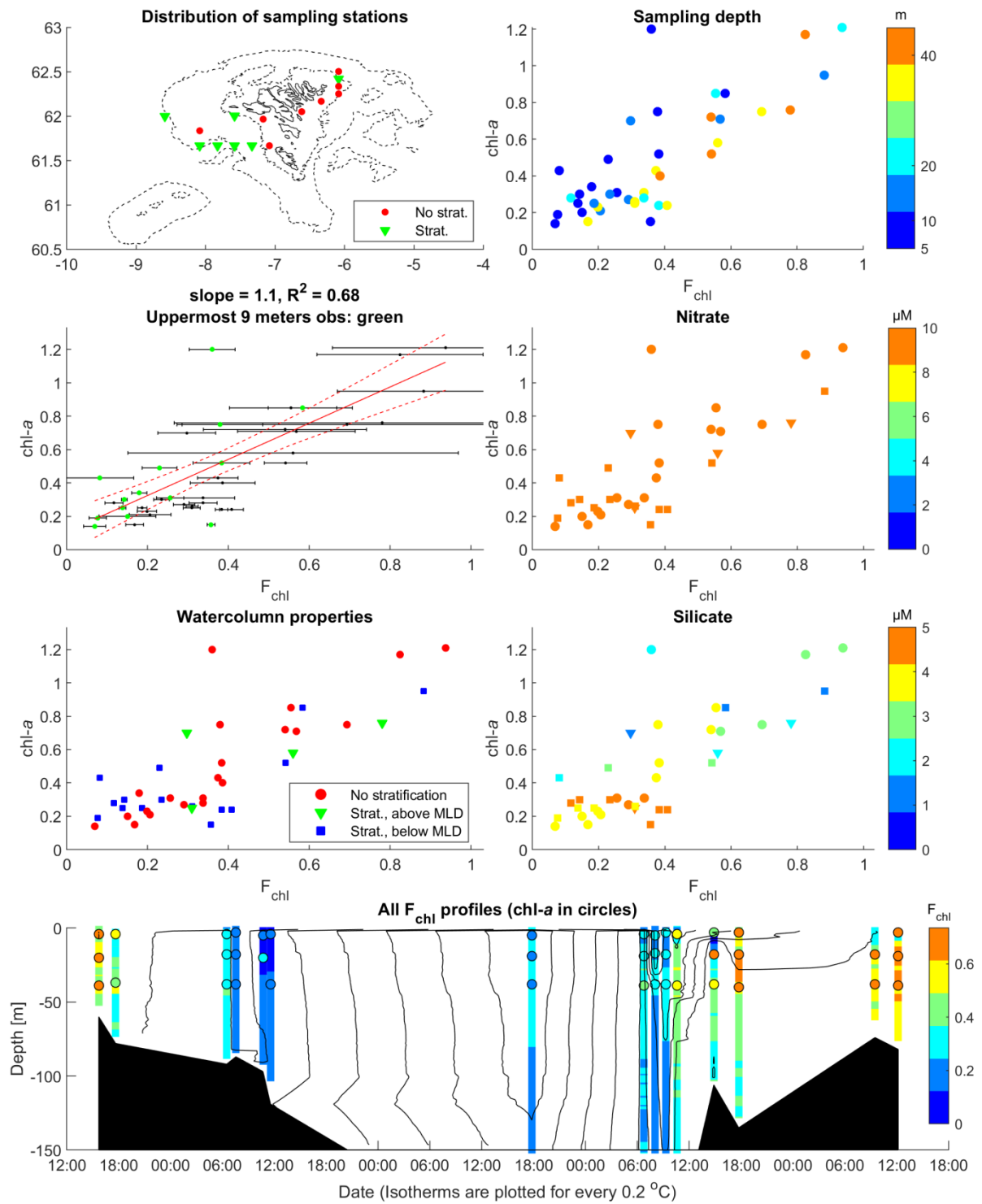
Cruise 1114, Biological oceanography and section K, 29/4-2/5, 2011



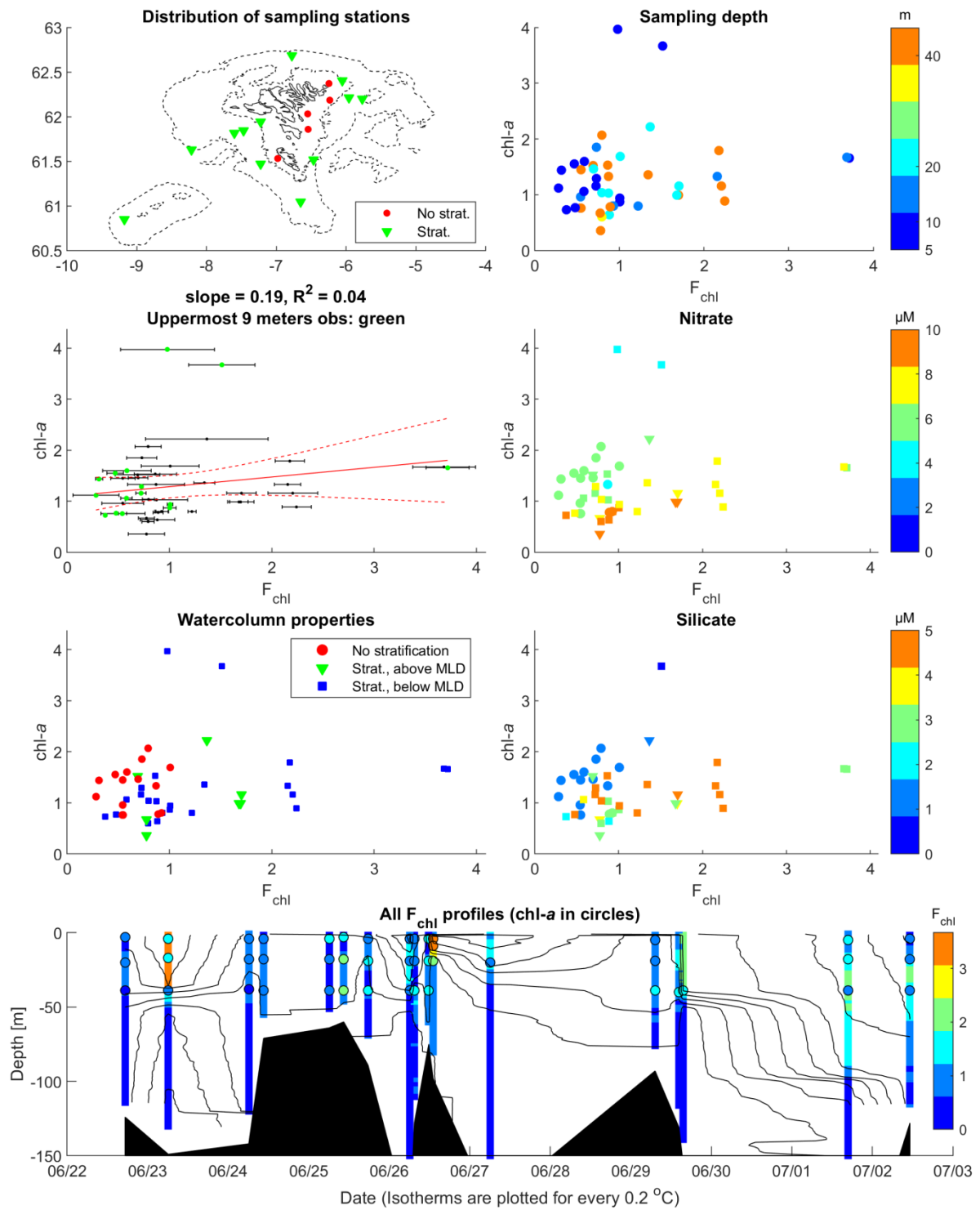
Cruise 1126, 0-group, 24/6-2/7, 2011



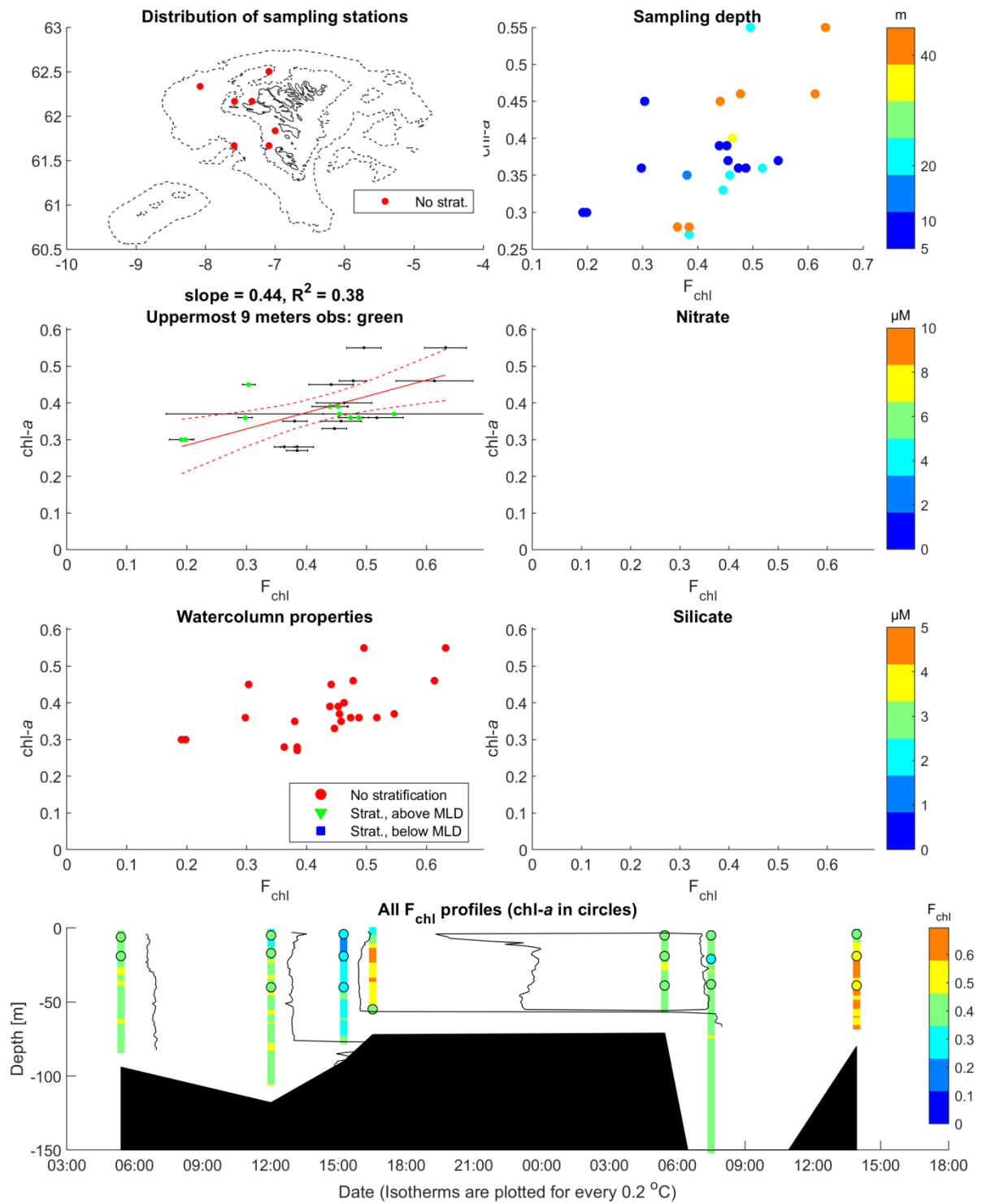
**Cruise 1216, Biological oceanography, 27/4-1/5, 2012**



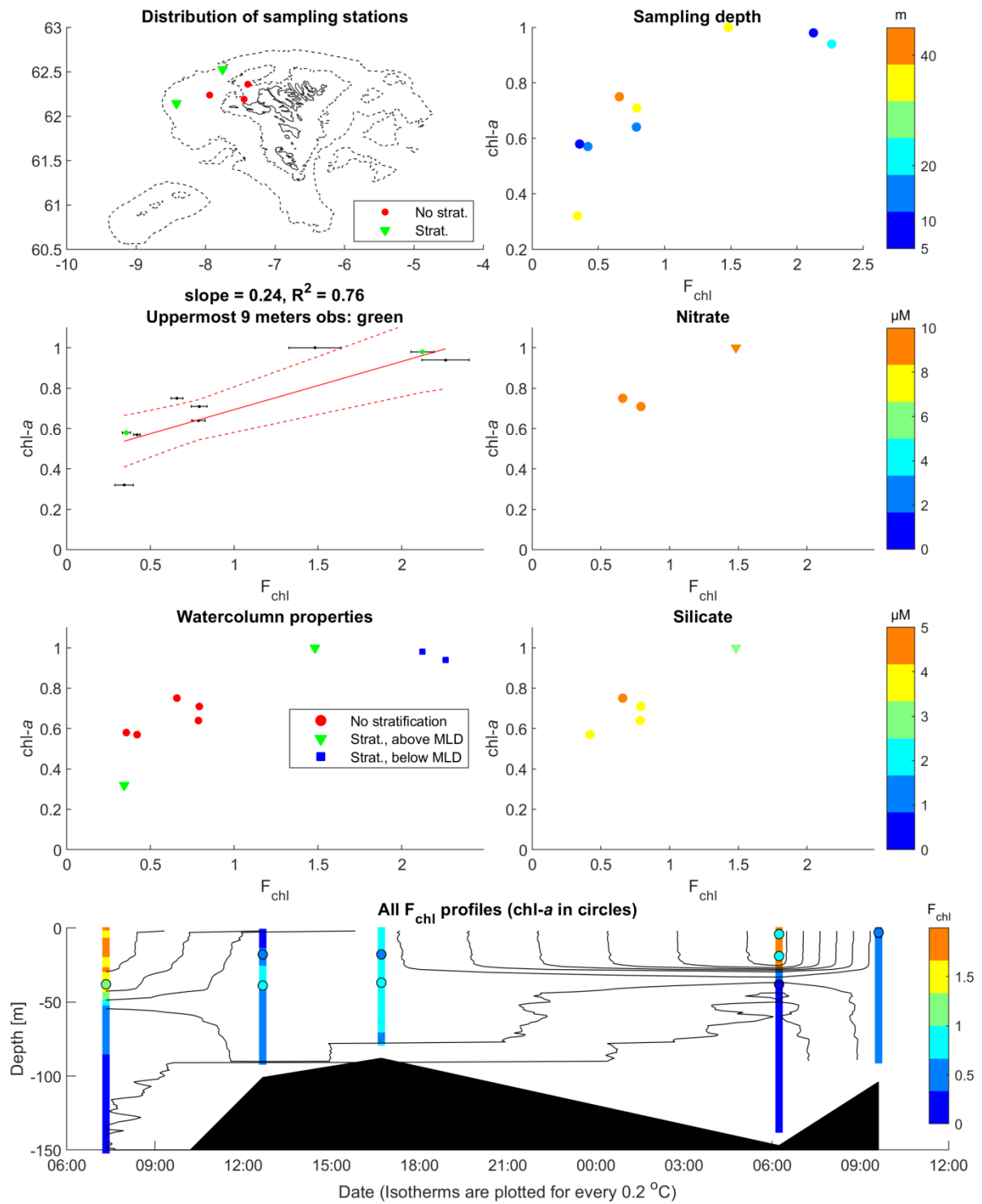
Cruise 1228, 0-group, 22/6-2/7, 2012



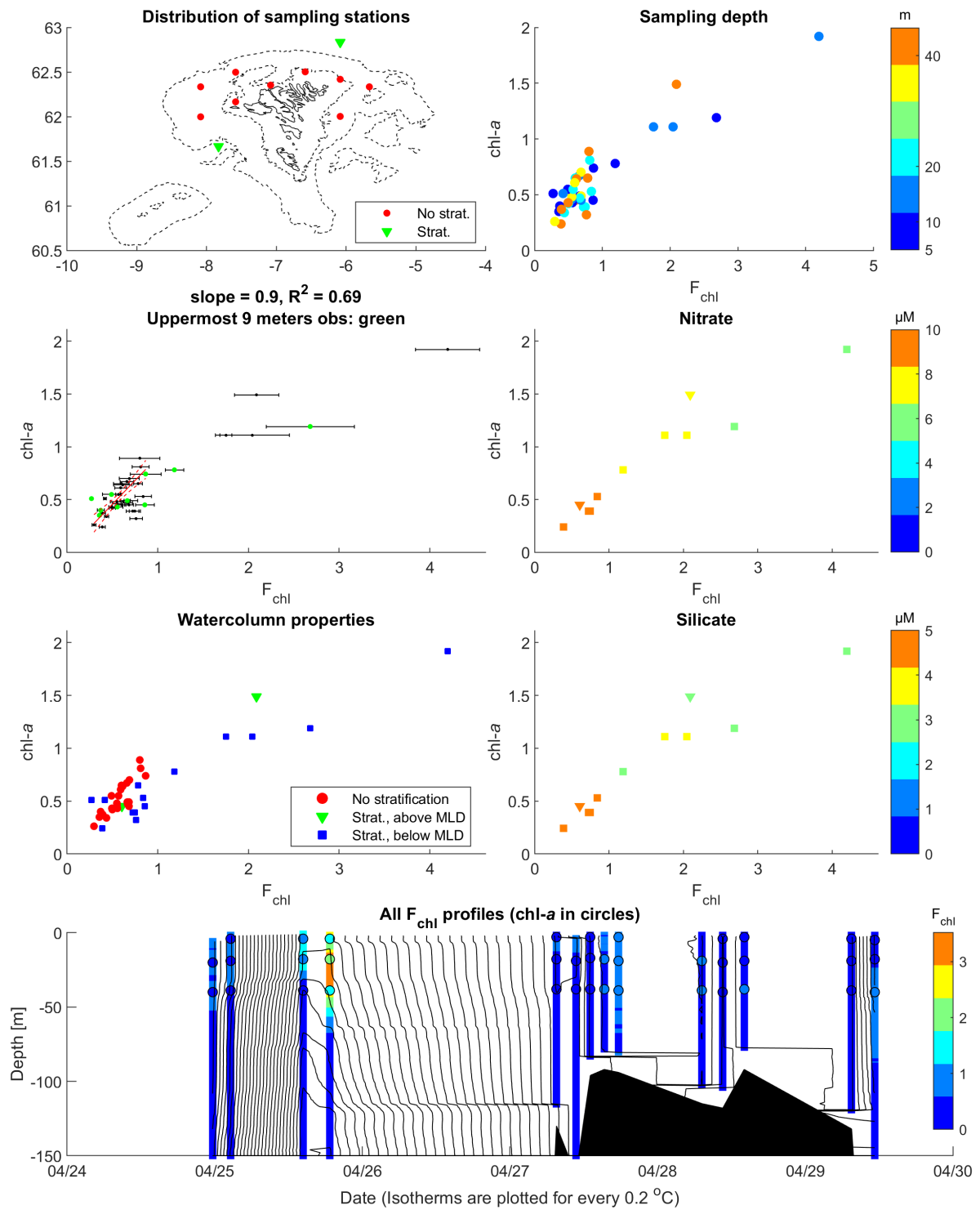
**Cruise 1318, Biological oceanography, 28/4-29/4, 2013**



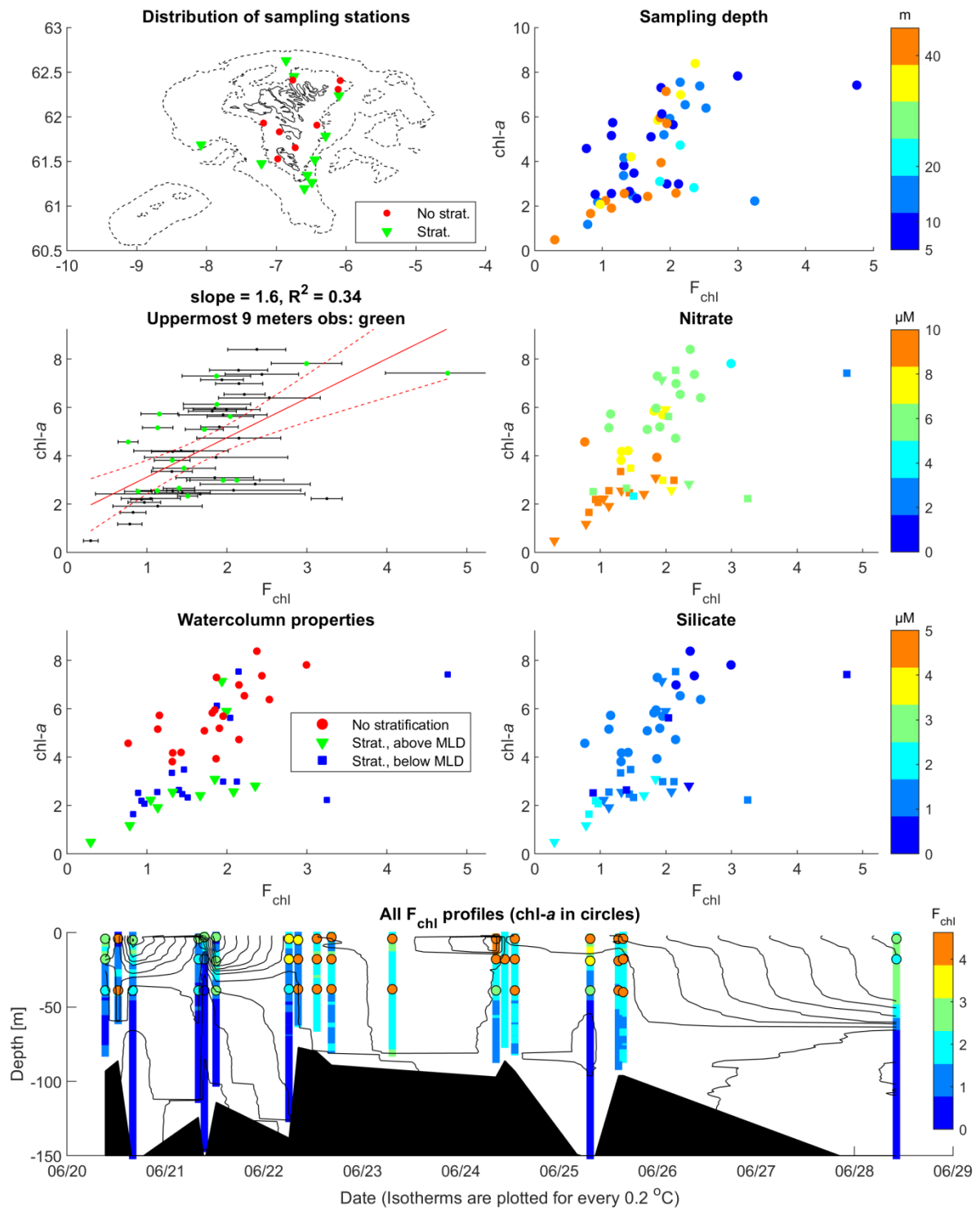
**Cruise 1330, 0-group, 28/6-29/6, 2013**



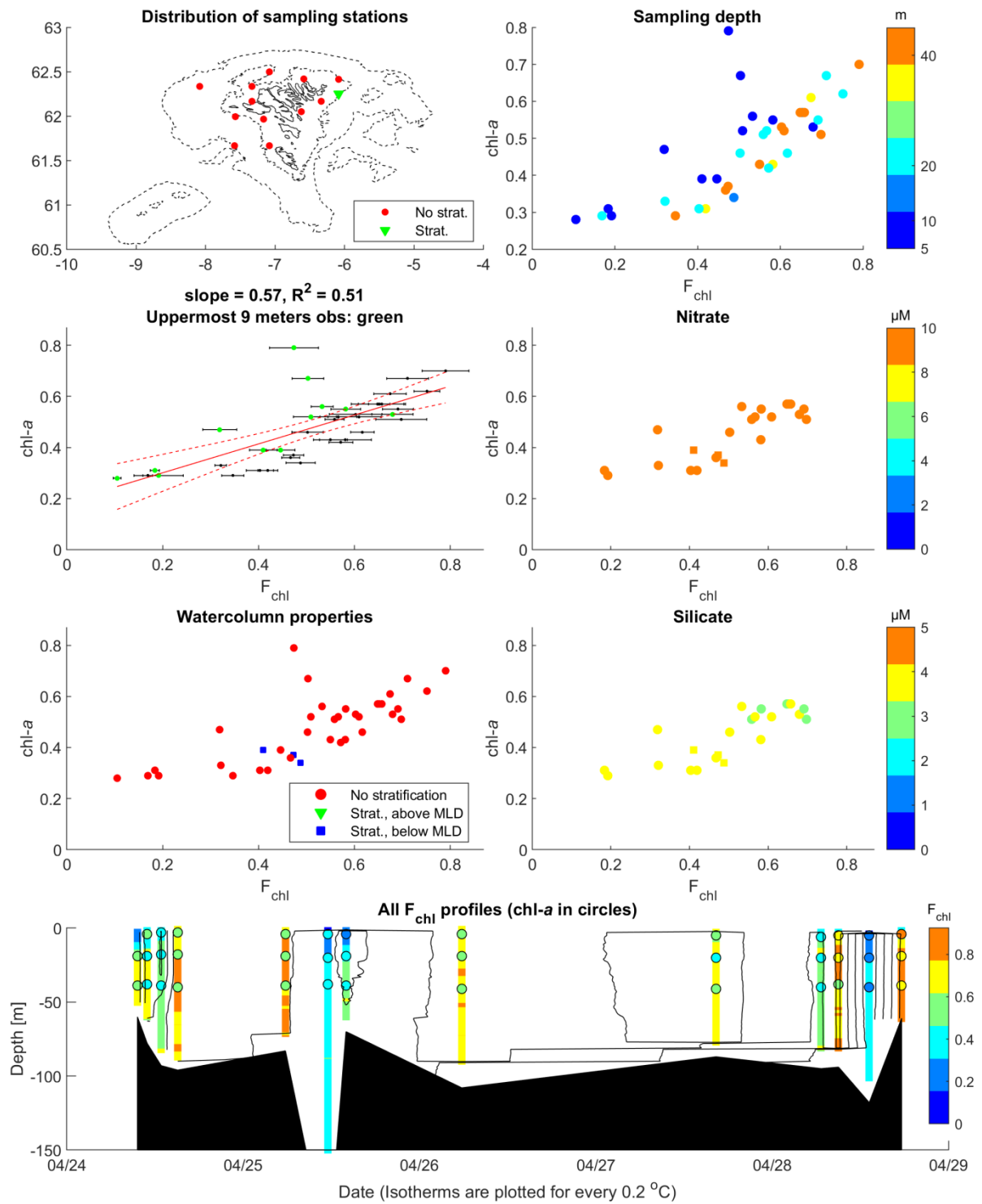
**Cruise 1414, Biological oceanography and section N, 24/4-29/4, 2014**



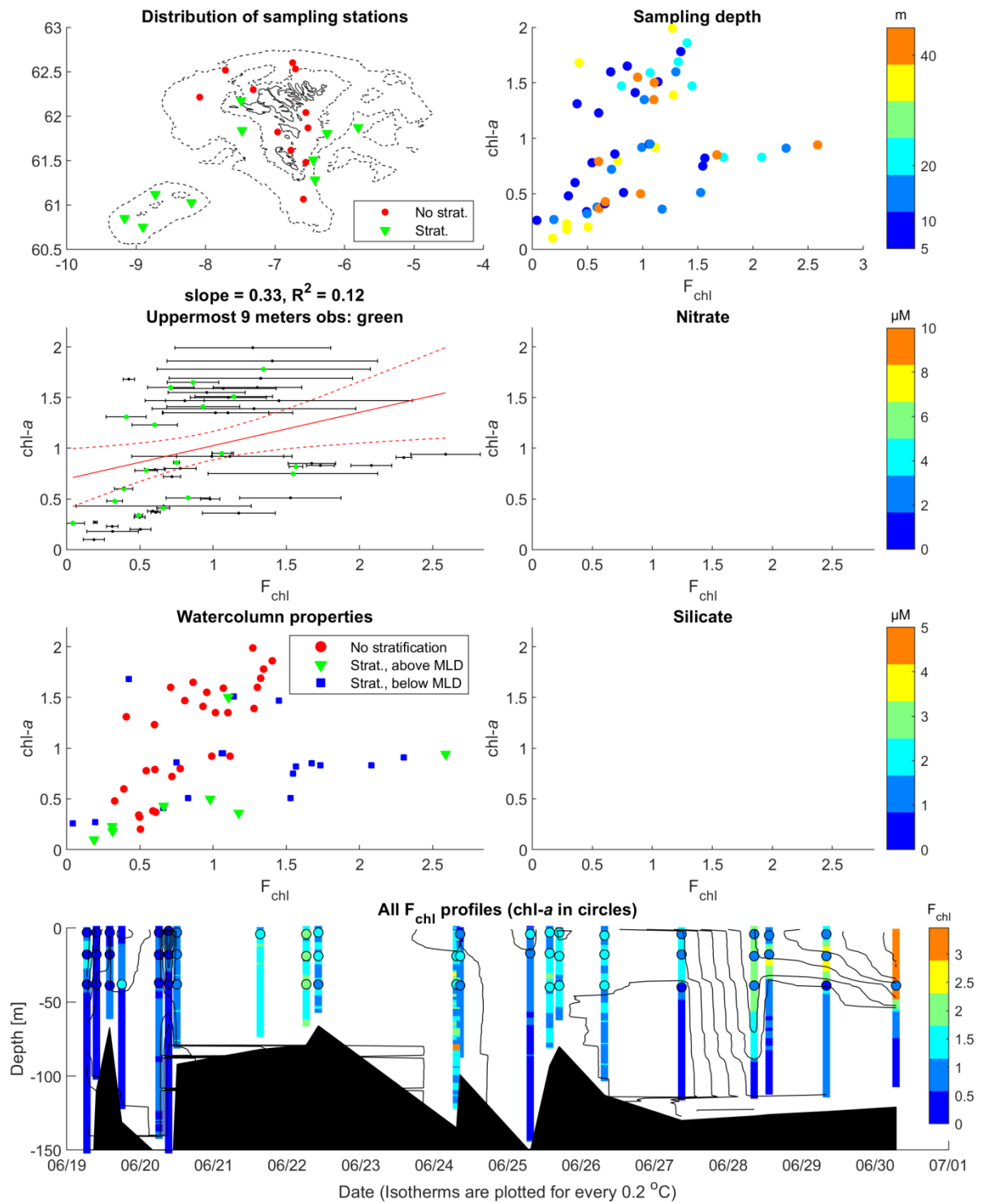
Cruise 1426, 0-group, 20/6-28/6, 2014



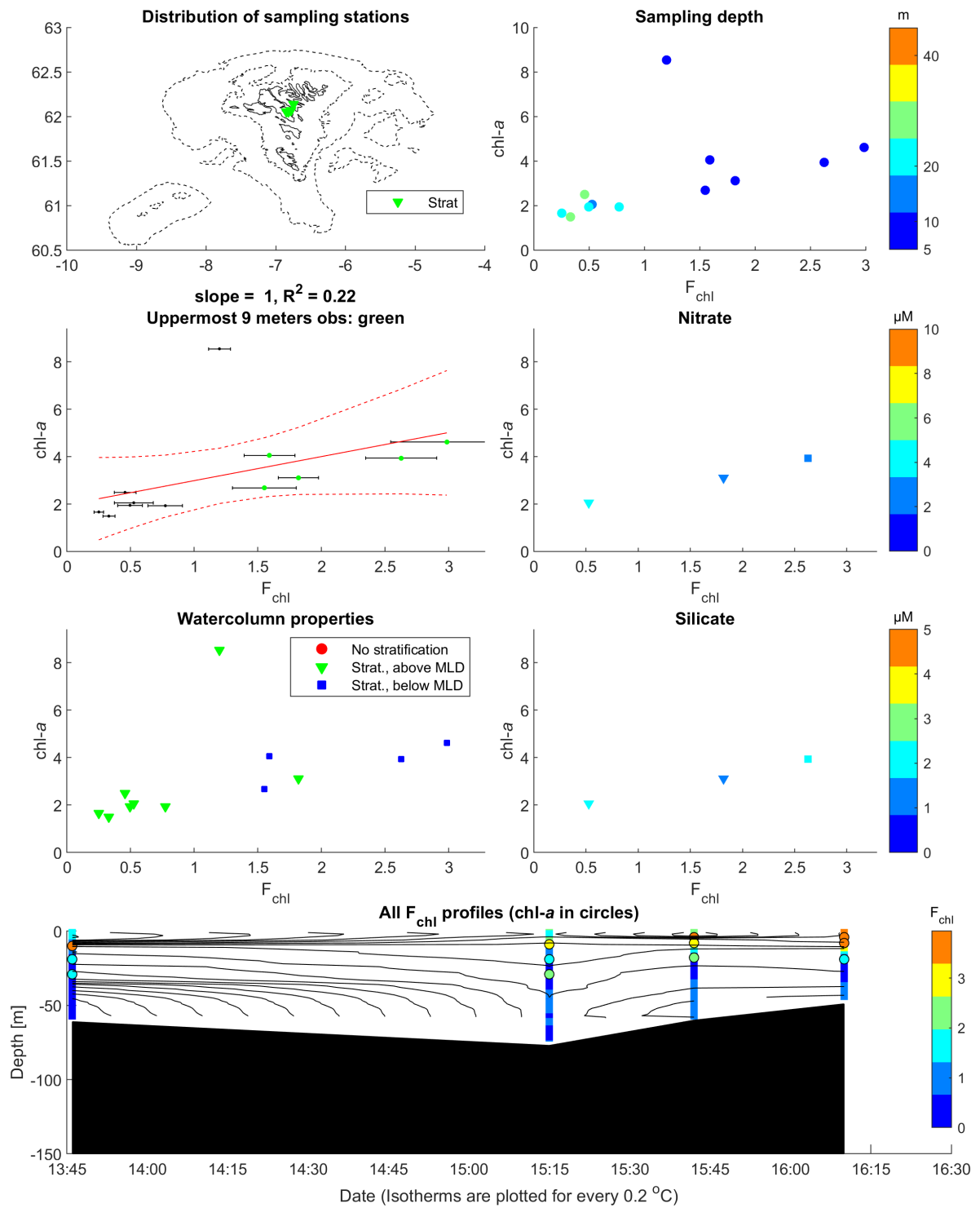
Cruise 1514, Biological oceanography, 24/4-28/4, 2015



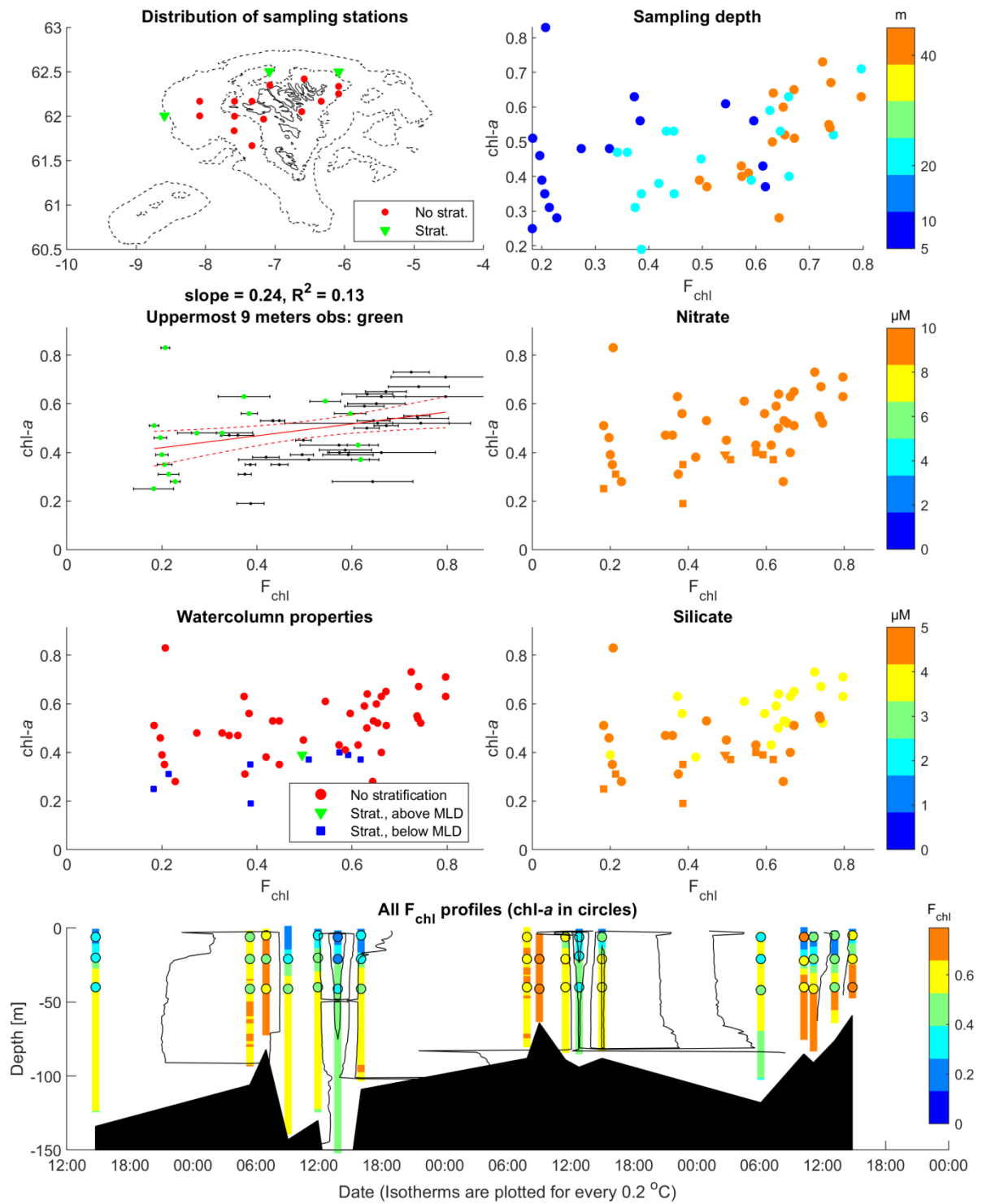
Cruise 1526, 0-group, 19/6-30/6, 2015



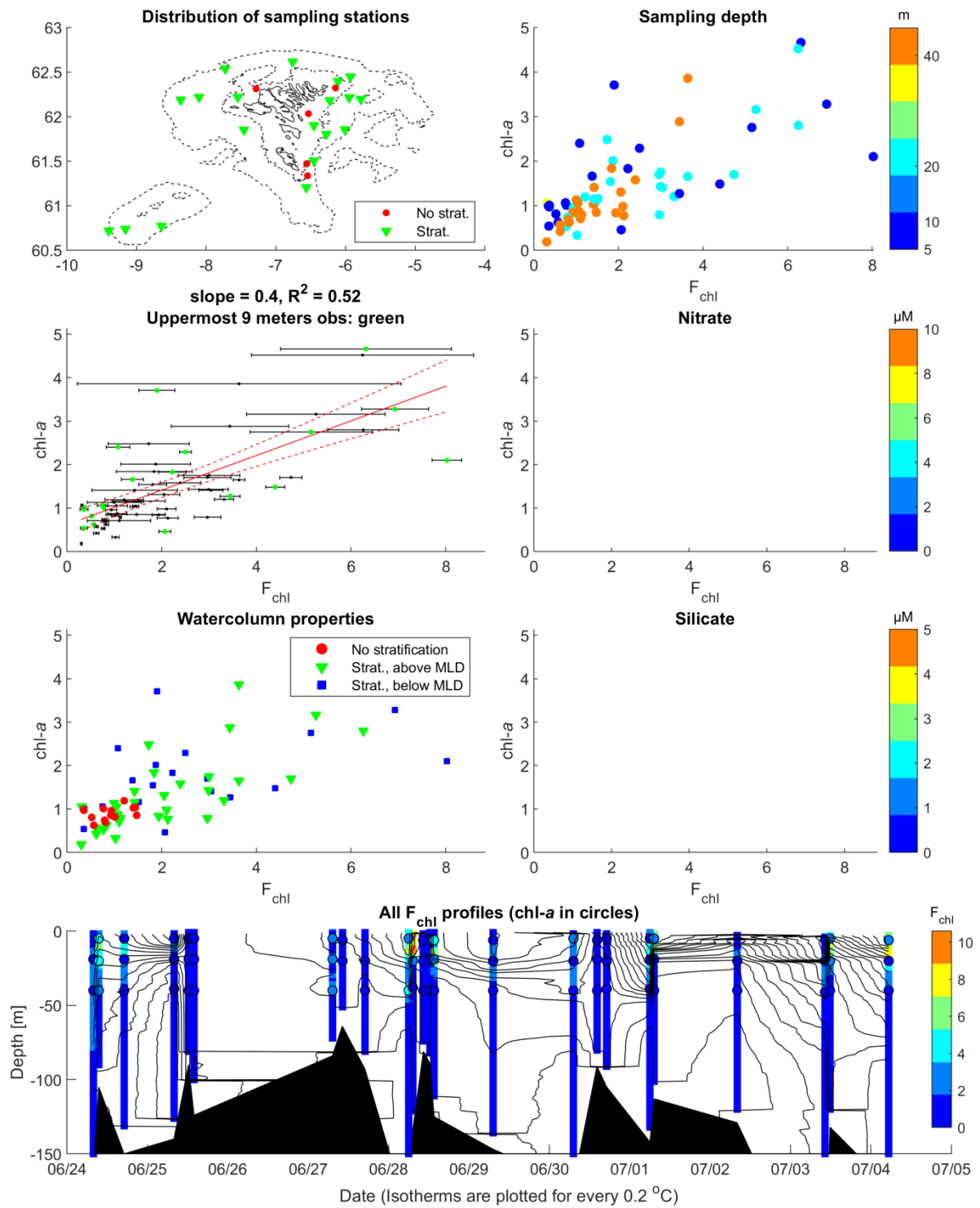
Cruise 1532, Fjords, 28/8-2015



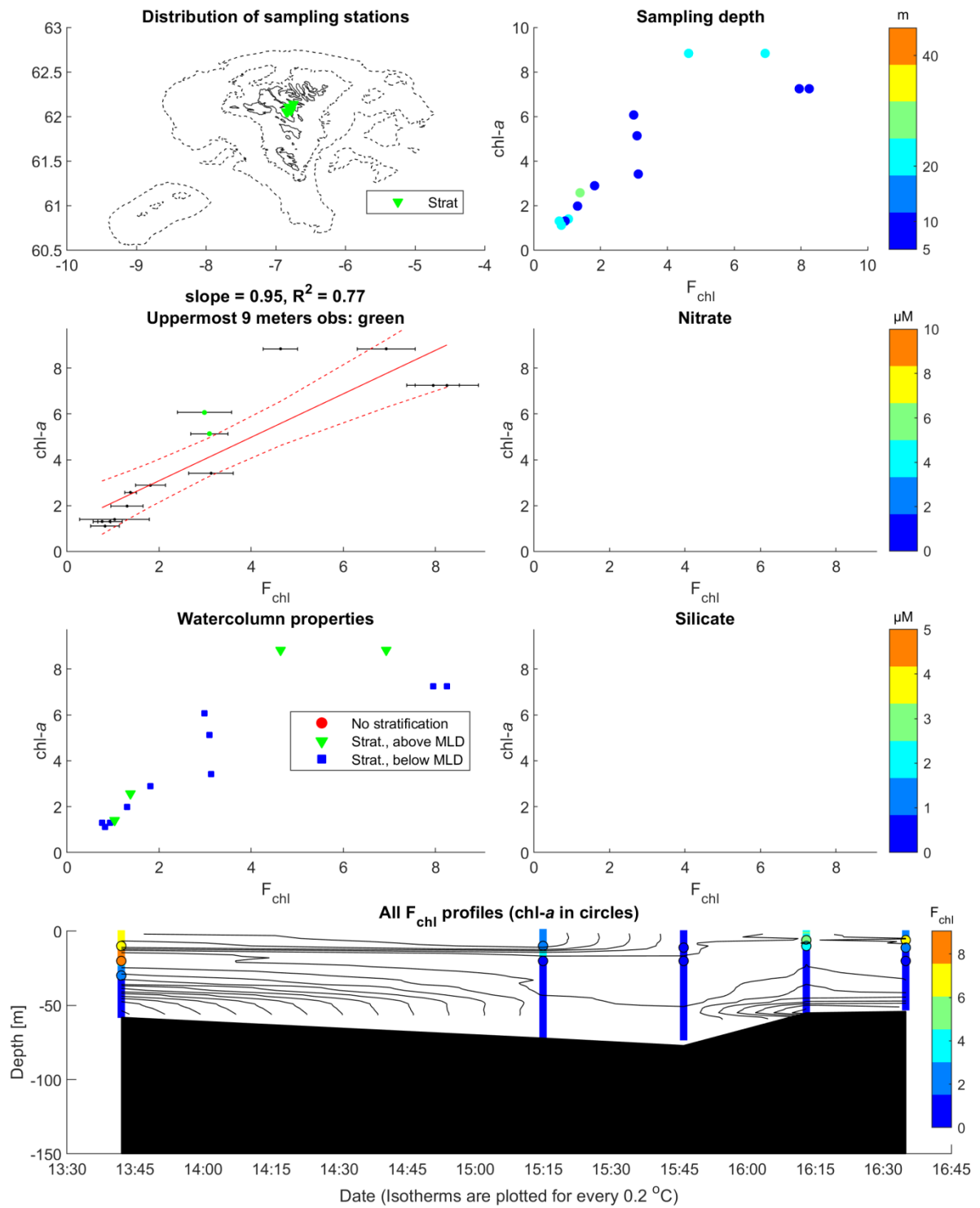
**Cruise 1616, Biological oceanography, 28/4-1/5, 2016**



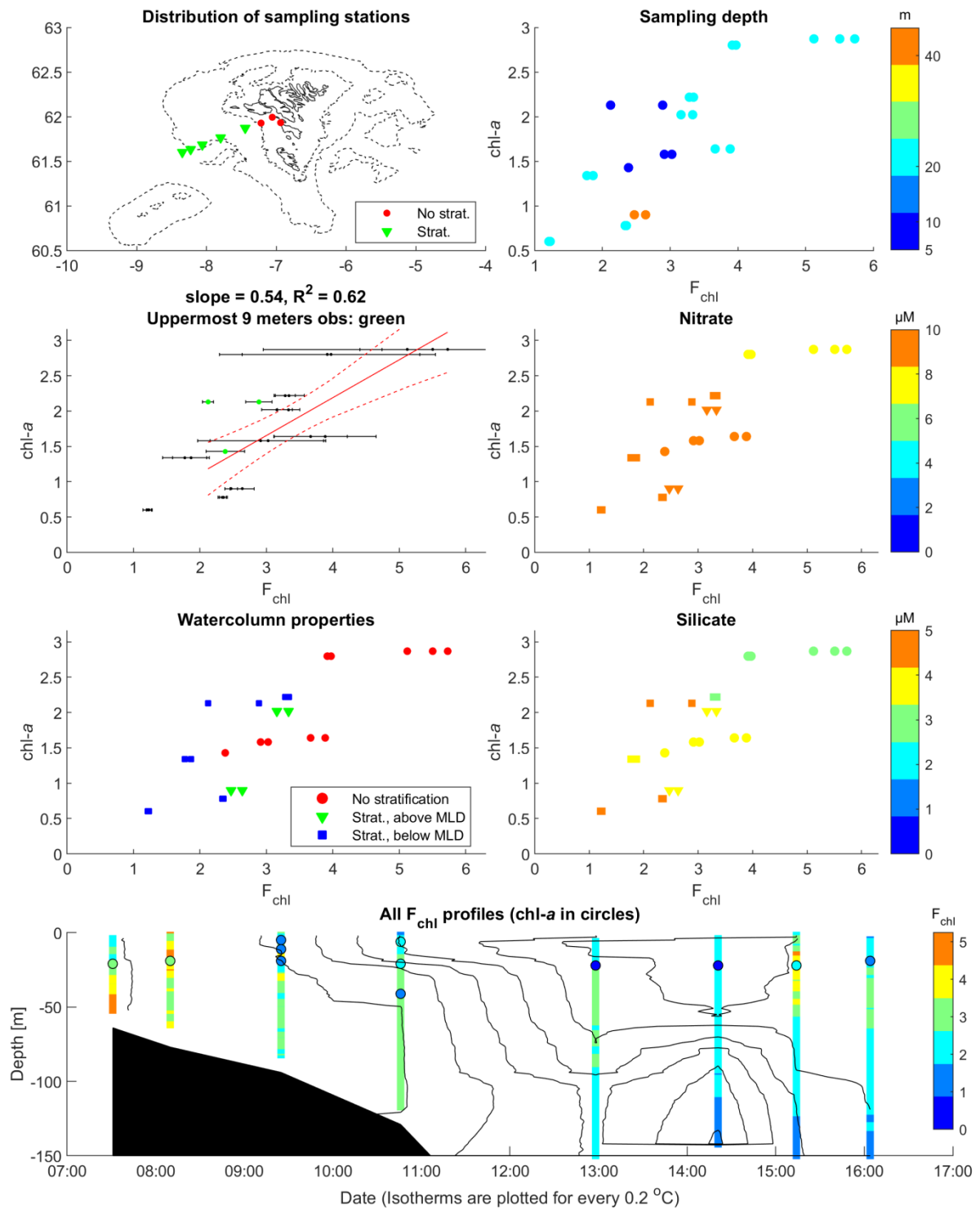
Cruise 1628, 0-group, 24/6-4/7, 2016



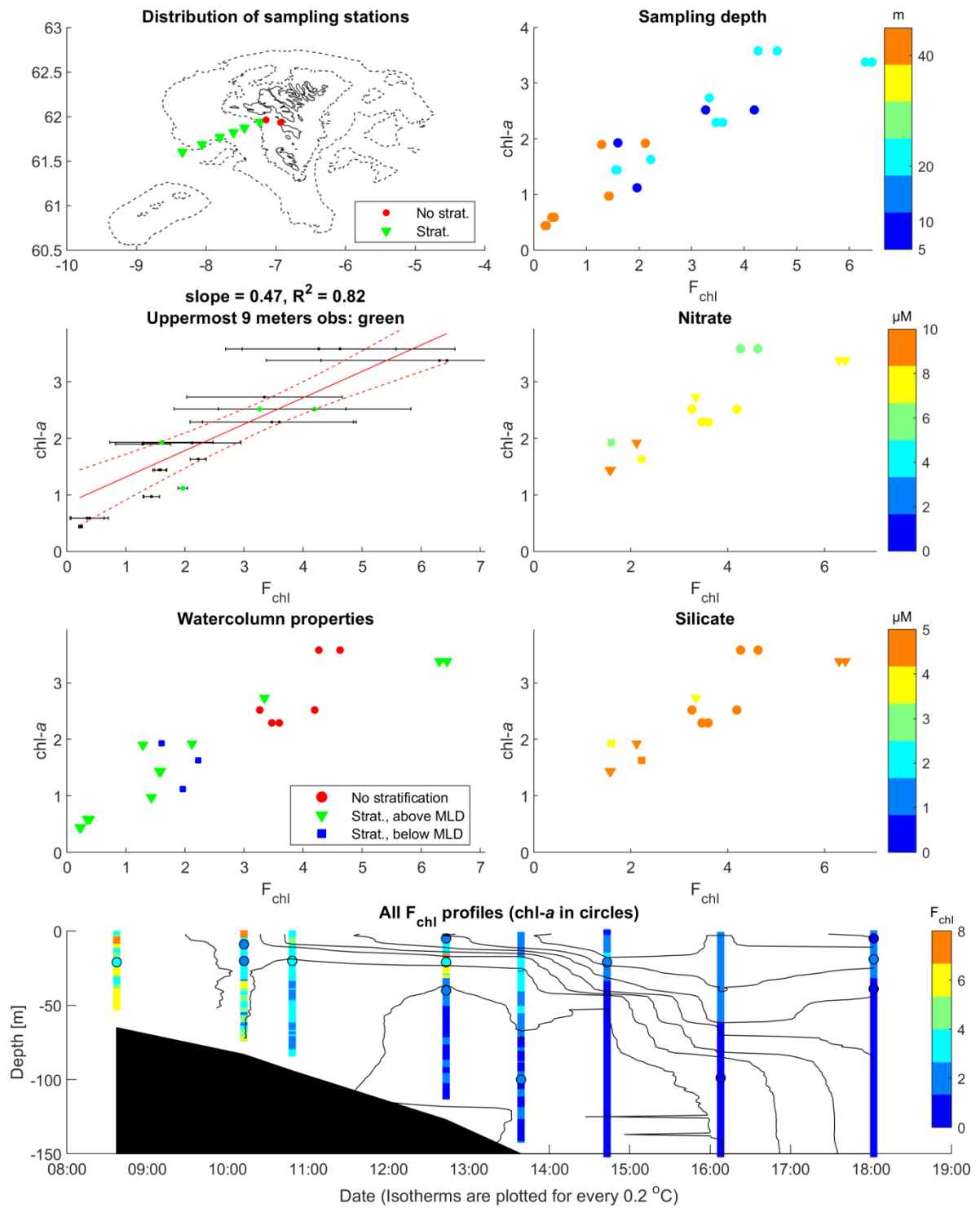
**Cruise 1634, Fjords, 30/8-2016**



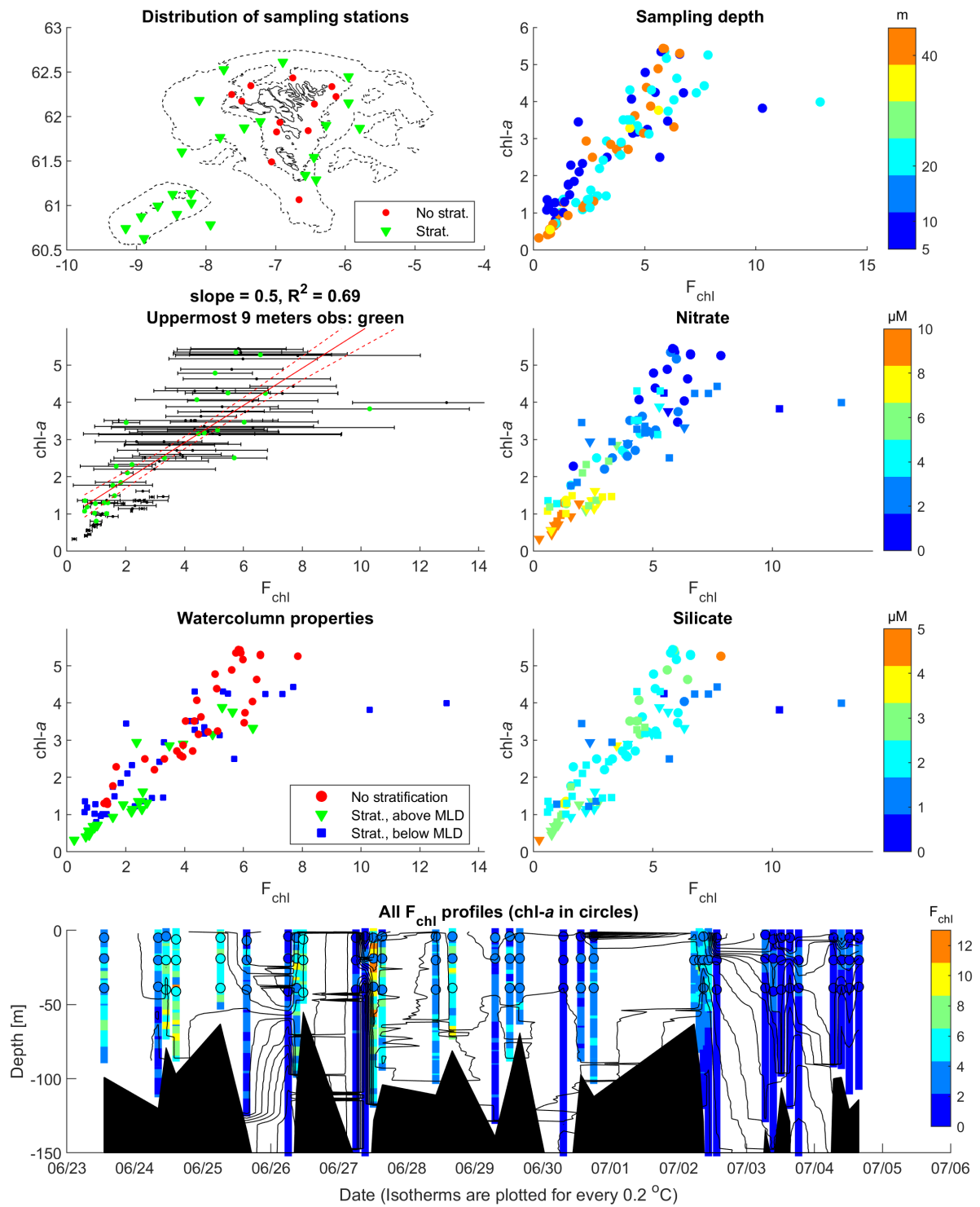
Cruise 1719, Section K, 15/5-2017



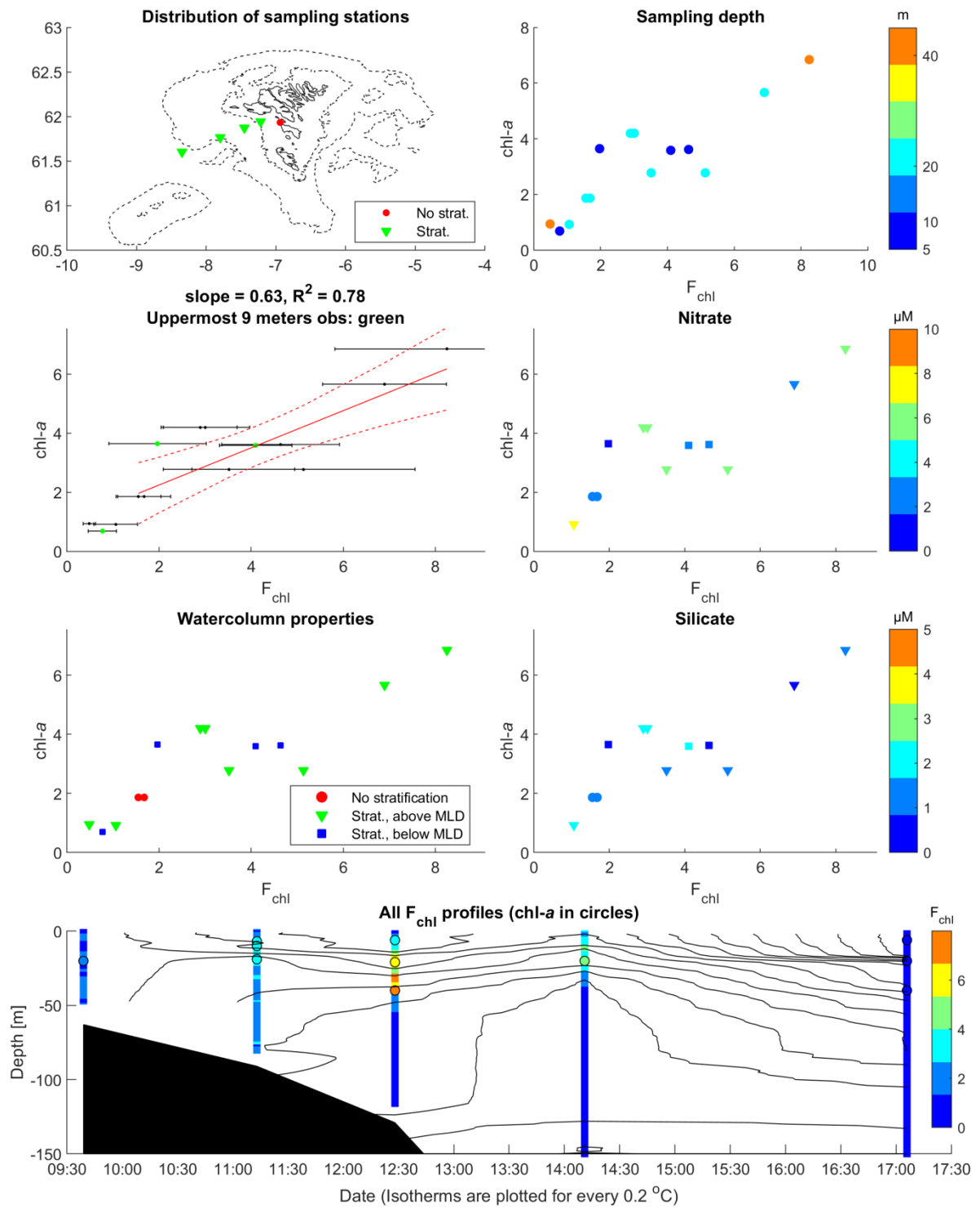
Cruise 1722, Section K, 25/5-2017



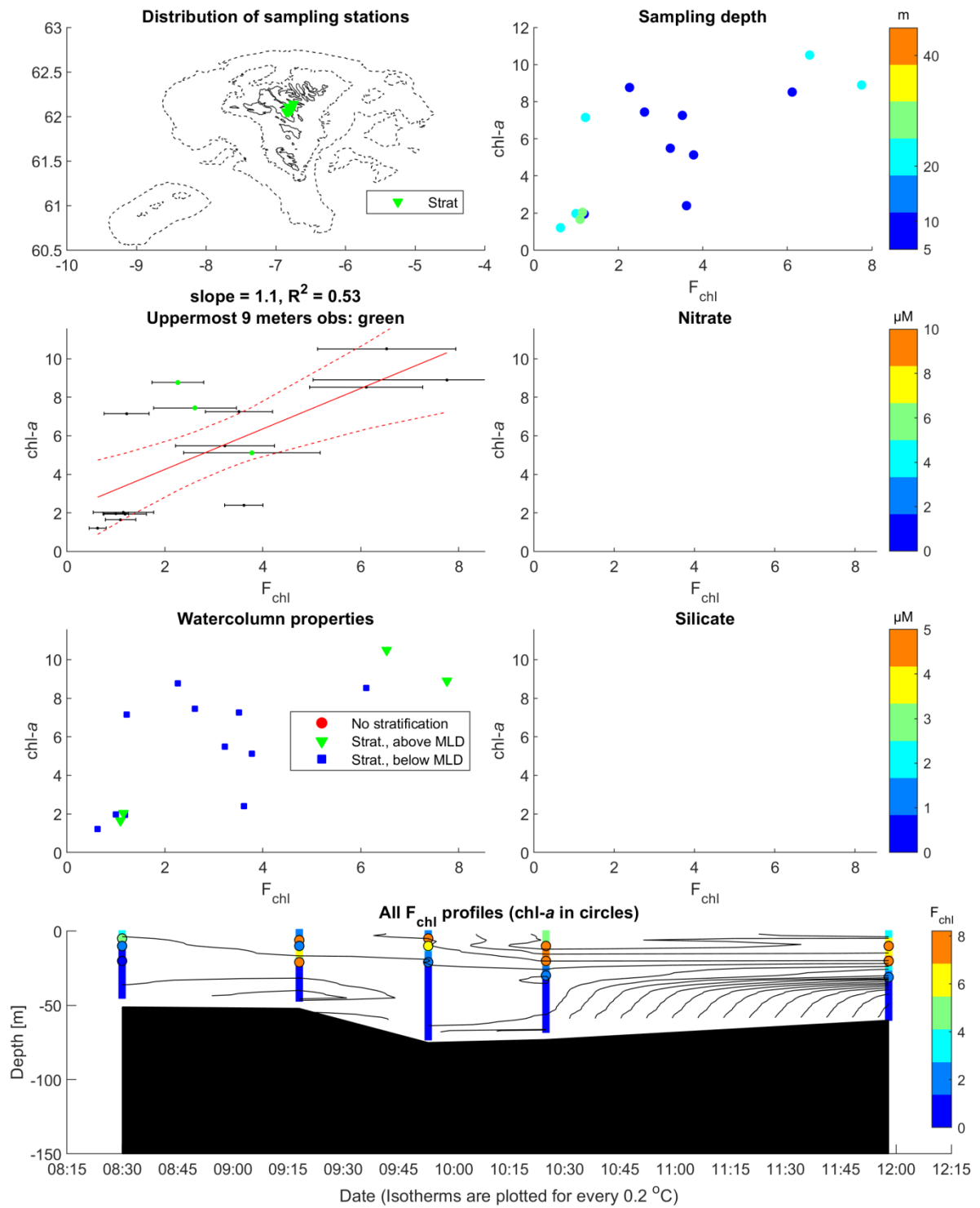
Cruise 1730, 0-group, 23/6-4/7, 2017



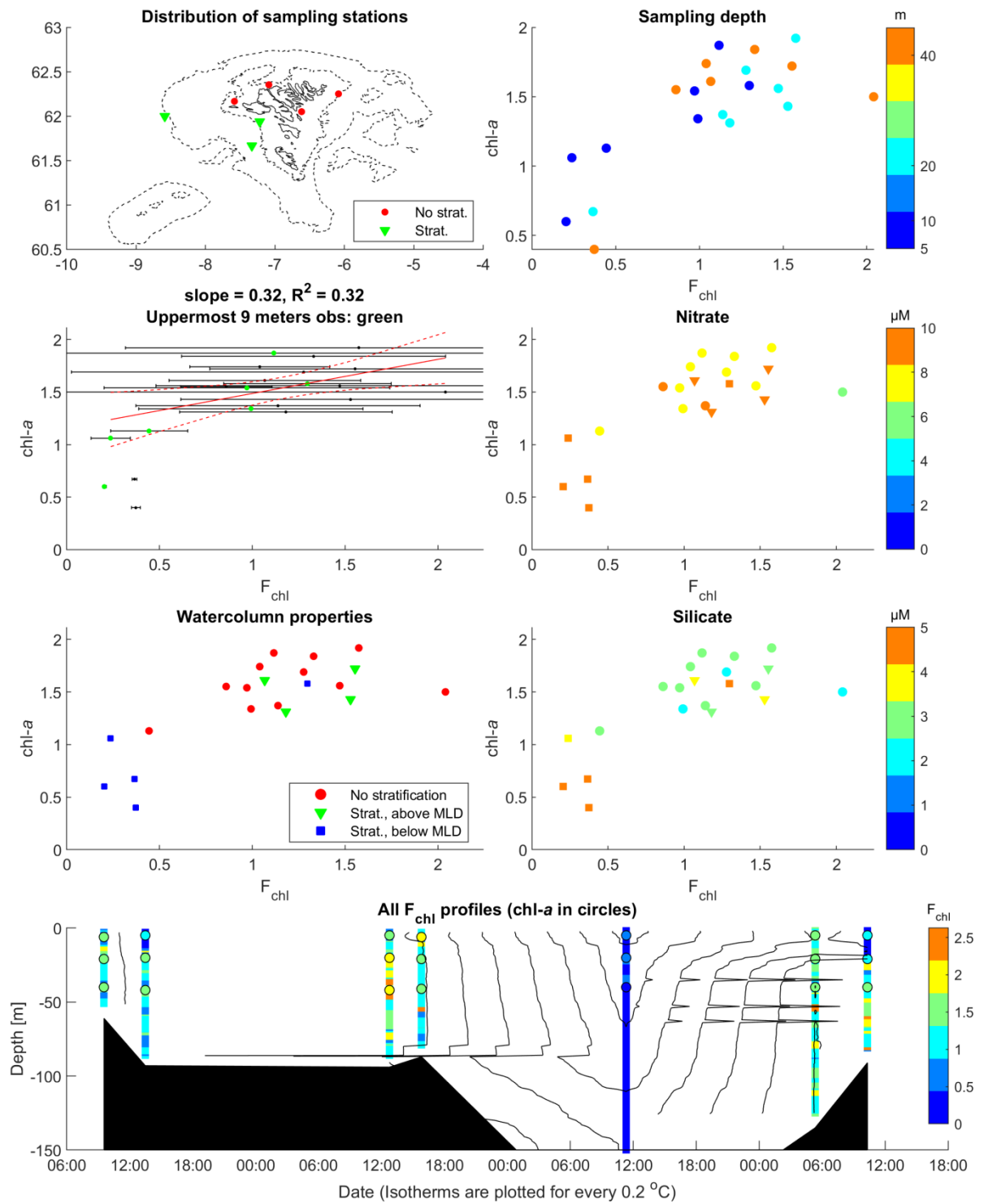
Cruise 1734, Section K, 1/8-2017



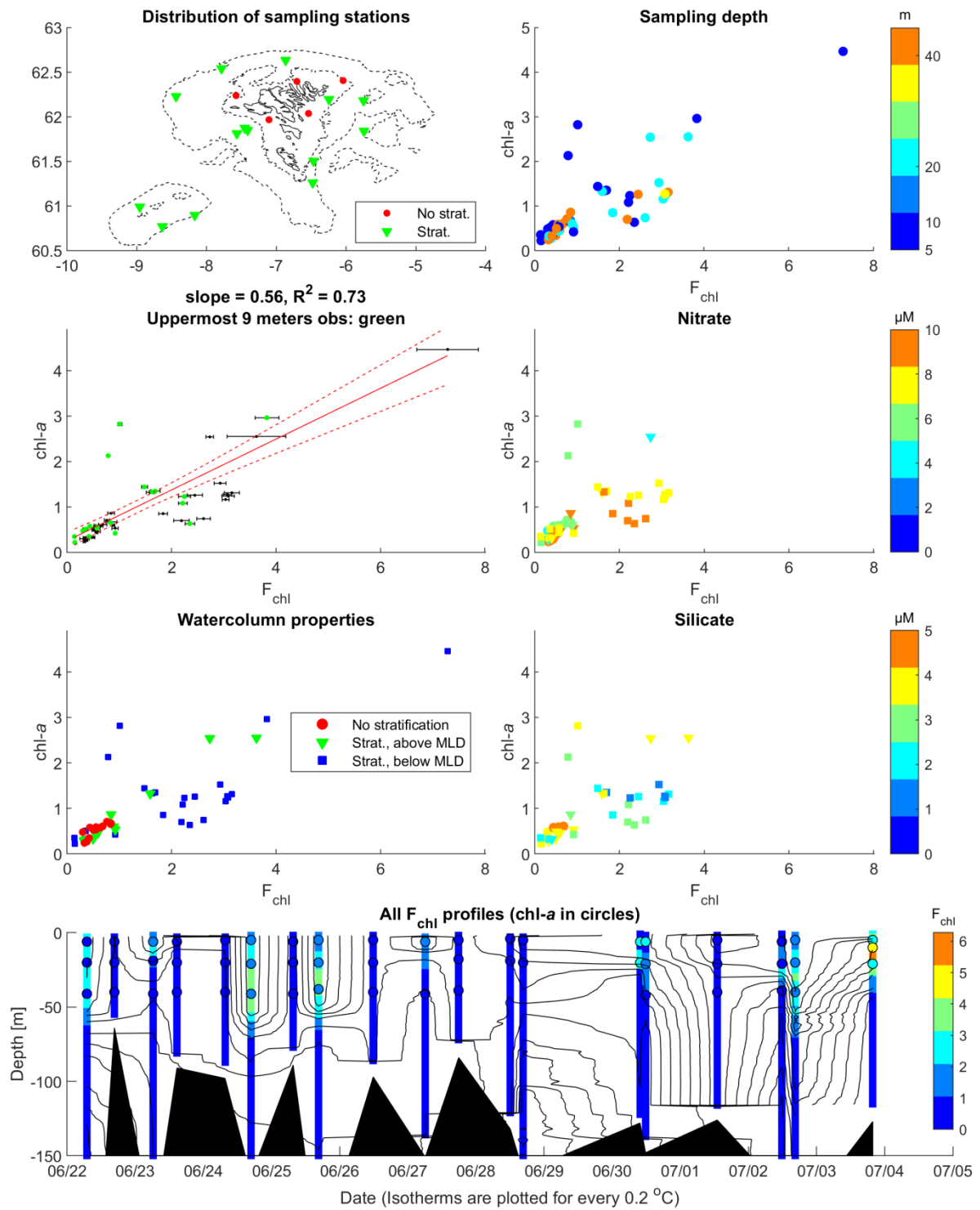
Cruise 1740, Fjords, 28/8-2017



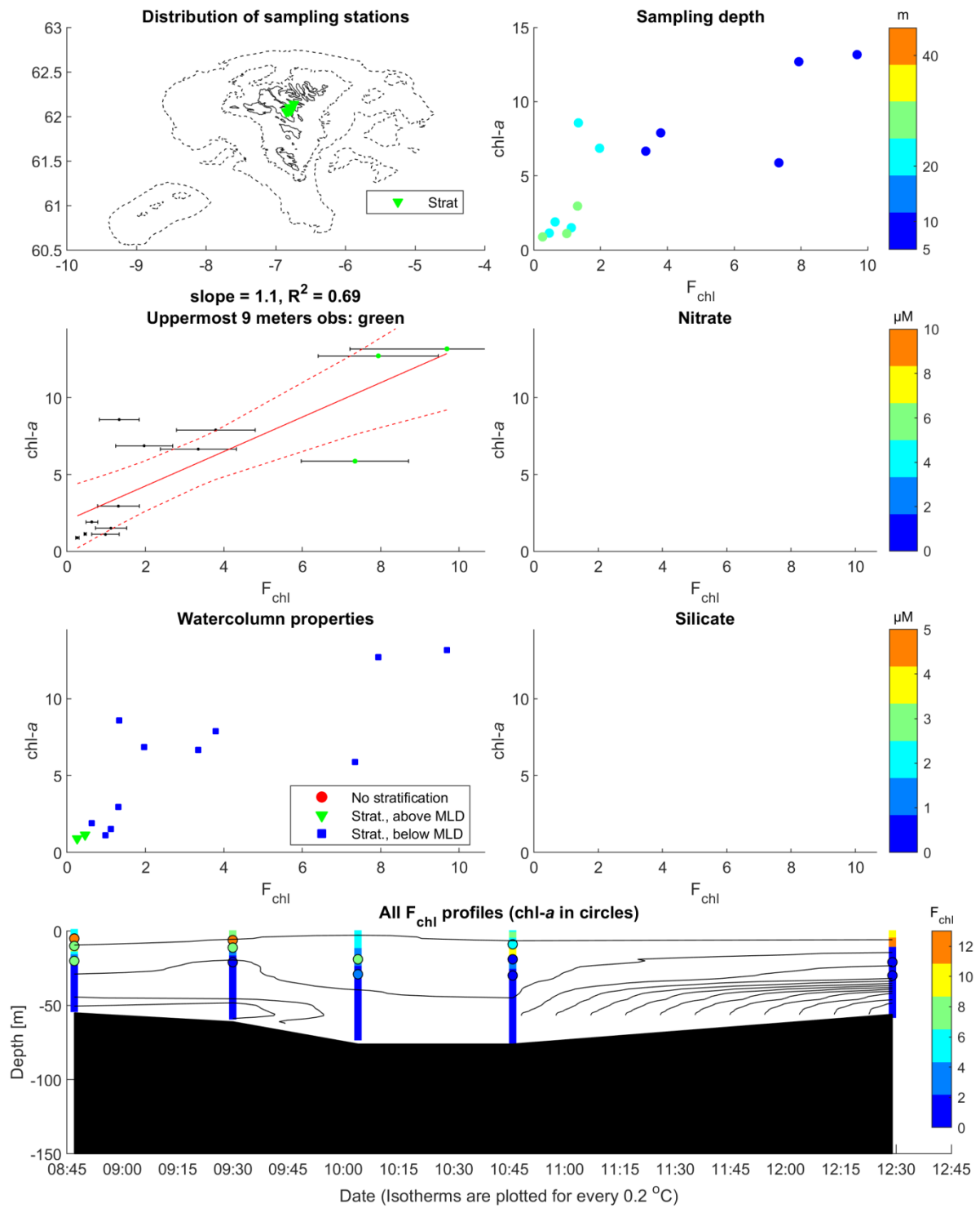
**Cruise 1818, Biological oceanography, 27/4-30/4, 2018**



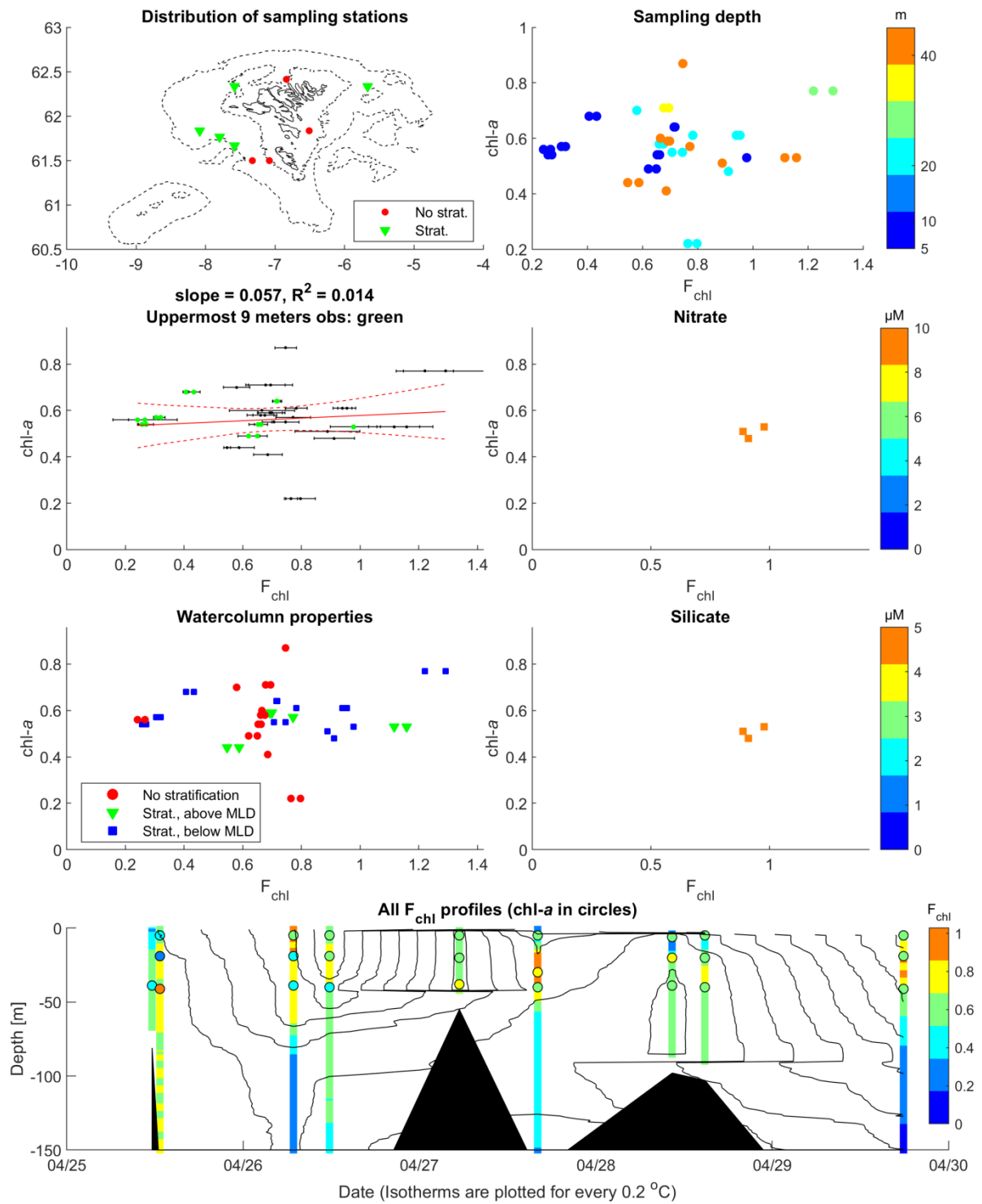
Cruise 1830, 0-group, 22/6-3/7, 2018



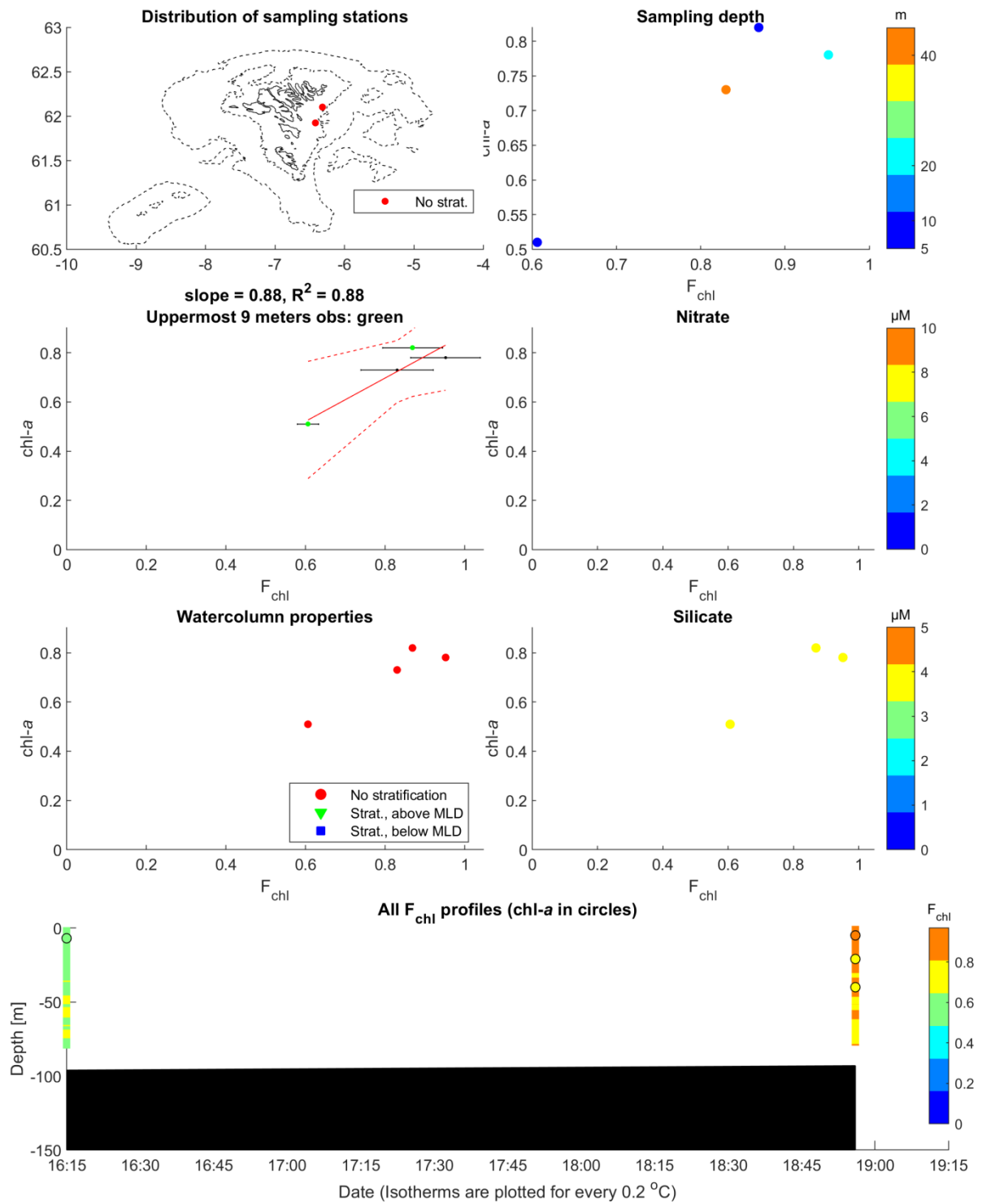
**Cruise 1836, Fjords, 27/8-2018**



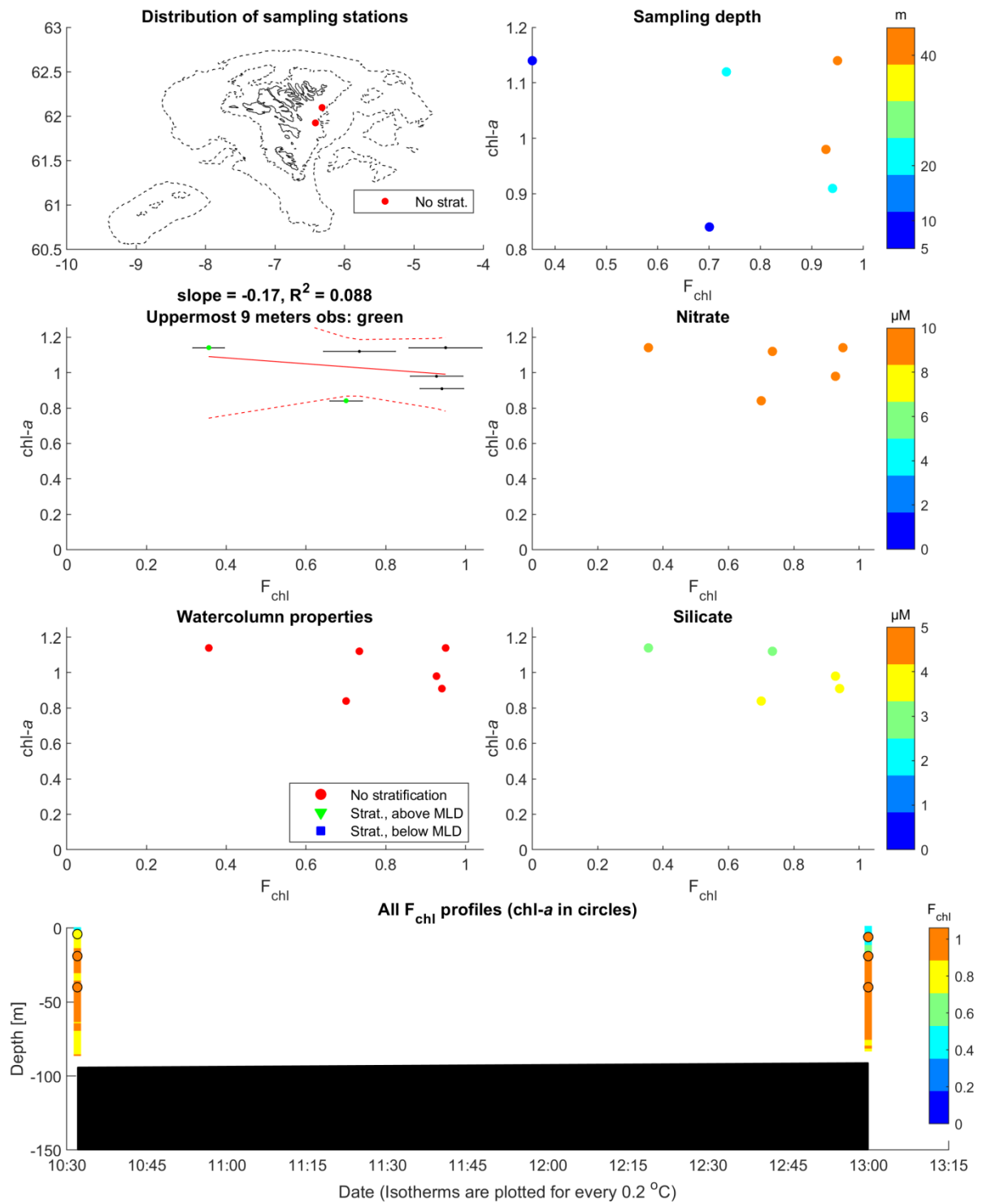
**Cruise 1916, Biological oceanography, 25/4-29/4, 2019**



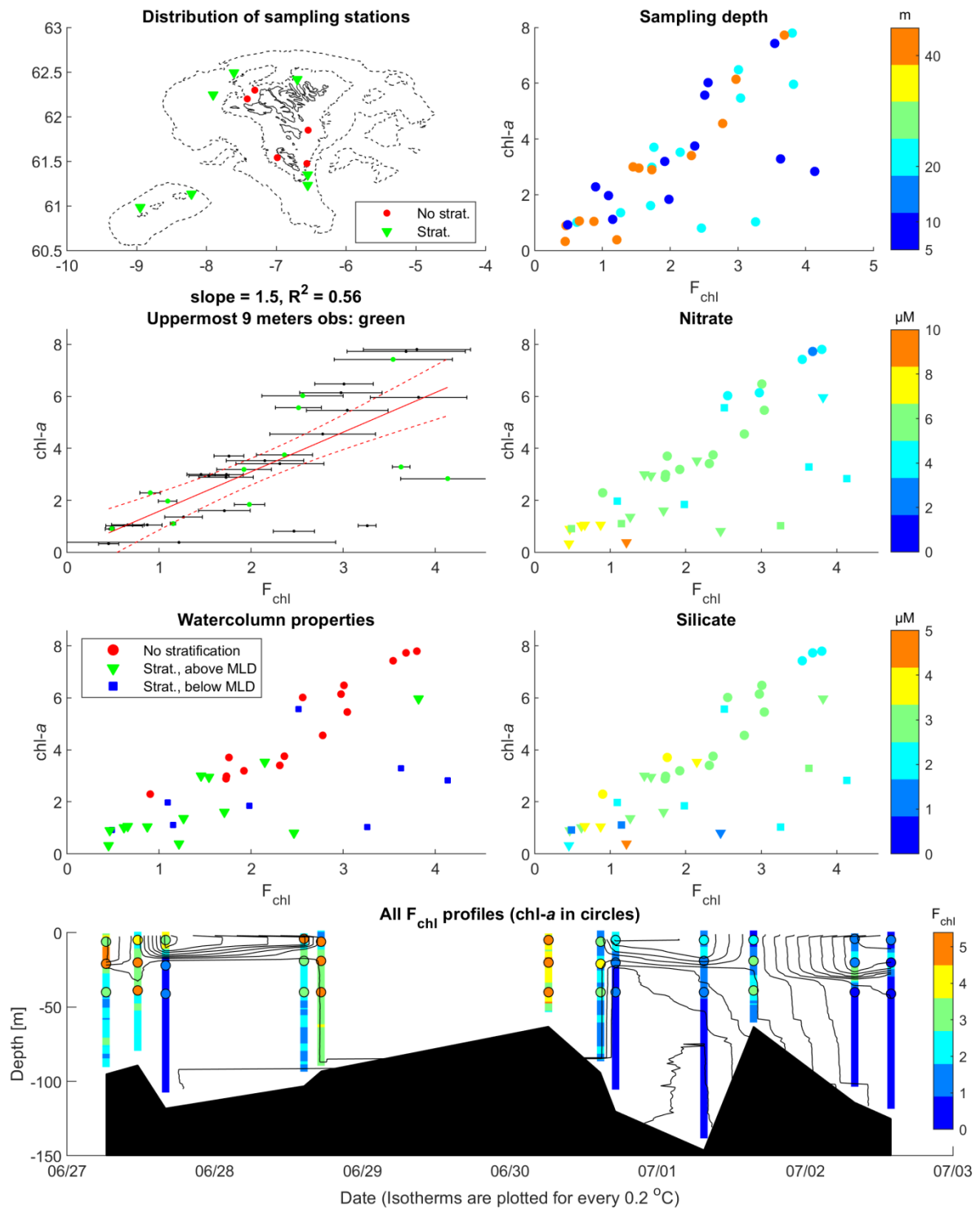
**Cruise 1921, Cod larvae, 23/5-2019**



**Cruise 1923, Cod larvae, 4/6-2019**



Cruise 1928, 0-group, 27/6-2/7, 2019



Cruise 1934, Fjords, 26/8-2019

